UNIVERSITÀ DEGLI STUDI
DELL'INSUBRIA

PhD course in Experimental and Translational Medicine

Medicine and Surgery Department

XXXIII cycle

Ph.D. Thesis

ACUTE STRESS, KETAMINE AND SYNAPTIC TRANSMISSION IN THE mPFC OF ADULT RATS

Supervisor: Dr Lia Chiara Forti

Co-Supervisor: Dr Emanuele Schiavon

Candidate:

Floramarida Salerno Scarzella

Index

SUMMARY

The work described in this thesis aimed at investigating the time course of the effects of acute stress, the foot-shock (FS) stress protocol, on excitatory synaptic transmission in pyramidal neurons (Pyrs) of cortical layers 2/3 and 5 in the prelimbic (PL) area of the medial prefrontal cortex (mPFC) of adult rats. Moreover, to investigate the possible use of ketamine at antidepressant doses for the rescue of FS effects on synaptic transmission, we extended the above measurements to animals undergoing FS and treated with systemic injection of low-dose ketamine.

Stress is an environmental risk factor for many neuropsychiatric disorders, such as depression and posttraumatic stress disorder (PTSD). The exposure to stressors can be chronic or acute (limited to a single traumatic event). A single acute stressor can lead to the establishment of either adaptive or maladaptive mechanisms. In PTSD, a single stressful event is enough to induce the alterations leading ultimately to the pathology, but it is not yet understood how a single event can be harmful in the long term in vulnerable subjects. Understanding the pathway leading to the maladaptive reaction could enlight new therapeutic approaches.

The mPFC plays a central role in the regulation of the stress response. In PTSD patients, the mPFC is smaller and this change correlates with symptoms severity (Holmes et al, 2018). The mPFC top-down control of the amygdala is impaired in stress-related pathologies (Lanius et al, 2010) and, given that the connections between the two areas are predominantly mediated by glutamate (Glu), studies on pre-clinical models of acute stress-related pathology have focused on the regulation of glutamatergic transmission. In the case of the acute FS stress paradigm, an early increase in depolarization-evoked Glu release from mPFC/FC synaptosomes was shown 1 hour after stress exposure, correlating with increased excitatory neurotransmission, as suggested by morphological (Nava et al, 2014), molecular (Treccani et al, 2014) and electrophysiological (Musazzi et al, 2010) evidence. Moreover, 1 day after acute stress exposure, an increase in the number of synapses and a decreased development of the dendritic arbour of layer 2-3 (L2-3) principal neurons in the prelimbic mPFC is observed (Nava et al, 2017). The latter event is similar to what seen in chronically stressed animals (Cook and Wellman, 2004).

The stress-induced impairment of glutamatergic transmission suggested the possibility to act on this system to contrast the pathological consequences of stress exposure. Indeed ketamine, an NMDA receptor antagonist used as anaesthetic, was tested at low doses in animal models of depression, demonstrating a fast-acting anti-depressant action (reviewed in Abdallah et al, 2014). The use of ketamine could be beneficial also for prevention of PTSD (Feder et al., 2020),

as a lower risk of developing PTSD was reported in soldiers treated with low doses of ketamine (McGhee et al, 2008). While the mechanisms underlying ketamine action are still debated (Duman et al., 2019), preclinical models demonstrated that its anti-depressant action involves an increase in the number of dendritic spines of layer 5 (L5) principal neurons in the mPFC, correlated with enhanced excitatory postsynaptic currents both in naïve and chronically stressed animals (Li et al., 2010; Liu et al, 2015).

Two main observations guided the work presented in this thesis. Firstly, some depressive-like behaviours (anhedonia and learned helplessness), typically arising in animal models of chronic stress, may be also present after acute stress (Mitra et al, 2014; Velbinnger et al, 2000), suggesting that the maladaptive mechanisms of the chronic stress response could already be activated 24 hours after a single traumatic event. This observation led us to investigate the time course of possible alterations, both early and sustained, of local synaptic transmission in the mPFC, induced by a single session of the unescapable foot-shock stress (FS), for revealing possible maladaptive mechanisms that could lead to the development of psychopathological conditions. Secondly, experimental pieces of evidence suggest that acute stress may have a preferential impact on the local network activation in specific mPFC layers (Hwa et al, 2019) and that ketamine may specifically affect distinct mPFC regions and subcircuits (Liu et al, 2015). This suggested us to evaluate the possible distinct effects of sub-anaesthetic doses of acute stress and ketamine on excitatory Glu transmission in different mPFC layers (L2-3 and L5) during the sustained phase of the FS-induced reaction.

In our experiments, the unpredictable FS protocol consisted of a 40 min session of 0.8mA electric shocks (2-8 second each), randomly occurring for a total of 20 minutes. We used the whole-cell patch-clamp technique in mPFC-containing brain slices from adult male rats, to record from cells in the PL mPFC region. In a part of our experiments, using a K^+-based intracellular solution, we could confirm that the recorded cells were regular spiking (RS) pyramidal neurons, as indicated by established functional criteria based on the assessment of neuronal firing responses and input resistance. We measured both the spontaneous excitatory postsynaptic currents (sEPSCs), arising from AP-dependent release, evoked by spontaneous firing activity in the slice and miniature excitatory postsynaptic currents (mEPSCs) arising in the absence of action potentials (APs), recorded in the presence of a cocktail of Na+ channels and GABAa receptors and Gly receptors blockers.

To investigate the time course of FS-induced alterations of local synaptic transmission in the mPFC, our first set of experiments studied sEPSCs and mEPSCs 1 hour after the exposure to stress in L2-3 neurons. Of notice, when recording the firing activity of these neurons, we could

not reveal any stress-induced regulation of neuronal excitability at this early time.

Contrary to the expectation based on the increase of spine density in this area (Nava et al, 2014), we could not detect changes in the frequency and/or amplitude of mEPSCs, suggesting that the newly formed synapses reported by Nava et al. might be non-functional, immature synapses. On the other hand, when looking at AP-dependent transmission, we showed that FS induces an increase in the peak amplitude of the sEPSCs, confirming previous results in younger animals, and in accordance with data on depolarization-evoked Glu release from mPFC/FC synaptosomes (Musazzi et al, 2010). Moreover, in some cells from stressed animals, we observed the intermittent presence of clusters of large-amplitude sEPSCs, not observed in control, suggesting the stress-induced activation of synapses with high efficacy. This is consistent with the report of enrichment in docked vesicles in the presynaptic compartment of mature (perforated) synapses in L2-3 (Nava et al, 2014).

As no alterations of inhibitory GABAergic transmission has been reported in the FS stress model (Musazzi et al, 2010) in parallel to the enhanced excitatory activity, the early stress response could imply the unbalance of excitation and inhibition in the mPFC local network. In a second set of experiments, we studied the ratio of average excitatory and inhibitory conductances (E/I) in L2-3 mPFC neurons, in the same experimental groups as above, to verify a possible E/I increase, similar to what reported after an unconditioned threatening stimulus (Hwa et al, 2019). We used a Cs^+-based intracellular solution to allow stable recording of spontaneous inhibitory postsynaptic currents (sIPSCs, +3 mV) at positive potentials, and we also measured sEPSCs (-58 mV) in each recorded L2-3 neuron in the PL mPFC. We observed a non-significant tendency to an increase of both excitatory and inhibitory total charge, and an invariant E/I, suggesting that the local network in L2-3 maintains the balance of excitation and inhibition 1 hour after FS. Given that in these experiments, due to the presence of intracellular Cs^+ ions, it was not possible to assess the cell firing behaviour, the identity of the recorded cells as RS Pyrs could not be verified, and our E/I result may derive from a less homogenous neuronal population.

We next turned to the study of synaptic current regulation at a later time (24 hours) after exposure to the stressor. In our third set of experiments, the E/I was measured 1 day after FS in L2-3 neurons. When comparing control and stressed animals, we found a significant increase in average excitatory conductance, paralleled by a significant increase of the E/I balance, indicating that 1 day after stress the local neuronal network still experiences enhanced excitation, even if only a non-significant tendency to the increase in sEPSCs frequency could be detected. This result is consistent with the previous finding of sustained enhancement of Glu

release from mPFC/FC synaptosomes (Musazzi et al., 2017). Interestingly, in experiments with the Cs-based intracellular solution, we also observed a slight tendency to a slower speed of rise of the sEPSCs, and this tendency was confirmed in a further set of experiments using the K-based solution, where we demonstrated a significant slowing of the rise kinetics of sEPSCs of stressed animals 1 day after stress. This kinetic change may arise from several factors, including changes in postsynaptic receptor composition, in the shape of the postsynaptic spines, or the electrotonic distance of active synapses from the somatic recording electrode. Whatever the underlying mechanism, this increase confirms a dynamical change in the excitatory transmission mechanisms occurring 1 day after a single acute stressor. In the latter experiments at 24 hours from FS, the experimental groups included stressed animals receiving ketamine or saline injection 6 hrs after FS (and saline-injected controls). We found that a sub-anaesthetic dose of ketamine induces an increase in the frequency of the sEPSCs and rescue of the FS-induced rise-time increase. The enhancement of frequency is consistent with the ketamine-induced increased number of spines in naïve animals and chronic stress models (Li et al., 2010, 2011; Liu et al, 2015; Moda-Sava et al, 2018; Ng et al, 2018; Phoumthipphavong et al., 2016). The rescue of the FS-induced rise time increase is reminiscent of the evidence that ketamine induces re-formation of spines in close proximity to spines eliminated by previous chronic restraint stress (Ng et al, 2018) or chronic corticosterone treatment (Moda-Sava et al, 2018). If ketamine has a similar effect in FS-stressed animals, this could imply a rescue of sEPSC kinetic parameters after restoring synapses impaired by previous stress. Additional studies should address this issue.

To further explore possible distinct effects of sub-anaesthetic doses of ketamine in different mPFC layers in stressed animals, we finally focused on ketamine effect on L5 RS Pyrs in the PL region. Preliminary recordings of sEPSCs and mEPSCs, performed with K^+-based intracellular solutions as described for L2-3 neurons, do not show any effect of either ketamine or foot-shock on the modulation of excitatory transmission. However, our sample should be increased in future experiments to reach more reliable assumptions.

In conclusion, our data confirm an early FS stress-induced enhancement of Glu transmission in L2-3 Pyrs in the prelimbic mPFC. This enhancement is due to the activation of a few strong synaptic contacts and is not paralleled by a detectable increase in the E/I balance in single neurons. On the contrary, 1 day after FS, the excitatory Glu conductance is increased in parallel with an increase in the E/I balance. Ketamine at this time increases the frequency of sEPSCs, consistent with the synaptogenic effect reported in naïve and chronically stressed animals.

INTRODUCTION

1. What is stress?

Stress is the physiological response to environmental changes, both psychological and physical ("stressors"), that are perceived as challenges. This process involves many different compartments in the human body, that work together to contrast the effects of stressors and return to a homeostatic state, possibly different from the physiological homeostasis ("allostasis"). When this occurs, we have an "adaptive" response. On the contrary, when the system is no longer able to regain some kind of homeostasis, we have a "maladaptive" response to stressors that usually lead to pathological consequences. The factors determining this switch are not clearly understood and many efforts have been put in the characterization of the pathways contributing to the stress response.

Research has failed until now to give a complete and univocal visualization of the so-called stress response system. Over the years, the stress response has been widely dissected and many distinctions have been made in the effort to explain the complex and multi-component pathways composing this system. The main distinction is between the physical and psychological stress, with the first related to the stimuli that produce actual disturbances of physiological status (e.g., haemorrhage or infection), and the latter regarding stimuli that threaten a balanced state (e.g. aversive environmental stimuli, predator-related cues and failure to satisfy internal drives). When analyzing the literature, a distinction can also be found based on the duration of exposure to the stressor, and hence the duration of the stress response activation, defining as "acute stress" the response to limited exposure to a stressor, and as "chronic stress" a repeated and prolonged exposure to stressors.

Regardless of these distinctions, the developing view of the stress response presents an interactive, time-tuned and tightly regulated harmonization of two distinct actors: the autonomic nervous system (ANS), both parasympathetic (PNS) and the sympathetic (SNS) systems, and the hypothalamic-pituitary-adrenal (HPA) axis. These systems were initially thought to play a distinct role, where the ANS was more involved in the physical/acute stress response, leading usually to a pro-adaptive outcome, while the HPA was engaged in the psychological/chronic stress response. However, the mounting evidence of the interplay between the different systems, the cross-regulation between the activation route of the ANS and the HPA, and the evidence of long-term maladaptive consequences after acute stress lead to hypothesize that what determines the extent of the stress response is not the type or the duration of stressor exposure, but rather the physiological state of the subject.

1.1 The stress response

In this section, an overview of the stress response and its main different actors will be presented, trying to give a general idea of the complexity of this system (Fig. I.1).

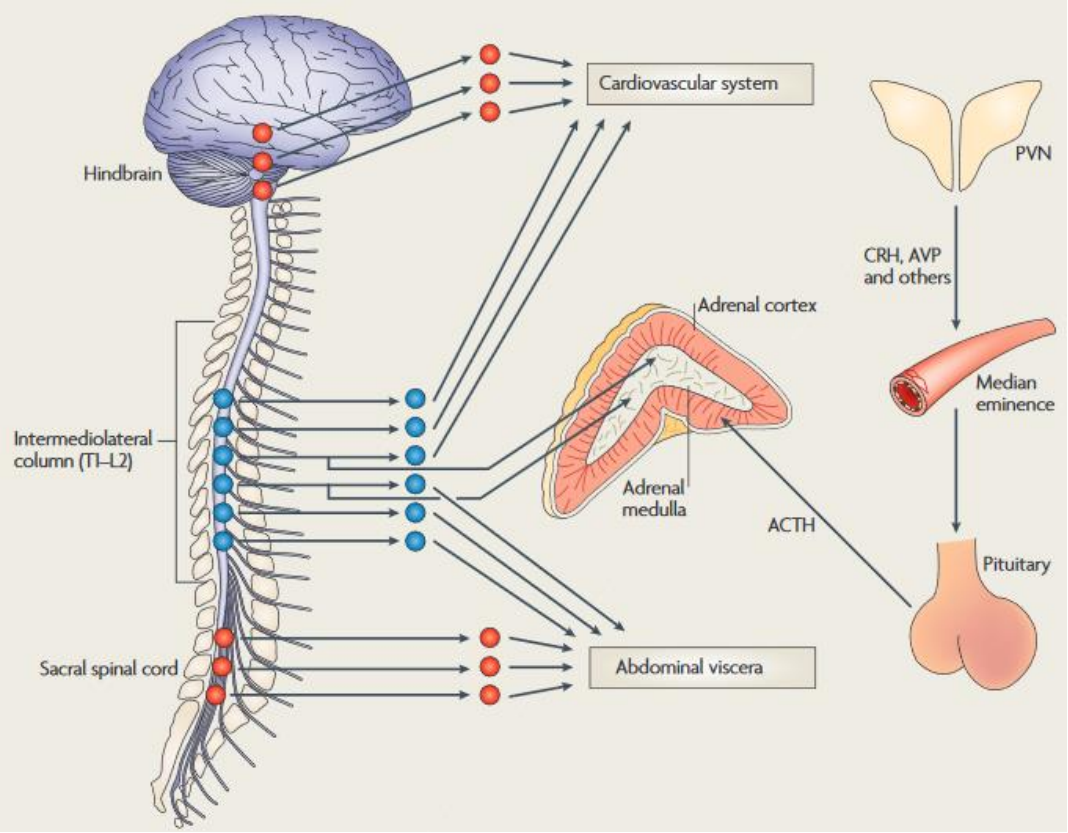

Fig. I.1. **Stress response main actors**. from Ulrich-Lai and Herman (2009). Visual representation of sympatho-adrenomedullary (SMA, left) and hypothalamic-pituitary-adrenocortical (HPA, right) axes as the principal systems acting on the activation, maintenance and restriction of the stress response. Activation after stressor exposure of the sympathetic neurons of the spinal cord (blue), induces the increase of epinephrine (from the adrenal medulla), norepinephrine (from sympathetic nerves) and heart rate, paralleled with energy mobilization. The parasympathetic tone (in red) contrast the sympathetic activation via activation of craniosacral preganglionic nuclei. Stressor exposure activates also the paraventricular nucleus (PVN), inducing the secretion of releasing hormones (CRH and AVP). These induce the pituitary gland to release ACTH, which acts on the adrenal cortex, promoting the production of glucocorticoid hormones.

The first response to a stressor is the so-called fight-or-flight response. The SNS activation originates from the preganglionic neurons in the intermediolateral cell column (IML), innervating sympathetic ganglionic neurons, which participate in somato- and viscero-sympathetic reflexes, inducing, for example, increase in the heart rate and raise of blood pressure thanks to its connection on the heart. Meanwhile, through the sympatomedullary arm

(SMA), the signals arrive at the adrenal medulla, causing the secretion of epinephrine and norepinephrine, which sustains the cardiac changes and promote hepatic gluconeogenesis. The final result of the SNS activation is that the body speeds up, tenses up and becomes generally very alert (Lewis and Coote, 1990).

The ANS response is short-lived, but stressor-related pieces of information, from the sensory system, are conveyed to the brain, enabling engagement of the neuroendocrine and neural systems. These brain circuits regulate both ANS and HPA axis responses to stress, with widely linked processes. It has been demonstrated, indeed, that the sympathetic inputs are received by the brainstem, which is composed of different nuclei regulating the tone of the SNS and PNS arms, thanks to descending information from the hypothalamus and the limbic forebrain. On the other hand, ascending pathways of the brainstem project to the paraventricular nucleus of the hypothalamus (PVN), participating to some extent in the HPA activation (Cunningham et al, 1990). This nucleus is the principal integrator of the stress signals, giving that its neurons respond to high-level of norepinephrine, corticotropin-releasing hormone (CRH) and arginine vasopressin (AVP) into the median eminence, generating the HPA signal. These hormones stimulate the anterior pituitary gland to produce and secrete adreno-corticotropic hormone (ACTH), which reaches the adrenal glands, inducing glucocorticoid production and release. These molecules regulate many compartments of the body such as behaviour, metabolism regulation, energy distribution, and pro-inflammatory state, in order to prepare the body to physically and psychologically respond to the stressor. This wide range of activity is due to the high and ubiquitous expression of its two main receptors: the mineral glucocorticoid receptor (MR) and glucocorticoid receptor (GR) (Joëls et al., 2012), that can trigger both rapid non-genomic effects (Groeneweg et al., 2012; Nahar et al., 2016) and delayed, long-lasting genomic effect (Grbesa and Hakim, 2017; Weikum et al., 2017). The principal glucocorticoid produced during the stress response, cortisol, is also the main inactivator of the HPA. Together with this negative feedback mechanism, multiple forebrain limbic structures cooperate to the PVN regulation, such as the hippocampus (HC) and the medial prefrontal cortex (mPFC), acting on the SNS and HPA regulation. The HC acts on the termination of the HPA axis, through direct inhibition of the PVN (Herman and Mueller, 2006), while the mPFC has a two-edged role, where one sub-region is involved in the termination of the stress response (Akana et al, 2001), another is involved in the initiation of this pathway (Radley et al, 2006).

In the end, the PNS is activated, under the control of descending preganglionic neurons in the dorsal motor nucleus of the vagus (DMV), medullary nucleus ambiguous (NAmb) and sacral parasympathetic nucleus, in order to facilitate return to a resting state by reducing the heart rate,

slowing the breathing, reducing the blood flow to muscles and constricting the pupils (Jones and Yang, 1986), through the release of acetylcholine. All these actions have the final purpose to act against the SNS activation. However, in abnormal conditions in which the stress response persists, an increase of peripheral levels of catecholamine and a decrease in the levels of acetylcholine occur (Chrousos and Gold, 1992). In these cases, the SNS continues to be activated without the normal counteraction of the PNS, generating a chronic stress response.

It is important to remember that the stress response can be anticipatory, if the stressor is expected and the brain can reference to prior experience, or reflexive, which requires immediate response by the system. In the first case, there is often the recruitment of forebrain and limbic circuit that projects indirectly to the PVN, while in the second, the activation of the hindbrain pathways projecting directly to the PVN is present (Ulrich-Lay and Herman, 2009).

2. Pathological effects of single stress exposure: PTSD

The fact that after being exposed to a single traumatic event people could have psychological consequences was evident at the beginning of XX century (Stephard, 2000), but the term post-traumatic stress disorder (PTSD) appeared in the American Diagnostic and Statistical Manual of Mental Disorders (DSM)-III only in the 1980s, referring to the mental health problems evident in soldiers returning from Vietnam's War.

PTSD is diagnosed when a person who has experienced or witnessed a major traumatic event, such as exposure to actual or threatened death, serious injury, and sexual violence, presents: at least one re-experiencing symptoms (e.g. flashbacks, dreams about the event, exaggerated reaction to cues of the event); active avoidance of reminders; at least two “alterations in cognitions and mood” symptoms, for example, pervasive negative emotion, diminished interest, detachment feeling, etc..; and at least two arousal symptoms, namely irritability, angry outburst, self-destructive behaviour, hypervigilance, problems with concentration and sleep disturbance. The combination of symptoms has to be manifested for more than one month after trauma exposure (American Psychiatric Association, 2013). Together with this definition described in the DSM 5, we have the one reported in the World Health Organization’s International Classification of Diseases (ICD), used by many non-American countries. These two definitions differ mostly in the focus of the criteria, with the ICD more focused on the fear circuitry, while DSM gives more importance to emotional reactions to the trauma, causing a slight discrepancy in the diagnosis of patients.

The risk factors for this disorder are shared with many others psychiatric conditions: female gender (2:1 female to male ratio), low social background, prior mental disorder, familiarity with mental disorders, and traumatic childhood (Brewin et al., 2000).

The prevalence of PTSD varies across countries and communities. It occurs in 5-10% of the population, varying from the civilian population and military ones, where the risk is more significant. For example, 10 years after the Vietnam war the rates of PTSD went up to 28% in those who had experienced combat exposure, while 40 years after the end of the war, 11% of Vietnam veterans were still experiencing PTSD symptoms (Dohrenwend et al., 2006). Furthermore, PTSD shows high comorbidity with other neuropsychiatric disorders, such as depression, anxiety and substance abuse, a fact that hinders the progression in the understanding of this pathology. In an attempt to understand better the data, many studies focus on elucidating if PTSD starts the modifications that lead to the other condition, or is the other way around.
In the next session, the currently available evidence on human patients and our understanding of the pathophysiology of the disease will be shown.

2.1 Pathogenesis

The Post–Traumatic stress is a disorder that involves many aspects of the human body, in particular of the human brain.
The first pathway supposed to change in PTSD was the one involved in the stress response, in particular, it was thought that high levels of stress hormones could be present. Contrary to what expected, cortisol levels were lower in patients, with respect to the general population (Zodaldz and Diamond, 2013). Further study on this topic confirmed the presence of an exaggerated negative feedback sensitivity of the HPA axis before and briefly after the trauma exposure in people who developed PTSD (Van Zuiden et al, 2011; Galatzer-Levy et al, 2014). This reduction in glucocorticoid signalling sustains the hypothesis that the consolidation of the traumatic memories lays in the unopposed activation of the SAM (Yehuda, 2002). On the other hand, as postulated, catecholamine levels are higher in patients (Yehuda, 2002).
The next step in trying to elucidate the mechanisms underlying the PTSD was in studying the functionality of the brain area involved in fear processing, memory formation and stress response. At first, research focused on the hippocampus, particularly because there was evidence that this area was smaller in patients (Bremner et al, 1997). Later on, this correlation has been found out as predictive of PTSD (van Rooji et al, 2015). This, together with the absence of recurrent changes in hippocampal functionality, led to switch the attention to other brain areas, in particular amygdala and mPFC. Unfortunately, it was not possible to determine common features, because of the variety of the pathology manifestations. For example, the existence of emotional undermodulation and overmodulation (Fig. I.2) (Lanius et al, 2010) reflects different regulations of some brain areas. In the first case, there is a decreased activity of mPFC, that results in increased activation of the autonomic responsivity guided by the

amygdala, as shown during re-experiencing, fear, anger, guilt and shame. In contrast, the second scenario is characterized by heightened inhibition of amygdala, related to the increased activity of the mPFC, resulting in a more detached behaviour (Lanius et al, 2010). In either case, the alteration of the fronto-limbic activity results in the struggling of the modulation of distress response, as a typical treat of the pathology.

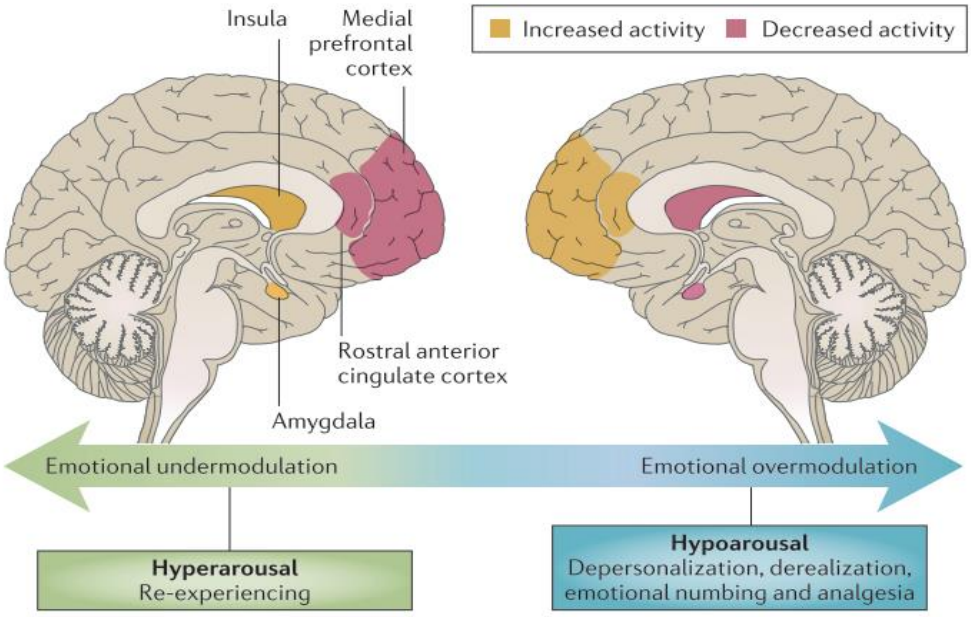

Fig. I.2. **Contrasting modulation in PTSD patients**. from Yehuda er al (2015). In PTSD patients two contrasting emotion dysregulation were described. Emotional overmodulation or hypoarousal (right) is characterised by increased control of emotional states, depending on the increased activity of the mPFC that inhibits the amygdala. On the other hand, in the emotional undermodulation or hyperarousal (left) state, there is less control on the emotional response, indeed the mPFC has a decreased regulatory activity onto the amygdala.

In an attempt to better understand the neurochemistry of the pathology, many studies involved the use of PET tracers for imaging. This line of research has been deeply impinged by the lack of good tracers for many interesting pathways. Lower levels of γ-*aminobutyric acid* $(GABA)_A$ receptor in combat veterans with PTSD has been described, with respect to healthy ones (Geuze et al, 2008). The number of endocannabinoid receptors in the brain, together with anandamide and cortisol concentrations in the blood could classify PTSD patients (Neumeister et al, 2013).

2.2 Treatments and novel strategies

Because of the complexity of this pathology, the elite treatment for PTSD is psychotherapy. Up today, regardless of the increasing understanding of the pathophysiology, psychological therapy, trauma-focused or not, represents the first-line treatment. In spite of the good results of this therapy, there are many limitations. First of all, not all health care systems provide psychotherapy as a treatment; secondly, the most efficient approach, the trauma-focused one, based on guiding the patient in re-experiencing the trauma in a safe context, has a high rate of dropping out (Schottenbauer et al, 2008); and lastly, the type of psychological approaches, the treatment duration and efficacy strongly depend on the causative trauma and the personal history of the patients. Despite these limitations, the pharmacological alternatives are quite limited. There are only two FDA approved and recommended drugs for PTSD treatment, sertraline and paroxetine, which are two selective serotonin reuptake inhibitors (SSRIs), firstly tried due to the high comorbidity with depression. Many medications have been evaluated based on existing studies of PTSD biology, with poor results. Among them, the most promising alternatives to SSRIs, emerged from a small trial using mifepristone, a glucocorticoid receptor antagonist (Golier et al, 2012), and several others using cortisol treatment (Aerni et al, 2004; Suris et al, 2010), but they need to be tested on a larger scale.

In recent years, new potential frontiers have been explored, such as the use of transcranial magnetic stimulation, deep brain stimulation and new neurofeedback (Novakovic et al, 2011; Karsen et al, 2014). For what concern the pharmacology approach, novel compounds have been proposed that could affect the endocannabinoid systems.

Particularly promising is the use of ketamine, a noncompetitive antagonist of N-methyl-d-aspartate (NMDA) receptors that affects learning and memory. Accumulating evidence for the role of glutamate in the pathophysiology of PTSD suggests a potential benefit for novel pharmacotherapeutic interventions for this disorder (Riaza Bermudo-Soriano et al, 2012). Moreover, intravenous ketamine administration has been used as an effective, rapidly acting intervention for patients with treatment-resistant depression, when administered at sub-anaesthetic doses of 0.5 mg/kg (Zarate et al, 2006; Mathew et al, 2012; Murrough et al, 2013). The trials carried out on PTSD with this drug give some contrasting results, and there are some concerns about the sympathomimetic effects and the acute psychological adverse effects, such as perceptual disturbance, dissociative symptoms, and short-term cognitive impairment (Krystal et al, 1994; Duncan et al, 2001), present after ketamine administration.

2.3 Models of pathology

Due to the high correlation between stress and neuropsychiatric disorders, many stress protocols on animal models have been established, even though the intrinsic complexity and variety of the psychopathology manifestations in humans hindered the possibility to relate a particular model to a single disorder. For this reason, the animal models address the need to elucidate the biological and molecular mechanisms of these disorders and/or to test the efficacy of a drug or a new treatment, and not the complete representation of every single manifestation of the human disorder. For what concerns PTSD models (Tab. I.1), some requirements have been established to evaluate the translational value: (1) the trauma must be relatively severe, (2) short duration of the protocol should be sufficient to provoke PTSD-like symptoms, (3) the intensity of the trauma should predict the severity of outcome, and (4) significant interindividual variability should be observed in outcomes (Siegmund and Wotjak, 2006; Flandreau and Toth, 2018). There are two main modalities for provoking a stress response in animal models: physical and social/psychological stressor exposure. Of note, a psychological challenge is present in many protocols of these two categories.

The physical stress protocols in use are primarily four:

a- Restrain/immobilization stress, where the animal is placed in a chamber with little to no movement availability.

b- Underwater holding, usually used with rats, where the rodent is forced to swim for 40 s, followed by a 20 s forced submersion (Richter-Levin, 1998)

c- Single prolonged stress, where animals are exposed to three different types of stressors, to induce psychological, physiological and endocrine challenges (e.g. restrain stress, forced swim and ether anaesthesia).

d- Electric shock, where rodents are exposed to a single uncontrollable and unpredictable foot shock (Bali and Jaggi, 2015). This represents the most common method of stress exposure due to the high reliability of amperage of shocks delivery and control, and the high reproducibility of context and environment. There are many different protocols for this stressful event, that mainly differ in the amperage of the electric shocks, in particular, higher amperage is known to induce PTSD-like symptoms, while lower intensity is used to study the fear response.

The social stress protocols are of two kinds:

a- Social Defeat Stress (SDS), used usually in mice and rats. It is the only stress that overcomes the first paradigm. It consists, in fact, of physical short exposure to an aggressive animal, followed by prolonged sensory exposure to the same animal, repeated for at least 5 days, using different aggressors. Some laboratories established a witnessed social defeat stress, where the animal doesn't face any physical aggression. This type of protocol usually lasts for 10 days (Warren et al, 2013). In the effort of accommodating all the requests for a PTSD protocol, a modified version of SDS has been developed. In this, the animal is partially restrained and put in contact indirectly with an aggressive rodent for 6 hours, during this time experimenters randomly allowed a few one-minute direct exposures between the two animals (Hammamieh et al, 2012).

b- Predator Stress, where rodents are exposed to their natural predators or their odour. In the first case, the predator has to be well fed and accustomed to the prey presence, to avoid any physical injuries, while for sensory stimulation either a porous container to avoid direct contact or a wad carrying their odour can be used.

It is hard to choose the best protocol, due to the high variety of results, influenced by the environmental challenges that can be different in each facility, but also due to the small changes introduced by different laboratories, in order to answer to different experimental needs. In the table below, the consensus validation of each stress protocol has been reported.

	Cluster B: intrusive symptoms	Cluster C: avoidance symptoms	Cluster D: negative alterations in mood and cognition		Cluster E: hyperarousal symptoms					Criterion F: lasting symptoms
	"Signs of" intrusive memories	Increased avoidance	Anhedonia/ decreased activity	Cognitive dysfunctions	Irritability/ aggression	Hyper-vigilance	Exaggerated startle	Concentration problems	Sleep disturbance	Symptoms present
Restraint/ immobilization stress	Freezing [3]	Plus-maze [3, 4]		Spatial memory [3]		Marble burying [5]			Increased REM [6]	>10 Days
Underwater trauma	Freezing [9]	Plus-maze [11]		Spatial memory [9]			Enhanced reactivity [10]			>Month
Single prolonged stress	Freezing [15, 17]	Plus-maze [8, 13]	Forced swim [18]	Disrupted extinction learning [14]			Enhanced reactivity [119]		Increased REM [20]	>2 Weeks
Electric shock	Freezing, fear generalization [29, 30, 31, 33]	Plus maze, social interaction, novelty- and social avoidance [29, 31, 32, 34]	Forced swim [29]			Object burying, hyper-locomotion [32, 34]	Enhanced reactivity, fear-potentiated startle [35, 120, 121]		Sleep fragmentation [34]	>Month
Social defeat	Fear generalization [122]	Plus maze, social avoidance [79, 75]	Self-stimulation and sucrose preference [80, 122]				Enhanced reactivity [78]		Sleep fragmentation	>Month
Predator stress	Freezing [100]	Plus maze [100]		Spatial and working memory [97, 99, 100]			Enhanced reactivity [90, 93]			>Month

Tab. I.1. **Animal models of PTSD alterations**. from Flandreau and Toth (2018). The table provides a summary of PTSD symptoms reproduced in the previously listed animal models. The symptoms are subdivided into clusters: cluster B reports intrusive symptoms; cluster C, avoidance symptoms; cluster D, negative alterations in mood and cognition; cluster E, hyperarousal symptoms; and the duration of symptoms is reported as criterion F. In the reference section of this thesis, a section dedicated to citations reported in this Table can be found.

3. Stress neurobiological effects

3.1 Structural modification

As illustrated, the stress response is regulated by different areas of the brain. Using animal models of stress, many pieces of information have been collected about the neurobiological mechanisms affected by the stress response. Many studies reported structural modifications in distinct brain areas, after acute or chronic stressor exposure, that mainly involve cellular and synaptic density, and dendritic length and arborization. (Fig. I.3)

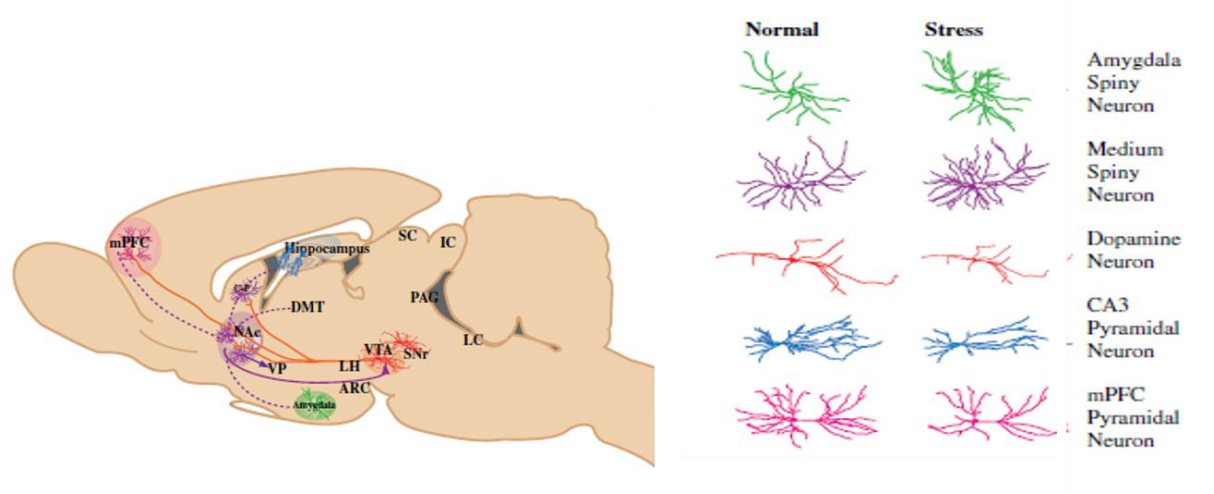

Fig. I.3. **Differential neuronal alteration in the stressed brain**. from Christoffel et al (2011). An example of long-range circuitry of the brain (reward circuit, left). Solid red lines represent dopaminergic projection from VTA; solid purple, the GABAergic afferents from NAc; dotted purple, glutamatergic projections received by the NAc. On the right, a colour-coded representation of stress effects onto specific neuronal types in the different areas (amygdala (green) and NAc(purple) spiny neurons, PFC (pink) and hippocampal CA3 (blue) pyramidal neurons, and VTA dopamine neurons (red)).

In the HC, the first deeply studied area in the field, after chronic stress there is a shrinkage and de-arborization of the apical dendrites in the CA3 area (Christian et al, 2011; Magarinos et al, 1997), while in the CA1 area apical branches are shorter in stressed animals (Brunson et al, 2005; Christian et al, 2011). On the other hand, the stress effect on the synaptic structures in this region is less clear, in particular in the CA3 area, where some studies reported dendritic spine density increase in the apical dendrites of CA3, while others observed a reversible decrease (Sandi et al, 2003; Stewart et al, 2005) or no changes (Magarinos et al, 1996). In the CA1 area, a decrease in spine density was reported (Pawlak et al, 2005), and in the thorny excrescences of the mossy fibres, a reversible retraction was present (Magarinos et al,1997). Similar effects on dendrite length have been reported in the PFC after chronic stress, where a decrease in spine density was also present (Wellman, 2001; Cook and Wellman, 2004; Radley and Morrison, 2005; Goldwater et al,2009) (Fig. I.4, right), even though, after repeated restraint stress, dendritic hypertrophy in interneurons, particularly in Martinotti cells, was noticed (Gilabert-Juan et al, 2013). In this region, Shansky and Morrison (2009) observed a subpopulation of neuron in the infralimbic (IL) area, projecting in the basolateral amygdala (BLA), which seems unaffected by stress. This suggests that the long-range connections of a neuron, rather than its anatomical localization, may be the relevant factors driving morphological changes. Interestingly, in other brain areas stress induces opposite changes.

Indeed, chronic stress causes hypertrophic dendritic arborization and increased spine density in the nucleus accumbens (NAc) (Christofell et al, 2011) (Fig. I.4, left). Similar effects were detected in the BLA (Vyas et al, 2003, 2004, 2006; Mitra et al, 2005), but not in the medial amygdala (MeA) of chronically stressed animals (Bennur et al, 2007), where a decrease in spine density was detected.

The spine plasticity stress effects do not involve just the number of the spine, but also their structures (Fig. I.4). Spines, indeed, can be categorized by their shape in thin, mushroom and stubby. The different types might subserve different functions, as suggested by the prevalence of thin and stubby spines in development, considered as immature plastic structures, while mushroom spines are more stable and stronger (Harris and Kater, 1994; Petrak et al, 2005). For this reason, researchers are now focusing on describing the type, rather than the number, of spines affected by stress. For example, the overall spine loss in the PFC after chronic stress (Radley et al, 2006a) is driven by the loss of mushroom spines, while the number of thin spines is increased (Radley et al, 2008).

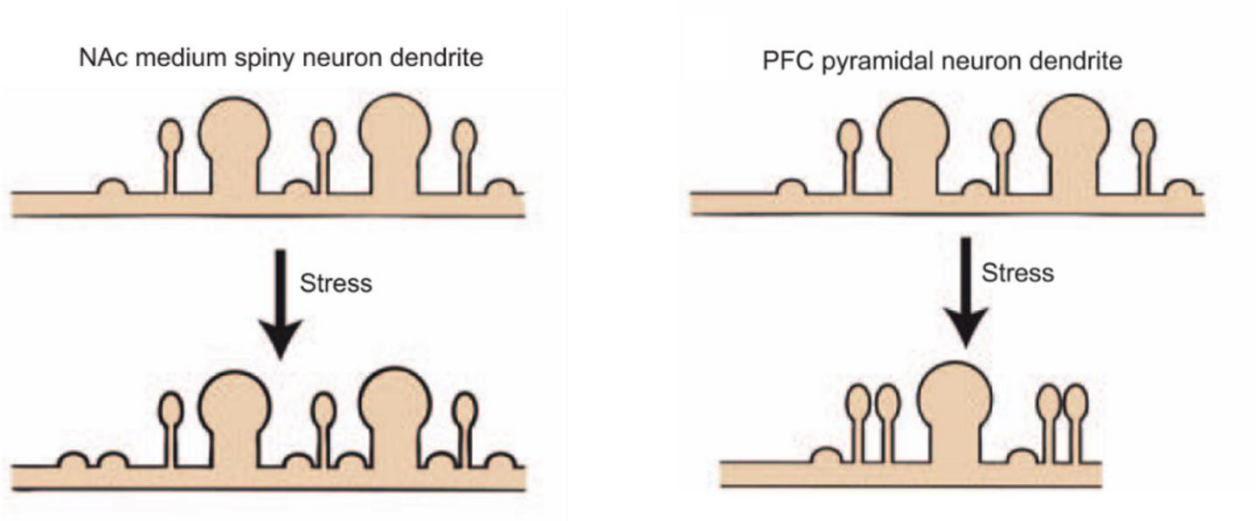

Fig. I.4. **Stress effects on spine plasticity**. adapted from Christoffel et al (2011). Examples of stress impact on the morphology of the neurons. Left, representation increase in the stubby spines of NAc dendrites from control (top) to stressed (bottom) neurons. Right, a scheme of the stress-induced alteration (bottom) on the dendrites of the PFC. In particular, it is represented the dendritic retraction and the differential action on spine density (increase of the thin spines, but decrease of the mushroom ones).

3.2 Stress effects on synaptic transmission

The morphological alterations induced by stress lead to hypothesize the presence of functional modifications involving synaptic transmission. Synaptic transmission may occur with different modalities (Kaeser and Regehr, 2014), mainly distinguished by the presence/absence of action

potential (AP) invasion of the presynaptic terminal (fig.I.5). In AP-independent release, a single central nervous system presynaptic terminal mostly releases a single neurotransmitter vesicle (with a few exceptions), while a single AP invading a terminal may release one or more vesicles (multivesicular release), moreover many terminals may be stimulated nearly synchronously, so that postsynaptic currents may be larger and prolonged. When neurotransmitter release is driven by APs spontaneously generated by afferent neurons in a brain slice preparation, the so-called "spontaneous" postsynaptic currents (sPSCs) are generated (fig.I.5a, centre panel). These currents, depending on the type of neurotransmitter released, can be excitatory (sEPSCs), generated mostly by releasing Glu, or inhibitory (sIPSCs), when GABA or Gly are released. They are generated by activation of ionotropic NMDA (NMDA-R) and 2-amino-3-(5-methyl-3-oxo-1,2-oxazol-4-yl) propanoic acid (AMPA-R) receptors, at Glu synapses, and by $GABA_A$ and Gly receptors activation, at inhibitory synapses. When monitoring the frequency and amplitude of these signals from the cell body of a neuron, information is obtained about the overall activation of the neural circuit that generates the APs in the axonal afferents, mixed with information on the pre- and postsynaptic mechanisms of the involved synapses. As a consequence, changes in sPSCs frequency or amplitude can indicate regulation of the overall neuronal circuitry and/or morphological and functional remodelling at specific synapses, making the interpretation of these changes difficult. A parameter describing the activation of excitatory and inhibitory neurons in a local neuronal network is offered by the E/I, defined as the ratio of the (time) average of the total excitatory synaptic conductance over the average of the total inhibitory synaptic conductance, in a given neuron of the network. The E/I is obtained from recordings of sEPSCs and sIPSCs, and reflects both the amount of network activity, and the relative number of excitatory and inhibitory connections to the neuron and their strength.

In studies focused on putative synaptic remodelling, another type of spontaneous activity is frequently studied, the AP-independent release of synaptic vesicles (Fig. I.5a, left panel). The related current, referred to as "miniature" (or "mini") postsynaptic currents (mPSCs) (Fig. I.5c), can be experimentally isolated using tetrodotoxin (TTX), a peptide blocker of voltage-gated Na^+ currents inhibiting the generation of APs. The production of these currents results from the spontaneous fusion of vesicles with the presynaptic membrane, releasing mostly Glu at excitatory terminals (mEPSCs) or GABA/Gly at inhibitory terminals (mIPSCs). Alterations of mPSCs are the consequences of truly synaptic alterations, such as changes in receptor-dependent modifications, including receptor internalization, structural modification and receptor modulation; changes in the amount of transmitter released; changes in the mechanisms

of spontaneous fusion, or other presynaptic alterations influencing the release probability of the vesicles. Lastly, alterations in mPSC frequency may signal the increase/decrease in the number of functionally active synapses. It is still debated if the mPSCs represent a sort of baseline noise affecting information transfer by AP-dependent release, or rather they carry specific functional information on a different time scale with respect to AP-dependent release, or both. In support of the last hypothesis, many studies have reported the involvement of mPSCs in electrical signalling of neurons (Mathew et al, 2008; Paré et al, 1997; Paré et al, 1998), biochemical signalling involved in synaptic stability and maturation (Turrigiano, 2012; McKinney,1999; Tyler and Pozzo-Miller, 2003; Verhage et al, 2000), local dendritic protein synthesis (Sutton et al, 2004), and control on the postsynaptic responsiveness in synaptic plasticity (Aoto et al, 2008; Frank et al,2006; Lee et al, 2000; Sutton et al, 2006). These studies have also shown specific effects of postsynaptic excitatory receptor blockade or inhibition of neurotransmitter release under resting conditions, which could not be achieved by inhibition of action potential-mediated signalling alone.

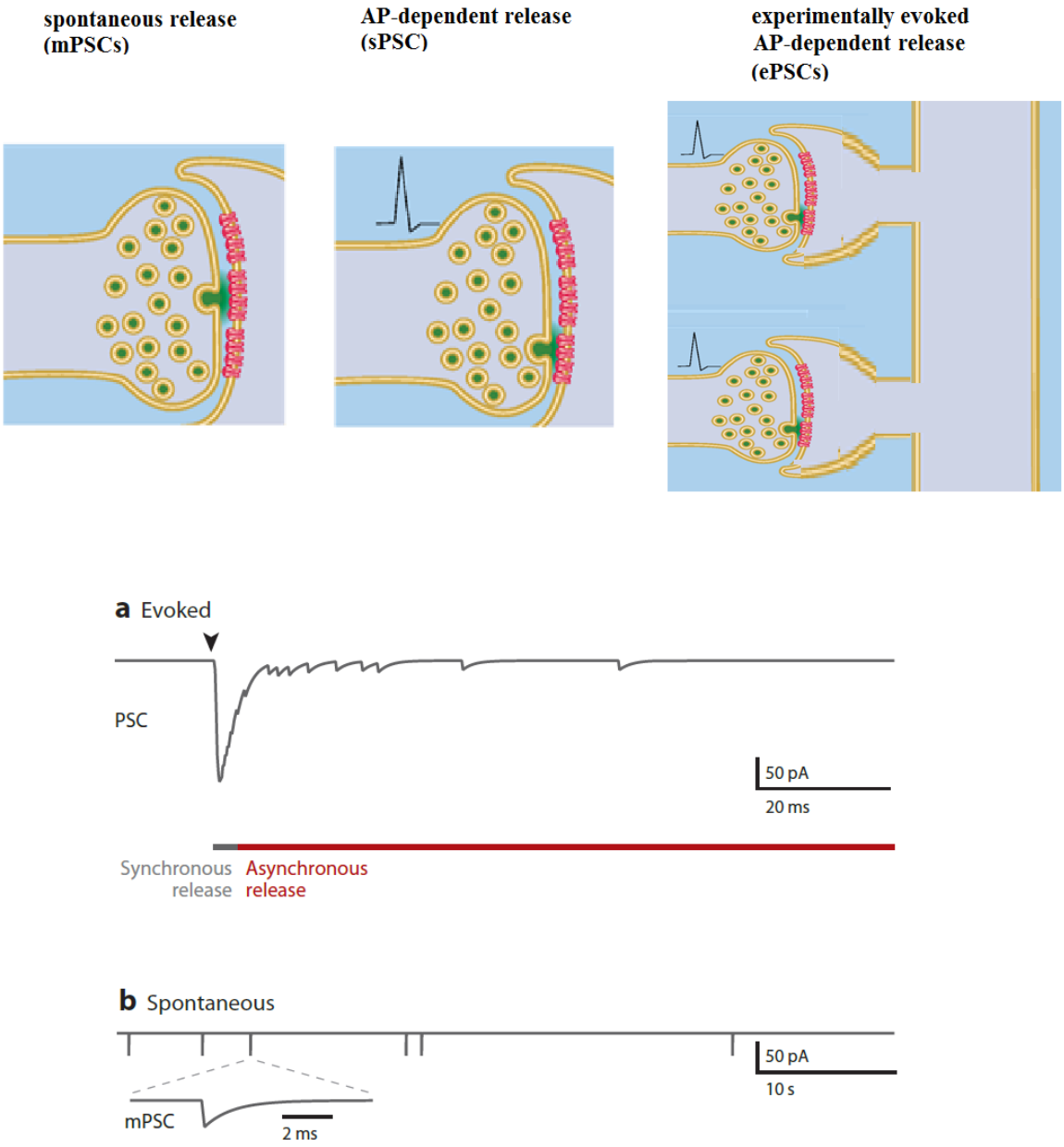

Fig. I.5 **Different types of transmitter release modalities and types of synaptic current recordings**. Adapted from Kaeser and Regehr (2014). Neurotransmitter release can occur through different mechanisms. According to release modality and experimental setting, different types of synaptic currents are recorded. (**a**) *Left*: spontaneous vesicle release in the absence of APs, giving rise to miniature currents (mPSCs). *Centre*: AP-triggered release (due to spontaneously network-generated AP) giving rise to sPSCs. If a single vesicle is released in a single terminal, the size of the sPSC can be similar to that of mPSCs. On the contrary, if multiple terminals are stimulated or multiple vesicles are released from a single terminal (multivesicular release; not depicted in the cartoon), larger and prolonged sPSCs may occur. *Right*: the experimentally provided electrical stimulation of afferent axons nearly simultaneously stimulates release from several terminals giving rise to evoked PSCs (ePSCs). Adapted from Kavalali et al (2011). (**b**) Model excitatory evoked synaptic current (eEPSC). A period of synchronous release, followed by a period of asynchronous release are highlighted. (**c**) Excitatory minis (mEPSCs).

The stress response generally seems to enhance glutamate release in many different areas of the brain, an expected action considering that glucocorticosteroids diurnal peak has the same effect (Lowy et al, 1995; Venero and Borrell, 1999). In the CA1 area, after application of corticosterone, an enhancement of mEPSC frequency was seen, suggesting an increase in Glu release probability (Karst et al, 2005), while chronic stress protocols induced an increase in Glu levels measured by microdialysis in the CA3 area (Yamamoto and Reagan, 2006). In this area, corticosteroid increase Schaffer collateral transmission both in the glutamatergic projection and in the feedforward and feedback GABAergic projections (Joëls and de Kloet, 1993; Birnstiel et al, 1995). Indeed, acute and chronic stress may also act directly on inhibitory transmission, for example, reducing mIPSCs frequency in the PVN, while the GABAergic interneurons surrounding this region increase their burst firing activity if exposed to stress hormones (Shin et al, 2011). Moreover, stress through norepinephrine can modulate the activity of BLA interneurons. In rat BLA, footshock stress facilitates GABA release (Galvez et al, 1996), and, in parallel, norepinephrine induces GABA release, as seen by increases of sIPSCs and mIPSCs frequencies. On the contrary, tail-shock stress severely compromised the release of GABA in the BLA, potentially contributing to the hyperexcitability of BLA output neuron mechanisms (Braga et al, 2004).

The plasticity of synapses (short-term and long-term synaptic plasticity processes: STP, LTP, LTD; Citri and Malenka, 2008) in different brain areas is known to be affected by stress. Severe stressful events impair LTP (Foy et al, 1987; Shors et al, 1989,1990a,b; Shors and Thompson, 1992; Kim et al, 1996; Garcia et al, 1997), while exposure to stressors can also facilitate LTD induction in the CA1 area (Kim et al, 1996; Xu et al, 1997, 1998; Manahan-Vaughan and Braunewell, 1999; Manahan Vaughan, 2000). LTP in the CA3 evoked by stimulation of commissural/associational input to CA3 is reduced, but this is not the case for the mossy fibre inputs (Pavlides et al, 2002), suggesting an effect on NMDA functionality (Lüscher and Malenka, 2012), since the commissural/associational synaptic potentiation is NMDA receptor-dependent, while mossy fibre LTP is NMDA receptor-independent (Joëls et al, 2005).
In vivo studies demonstrated that after acute stress LTD facilitation was present in the dentate gyrus (Pavlides and McEwen, 1999), while chronic stress in vitro (Alfarez et al, 2003) and in vivo (Pavlides et al,2002) studies reported a hampering of synaptic efficacy.

Acute restraint stress (20 min), mild footshock stress and initial exposure to nicotine all facilitate induction of LTP in vitro (Sarabdjitsingh et al, 2012). However, a study in vivo found that elevated-platform stress enhances baseline electrophysiological responses in BLA and inhibits LTP induction, whereas administration of corticosterone does not affect LTP (Kavushansky et al, 2006). These divergences could relate to the loss of some regulatory circuit in the in vitro preparation.

Greatly affected by stress is also the synaptic plasticity involving inter-area circuit, in particular, LTP in amygdala- PFC and HC- PFC are inhibited by acute stress (Maroun and Ritcher-Levin,2003; Rocher et al, 2004), while chronic stress inhibits LTP in the HC- and thalamus- to-PFC pathway (Quan et al, 2011; Cerqueira et al,2007).

Stress hormones are also able to modulate the expression, trafficking, and channel properties of receptors. For example, $GABA_AR$ subunit expression seems to be differentially modulated in different areas by stress hormones. $GABA_AR$ β1 and β2 subunits expression are decreased in the stressed PVN expression (Verkuyl et al,2004), while in the hippocampus these are increased (Cullinan and Wolfe,2000).

After chronic stress, the HC seems to undergo a process of receptors rearrangement. The CA3 NMDA response is characterized by an increase in the decay and amplitude of evoked EPSCs (Karst and Joëls, 2003). Moreover, chronic unpredictable stress increases NMDA receptor protein levels in the ventral hippocampus (VH) (Calabrese et al.,2012), where an increase in the transcription level of AMPA-R GluA1 subunits (Pacheco et al, 2017) is also present. A selective increase in the AMPA-R mediated transmission was seen specifically in CA1 neurons (Karst and Joels, 2005), but also in other neurons, like the midbrain dopaminergic (Saal et al, 2003) and nucleus accumbens shell (Campioni et al, 2008) neurons. Stress can also modulate the phosphorylation of different sites of the AMPAR. It has been reported that phosphorylation of GluA1 subunit after acute stress is diminished in the Ser831 site in mPFC and dorsal hippocampus (DH), while the phosphorylation of Ser845 is increased in the Amygdala and VH, while Ser880 of GluA2 is downregulated in the amygdala and VH (Caudal et al, 2010), and upregulated in the mPFC (Caudal et al, 2010; Bonini et al, 2016). These three phosphorylation sites are recognized by different kinases that act in different ways depending on the region or even the subregion. The phosphorylation of Ser831 and 845 increases the channel conductance, and insertion in extra-synaptic sites, respectively, suggesting a proneness to LTP. On the contrary, Ser 880 increases the internalization of the AMPARs, diminishing the excitatory transmission.

4 The medial Prefrontal Cortex

4.1 mPFC: a multitasking area

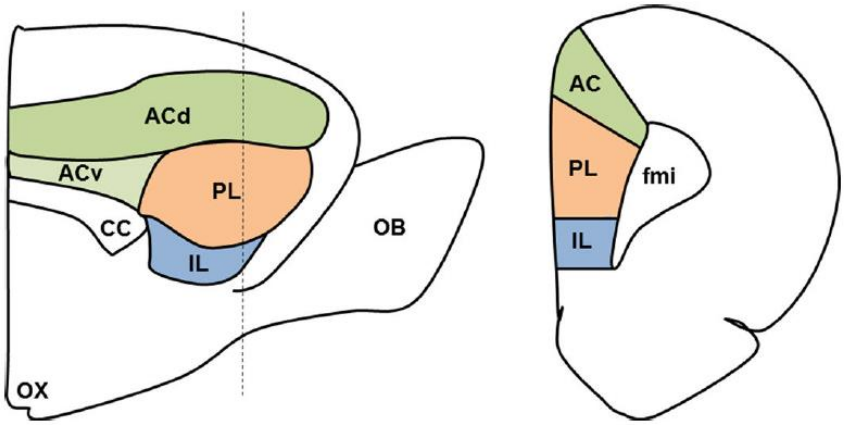

Fig.I. **mPFC in the rat brain**. from McKleeven et al (2015). Coronal (right) and sagittal (left) view of the medial prefrontal cortex (mPFC), showing the different areas: anterior cingulate (AC) implicated with motor behaviour and spatial navigation, prelimbic (PL) involved in the regulation of the HPA and fear consolidation, and infralimbic (IL) implicated in visceral-autonomic responses regulation. In the picture are represented also neighbouring areas: olfactory bulb (OB), forceps minor of the corpus callosum (FMI), corpus callosum (CC), dorsal AC (dAC), ventral AC (vAC), optic chiasm (OX).

The mPFC is a region of the prefrontal cortex area, involved in many different tasks, due to the extensive innervation to and from diverse brain regions. It is divided into two functional subregions: the dorsal and the ventral. The dorsal regions include the anterior cingulate (AC, Fig.I.6), implicated with motor behaviour and spatial navigation (Vertes, 2004; Vogt et al, 2004), and pre-limbic (PL, Fig.I.6) cortex, projecting to many regions involved, for example, in the regulation of the HPA, like the bed nucleus of the stria terminalis (BST), or the consolidation of fear. The ventral region, including the infralimbic (IL, Fig.I.6) cortex, innervates many regions typically involved in the regulation of visceral-autonomic responses. The mPFC plays a critical role in the formation, consolidation and retrieval of remote, recent, or short-term memories, as suggested by the mPFC-HC connection (Fig.I.7). The subgenual area of the mPFC is particularly implicated in forming abstract event representations (Schlichting et al., 2015), while, through inhibition of the amygdala, the mPFC-amygdala connection is involved in anxiety control (Fig.I.7). The mPFC-HC connection is more active when new events overlap with existing knowledge (Zeithamova et al., 2012; Schlichting and Preston, 2016), indicating a role of the mPFC in remote memory recall. The connection with the HC could justify also the role of mPFC in the stabilization of recently acquired memory, as reported by many independent studies where induction of mPFC lesions after training sessions to different learning tasks severely impair the memory (e.g. Tronel and Sara, 2003; Leon et al, 2010). Moreover, inactivation of the mPFC in rats also impairs recent memory recollection, in

particular in the recall of recently acquired fear-associated memories (Corcoran and Quirk, 2007). The mPFC is not involved solely in the recollection of memory, but also in "short term" memory formation (Seamans et al., 1995). A particular type of "short term" memory is the working memory, which spans intervals shorter than a minute. Working memory is modulated by the mPFC, as reported in studies on rats where this area was damaged, that showed a deficit in the delayed response (e.g., Horst and Laubach, 2009). Both PL and IL are involved in the drug-seeking behaviours which are regulated by the connection of these regions with NAc (Fig.I.7). The dorsal part of the mPFC is connected to the core of NAc, while the ventral part projects to the NAc shell (Berendse et al, 1992). Finally, the mPFC is deeply involved in the regulation of the HPA axis response. The dorsal part seems to be a site for indirect glucocorticoid negative feedback signalling, as demonstrated by the absence of direct connection to the PVN, but a deep association to the BST and many other non-PVN projecting regulatory regions. On the other side, the ventral region may be involved in the stress excitation, due to the heavy innervation to subcortical autonomic sites.

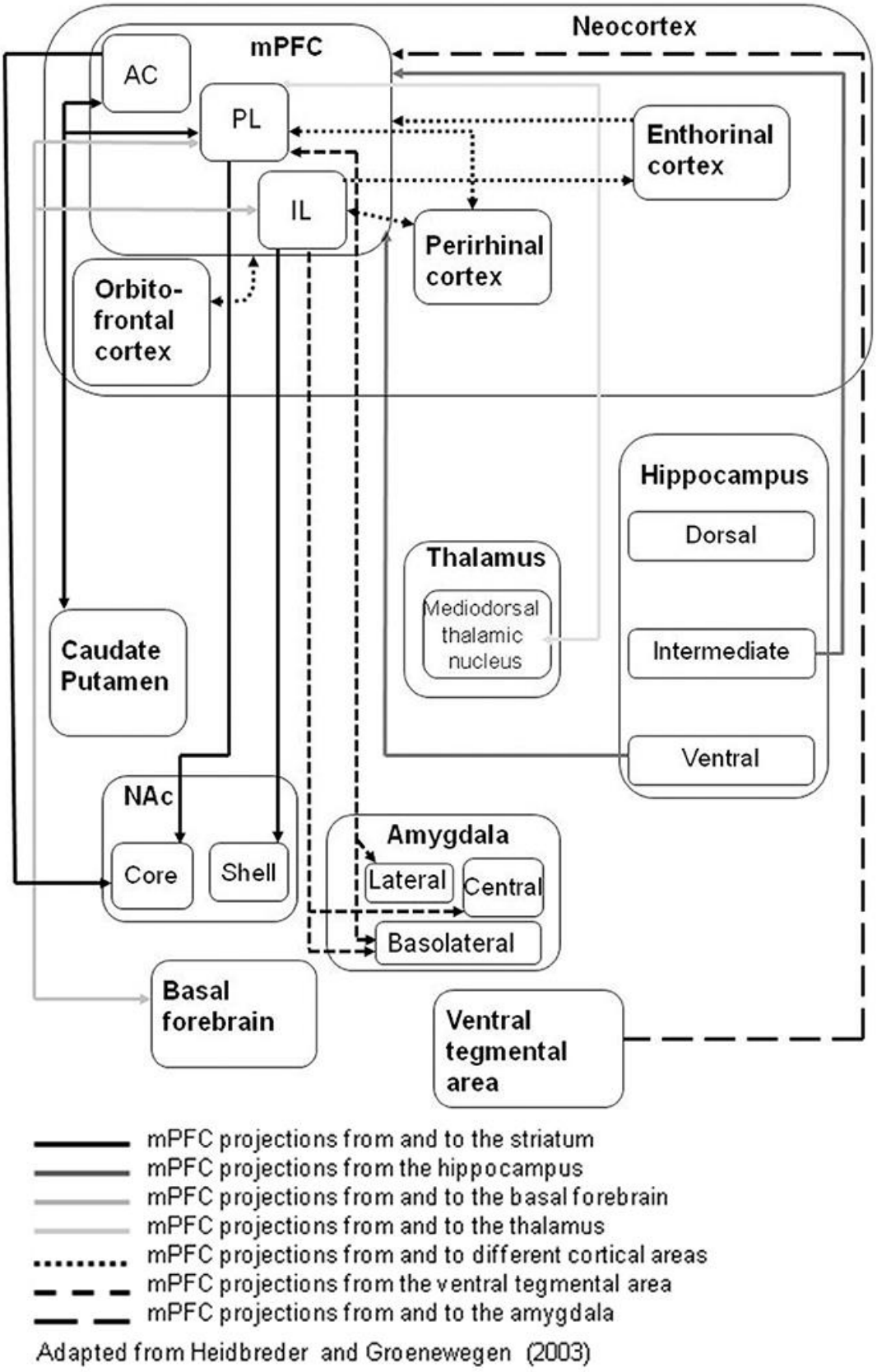

Fig. I.7 **Connections of the rat mPFC areas with key brain regions**. from Heidebreder and Groenewegen (2014).

4.2 Stress effects on mPFC Glu transmission

Because of the multiple functional roles of the mPFC, many studies have focused on the characterisation of stress effects in this area.

In the case of acute stress, using the foot-shock (FS) acute stress protocol in adult rats, an enhancement of Glu release was described, as measured by the increase in the depolarization-evoked Glu release from mPFC/FC synaptosomes (obtained from frontal and prefrontal cortex). A corresponding decrease in the paired-pulse facilitation of evoked release (considered as an indication of an increase in presynaptic release probability; Regehr, 2012) was measured in layer 2-3 pyramidal neurons of the prelimbic mPFC (Musazzi et al, 2010). In the case of juvenile (3-4 weeks old) rats subjected to a milder acute stress protocol (forced swim), an increase in AMPAR- and NMDAR-dependent sEPSCs was reported (Yuen et al, 2011). This was supposed to entrain disinhibition of the area, correlating with results from a study where the acute application of corticosterone induced a decrease in the inhibitory neurotransmission (Hill et al, 2011). In order to verify this inference, a recent study evaluated the E/I ratio in the mPFC after acute stress exposure in adult mice, finding that an increase in this ratio is present only in layer 2-3 of the PL, driven solely by an enhancement in the sEPSCs in principal neurons (Hwa et al, 2018).

In the case of chronic stress, per the morphological changes in the mPFC, described in par. 3.1, a decrease in NMDA- and AMPA- mediated sEPSCs was observed, together with an increase in the rate of degradation of these receptors (Yuen et al, 2012). While this study was conducted on adolescent animals (25-28 days), when the mPFC is still developing, these results were confirmed by an independent work on adult animals (10-12 weeks) to which corticosterone was administered orally, where a decrease in NMDA and AMPA subunits in ventral mPFC was reported (Gourley et al, 2009). Overall, the modifications induced by the stress in the mPFC evolve with time after the first stressor presentation, as suggested by the evidence that after acute stress there may be an enhancement of the excitatory transmission (in adult animals), while chronic stress decreases excitatory transmission (in adolescents).

In addition to stress effects on neurotransmission in the mPFC, many studies investigated the role of the mPFC in the regulation of the stress response. Due to the projection in pre-autonomic nuclei in the brainstem, such as the nucleus of the solitary tract (NTS) (Gabbott et al, 2005; Resstel et al, 2004; Varbene et al,1997), it has been thought that this area could participate in the ANS regulation. Studies focused on the involvement of PL and IL in autonomic response suggested the opposite role of these subregions. While PL is inhibitory for cardiac stress

response (Tavares et al, 2009) and its stimulation increases the parasympathetic activation (Powell et al, 1996), IL has excitatory activity on the tachycardiac stress response (Tavares et al, 2009) and promotes sympathetic activity (Powell et al, 1996). For what concern the involvement of the mPFC in HPA regulation, a coherent function seems to exist, inhibiting the HPA axis, as demonstrated by injecting corticosterone in PL and IL which induced an enhancement of the negative feedback, reducing corticosterone secretion (McKleeven et al, 2013). Interestingly, it has been found that in chronic stress glucocorticoid inhibition is specifically carried out by IL. Even though it is not clear how IL can act on the HPA, given that the mPFC has not direct projection on the PVN, the PL probably exerts this role via glutamatergic innervation of the BST, a region that is connected to the PVN by GABAergic projections (Radley et al, 2009). In general, it appears that the IL has an activating role on the ANS, but a negative role on the HPA, while the PL exerts a negative role on both axes.

4.3 The synaptogenic effect of ketamine at sub-anaesthetic doses

Ketamine is a non-competitive antagonist of NMDA-Rs used as anaesthetic, which also shows rapid and sustained antidepressant activity in treatment-resistant patients when used at low, subanesthetic doses (Duman et al, 2019). The use of ketamine could be beneficial also for the prevention of PTSD (Feder et al, 2020), as a lower risk of developing PTSD was reported in soldiers treated with low doses of ketamine (McGhee et al, 2008). Low-dose ketamine in naïve subjects has a complex action, with an early psychotomimetic effect (1-2 hrs after systemic administration) followed by a rapid antidepressant action (>2 hrs, peaking at 24 hrs) (Duman et al., 2019).

Preclinical and clinical studies demonstrated that chronic stress and depression cause neuronal atrophy and decreased synapse number in the mPFC (Li et al., 2010), as well as hippocampus, that are associated with depressive behaviours in rodent models and symptoms in patients (rev. in McEwen et al., 2015). In contrast, rapid-acting antidepressants, notably ketamine, rapidly increase synapse number and function, and reverse the synaptic deficits caused by chronic stress. Indeed, it was shown that the anti-depressant action involves an increase in the number of dendritic spines of layer 5 (L5) principal neurons in the mPFC, correlated with enhanced excitatory postsynaptic currents both in naïve and chronically stressed animals (Li et al., 2010; Liu et al, 2015). The synaptogenic action of ketamine was preliminarily demonstrated in naïve animals, were ketamine (10mg/kg) increases spine number and synaptic proteins translation in the apical dendrites of layer 5 pyramidal neurons in the PFC, peaking 24 hours after its

administration (Li et al, 2010). This effect may last up to 14 days after ketamine systemic injection (Phoumthipphavong et al., 2016). The increased synapse density induced by ketamine is also present in animals undergoing chronic corticosterone treatment (Moda-Sava et al, 2019) or chronic restraint stress (Ng et al., 2018). Interestingly, in both models, the newly formed spines were usually in correspondence of the ones destroyed by corticosterone treatment or restraint stress.

In parallel to these effects on synaptogenesis, a functional ketamine effect on excitatory synaptic currents in the mPFC was demonstrated. It was shown that, in naïve animals, ketamine induces a robust and long-lasting increase in the frequency and amplitude of sEPSCs induced by 5-HT or hypocretin (orexin) in layer V pyramidal cells in the mPFC, indicating that the newly generated spines are functional (Li et al, 2010; Aguilar-Valles et al., 2018). Moreover, ketamine rapidly reverses the deficit in EPSC responses to 5-HT and hypocretin that is caused by chronic stress (Li et al, 2011).

The mechanisms underlying ketamine action are still debated. In the rodent PFC, the antidepressant action is associated with a fast transient increase of extracellular Glu and dopamine (Moghaddam et al., 1997). It is believed that this effect of ketamine, as well as several other channel blockers (Esketamine), negative allosteric modulators (Ro 25–6981), ketamine stereoisomers and metabolites ((S)-ketamine, (S)-norketamine, 2R,6R)-HNK), and muscarinic receptor antagonists (scopolamine) is obtained via blockade of NMDA receptors on tonic firing GABA interneurons, resulting in decreased interneuron firing and disinhibition of principal neurons, leading to increased glutamate transmission. The burst of glutamate causes activity-dependent release of Brain-derived neurotrophic factor (BDNF), stimulation of tropomyosin-related kinase receptor B (TrkB)-Akt and mammalian target of rapamycin complex 1 (mTORC1) signalling; these pathways lead to rapid induction of synaptic protein synthesis that is required for new synapse formation (Duman et al., 2019). In addition to glutamate, ketamine also rapidly influences levels of other neurotransmitters and there is evidence that some of these systems are required for the antidepressant actions of ketamine. In particular, dopamine could contribute to ketamine-induction of synapse formation and function in the mPFC (Hare et al., 2019). The serotonin system also has a role in the actions of ketamine, as the antidepressant behavioural effects of ketamine are blocked by 5-HT depletion or 5-HT1A receptor antagonists (Fukumoto et al., 2018).

The involvement of specific mPFC subcircuits in the antidepressant action of ketamine has been reported. The study of Liu et al. (2015) demonstrates that in layer 5 (L5) the excitatory sEPCSs evoked by stimulation with serotonin (acting at apical dendrites), or CRF hormone (acting at

basal dendrites), are enhanced by treatment with ketamine; however, the ketamin-induced enhancement of CRF-evoked sEPSCs is only present in the PL area (and not in the IL).

AIM

Various pieces of evidence prove the early effects of the acute foot-shock (FS) stress on glutamatergic neurotransmission in the mPFC of adult male rats, including the increased depolarization-evoked release of glutamate (Glu) in synaptosomes derived from FC/mPFC, the increased amplitude of spontaneous excitatory synaptic currents (sEPSCs) in L2-3 pyramidal neurons (Pyrs) in young adult rats (Musazzi et al, 2010) and the increased density of small, possibly immature excitatory synapses in the L2-3 of prelimbic (PL) area (Nava et al, 2014). Moreover, some functional and morphological alterations of the glutamatergic system were shown to be sustained after exposure to a stressor, such as the persistent increase of Glu release from FC/mPFC synaptosomes (Musazzi et al, 2017) and the apical dendritic retraction in L2-3 mPFC neurons (Nava et al, 2017) 1 day after FS. The latter effect has been reported also in animal models of chronic stress (Cook and Wellman, 2004), suggesting that similar maladaptive changes may occur in the acute reaction to a traumatic event and chronic stress. The **first aim** of this study was to verify, in adult rats, the presence of both early and sustained alterations of excitatory synaptic transmission in L2-3 Pyrs of the PL mPFC, induced by a single session of unescapable FS stress, in order to reveal possible maladaptive mechanisms that could lead to the development of psychopathological conditions.

Ketamine at sub-anaesthetic doses demonstrated therapeutic effect in depressed (Murrough et al, 2012) and PTSD patients (Federer and al, 2014). In animal models, ketamine increased the number of apical dendritic spines of mPFC L5 Pyrs both in naïve and chronically stressed animals, and the frequency and amplitude of excitatory postsynaptic currents (Liu et al, 2015). For this reason, our **second aim** was to verify the action of a sub-anaesthetic ketamine dose (10mg/kg) on the sustained effects of FS stress on synaptic transmission in PL mPFC principal neurons in L2-3 and 5. Given that the morphological and functional effects of sub-anaesthetic ketamine in the mPFC reach their peak 24 hours after drug administration in a chronic stress model (Li et al, 2011), intending to devise a rapid therapeutic intervention after acute stress, we examined the ketamine effect on synaptic transmission 24 hours after exposure to the stressor, with ketamine injection occurring 6 hours after stress.

Our recordings were restricted to regular spiking (RS) Pyrs, identified by their soma shape and electrophysiological characteristics. Focusing at first on L2-3 neurons, we performed whole-cell recordings at -60mV from RS Pyrs, assessing synaptic activity in the presence or absence

of spontaneously occurring action potentials, namely sEPSCs or mEPSCs. The first set of experiments aimed at studying alterations induced 1 hour after FS**.** We then studied the progression of the acute stress-induced alterations by analysing stressed subjects 24 hours after stressor exposure.

Layer 2-3 of the mPFC is the only cortical layer where an alteration of the excitatory/inhibitory conductance ratio (E/I) was reported, 90 minutes after acute psychological stress (Hwa et al, 2019), implying an unbalance of local network activity towards excitation. Therefore, our **third aim** was to test if FS stress would induce a similar E/I alteration. Using a Cs-based internal solution, we simultaneously measured sEPSCs (at -58 mV) and the spontaneous inhibitory currents (sIPSCs; at +3 mV) from each recorded neuron. We examined early (1 hour after FS) and sustained (24 hrs after FS) stress effects on the E/I.

Finally, we focused on the effect of systemic ketamine treatment on glutamatergic inputs to L5 Pyrs in the PL region, which are key targets of ketamine action in chronically stressed models. We present a preliminary study of 4 different experimental groups including ketamine treated or untreated stressed animals, and naïve or ketamine treated unstressed animals.

METHODS

1. Animals

All experimental procedures involving animals were performed in accordance with the European Union Directive 2010/63 and followed guidelines of the Italian Ministry of Health (D.Lgs 2014/26).

We used Sprague-Dawley outbred adult male rats, 9-13 weeks of age. The animals were housed in plastic cages, three rats per cage in a room maintained at a constant temperature of 22°C and 12-h light-dark circle (lights on from 7am to 7pm) and provided with environmental enrichment. Food and water were dispensed ad libitum. Animals used to study the early effects of acute stress on synaptic transmission were randomly separated into two groups: FS1h, animal that underwent the stress protocol described later and sacrificed 1 hour after the start of the stress, and their relative control group (CTR 1h), which were naïve animals (fig. M.1).

For experiments dedicated to the investigation of late effects of stress, rats were separated into four groups: i) FS24h (animals that underwent the stress protocol and a saline injection 6 hours later), ii) FSKet (animals that underwent the stress protocol and a ketamine injection (10mg/kg) 6 hours later); iii) CTR24h (animals that received only a saline injection), and iv) CTRKeta (animals that received only a ketamine 10mg/kg injection); animals in the latter two groups were sacrificed 18 hrs after injection (fig. M.1).

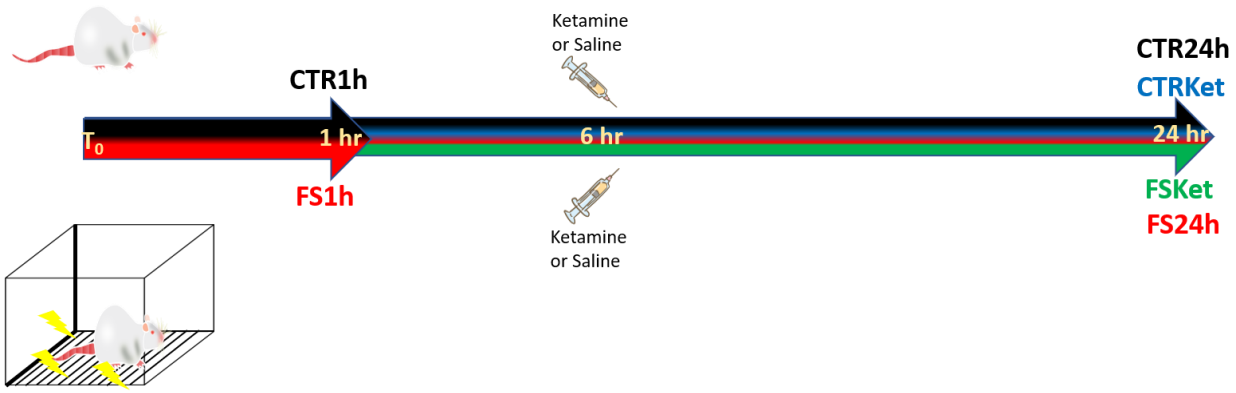

Fig. M.1. **Experimental groups**. Scheme of the protocols used to select animals belonging to different groups. The protocols are colour-coded and each arrow tip corresponds to the time of the sacrifice. In red, animals sacrificed 1 hour after FS (FS1h); in black, the respective controls (naïve animals; CTR1h). In dark grey and blue, animals that received saline (CTR24h) or ketamine (10mg/kg) (CTRKet) injection, respectively. In purple and green, animals that received the foot-shock and were injected with saline (FS24h) or ketamine (10mg/kg; green) 6 hrs later.

2. Acute Stress Protocol

2.a) Foot-shock apparatus description

- To perform the foot-shock stress treatment, a conditioning chamber (Shuttle Box LE916, PanLab) was used, provided with a frontal door allowing easy access inside the box. Walls were in plexiglass and all but two covered with black cardboard to allow constant monitoring during the test; the metallic grid floor was connected to an external power supply that switched on and off under computer control (the "shocker"); no lever or signal light was present in the chamber.
- The shocker (LE100_26, PanLab; also called scrambler) generates rectangular current pulses, switching on consecutively over 6 bars of the grid floor. Current was isolated with respect to ground, as a basic safety precaution to avoid electrical interference with other equipment. The output current depended entirely on the value selected by the user and not the resistance of the animal or the number of bars it was touching when it received the electric shock.

2.b) Stress protocol

Every stressed rat was transported into the dimly lighted experimental room, weighed, and placed in the conditioning chamber by holding its abdomen and thorax. Taking into account the hormone circadian cycle, we performed all the stress sessions in the late morning. A 40-minute session of 0.8 mA inescapable foot-shock was delivered by the shocker, controlled by a computer program custom made at the Department of Pharmacological and Biomolecular Sciences of the University of Milan. The session consists of single shocks ranging from 2 to 8 seconds, for a cumulative shock duration of 20 minutes randomly interspersed in the total time of the session. At the end of this procedure, animals were picked up by the tail and single caged. The rat placed in the box waited 1 minute before beginning of the FS procedure, to allow adaptation to the new environment, and 1 minute after its end.

3. Pharmacological treatments

Six hours after the foot-shock protocol, animals in the FS24h and FSKet groups were intraperitoneally injected with saline or ketamine (10 mg/Kg), respectively. Animals used as controls (CTR24h and CTRKet) were weighted and received an intraperitoneal injection of saline or ketamine (10mg/Kg) at the same time of the day as the previous two groups.

4. Slice preparation

At the time of the sacrifice, animals were gently handled and put in an empty cage for transferring to the surgery room to be sacrificed by decapitation, which occurred without sedating the animal.

After the decapitation, the head was put in a beaker containing an icy solution (Slicing Solution) and drained manually thanks to friction with the beaker surface. In order to slow down the warming of the solution, a part of the oxygenated Slicing Solution was slushed using an ice-cream maker and placed in the beakers.

When drained, the head was placed in a plate containing iced Slicing Solution and the skin was cut to gain access to the skull. Using a pair of scissors, the skull was cut open into two pieces, following the midline from the brain stem to the olfactory bulb (more or less at the base of the nasal septum, at the same level of the ocular orbs), paying attention not to cut the underlying brain tissue by keeping the scissors edge up-verse. After the cut, the scissors were used as a lever to remove the bones, in order to gain access to the brain and to gently remove it and put it in a beaker with oxygenated icy Slicing Solution.

The brain was then cut in two with a coronal cut, at the point corresponding roughly to -5mm from bregma and glued to the magnetic part of the specimen disc, that was then placed inside the buffer tray of the Vibroslicer (Leica VT1000), filled with icy bubbled Slicing Solution. Cortical slices from bregma mm 4.2 to 2.7 (fig. M.2A), containing the mPFC, with a thickness of 300 µm, were recovered in an interface-style chamber (fig.M.2B) containing the Slicing Solution, immersed in a thermostatic bath prewarmed at 34°C. After 30 minutes, the bath heating was switched-off and slices allowed to cool down at room temperature until use, occurring 1-6 h from the end of the slice cutting. In the interface chamber, slices were placed on a piece of lens paper laying on a nylon mesh, and the fluid level was adjusted to the upper surface of the slice, thus stabilizing the tissue by surface tension. The chamber was covered, to allow the formation of a humid and oxygen-saturated environment (fig.M.2B). The choice of this maintenance style was dictated by the necessity to ameliorate the survival rate of the adult brain slices, assured by better oxygenation of the tissue in this maintenance configuration.

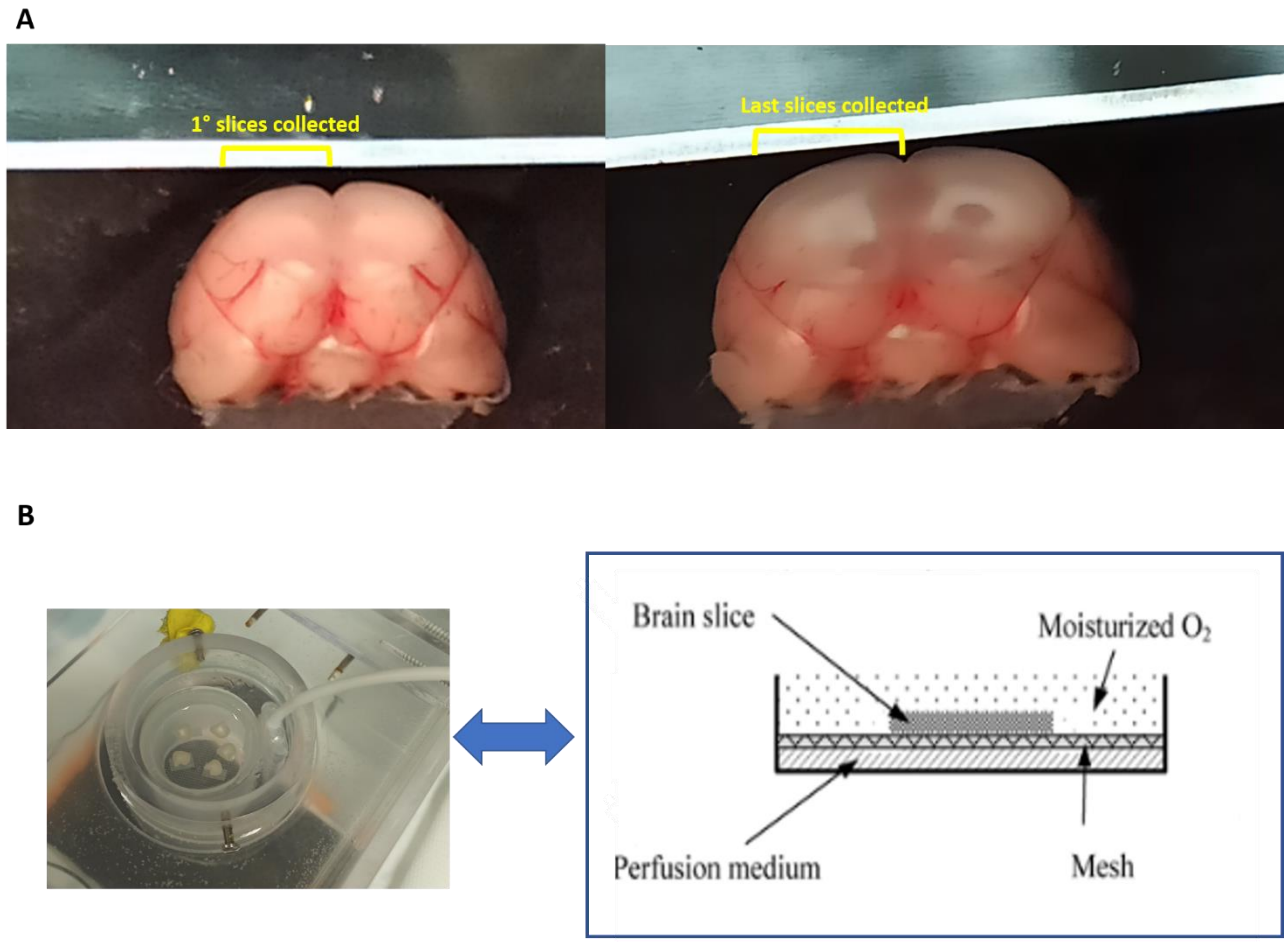

Fig. M.2. **mPFC slices collection and maintenance**. **(A)** Collection of slices started when the forceps minor of the corpus callosum (f.m.i.) was visible (left) and finished when it started to open (right). **(B)** Maintenance chamber where the slices were kept from the end of the cut till the start of the recording. On the right a scheme of the interface chamber used for maintenance.

5. Measurement of Corticosterone levels

After decapitation, blood was collected from the trunk of the animal in a 50 ml tube, that was placed in ice till the time of the processing. Blood serum was separated by two centrifugation steps, the first occurring in the 50ml tube (4500g x 5'); for the second, 1ml of supernatant was collected in a 1ml tube and centrifugated at 10000g x 10'. 500µl of plasma were placed in an empty tube and stored at – 80°C. Measurement of serum corticosterone (CORT) levels was performed through a commercial kit (Corticosterone ELISA kit, ADI-900-097, Enzo Life-Science), using the protocol for small volumes.

The optical density of the ELISA plate was detected as the ratio between 415nm (emission wavelength) and 595nm (correction wavelength), using an iMark Microplate Absorbance

Reader (Bio-Rad). A calibration curve was obtained by plotting the logarithmic value of the per cent bound versus the logarithm of the concentration of each standard. Samples concentration was attained using the interpolation with a sigmoidal dose-response curve, calculated using GraphPad Prism software (GraphPad Software, LLC). The mean CORT concentration for CTR, FS1h and FS24h were compared by 1-way ANOVA test, after confirming that the values for each group were normally distributed.

6. Electrophysiological Apparatus

After recovering at room temperature for at least 1 hr, slices were transferred for recordings to a submerged chamber and perfused with a solution simulating cerebrospinal fluid (Artificial Cerebrospinal Fluid Solution, ACSF, see below), bubbled with carbogen (5% CO_2, 95% O_2), maintained at constant temperature using a 2-channel temperature controller (TC02, MultiChannel Systems, Reutlingen, Germany) separately heating the inflowing solution into the perfusion cannula (PH01, MultiChannel Systems, Reutlingen, Germany) and the chamber holding plate (fig. M.3). The settings of the temperature controller were chosen so as to obtain in the bath a temperature of 33±1°C, that was periodically checked with a thermocouple thermometer.

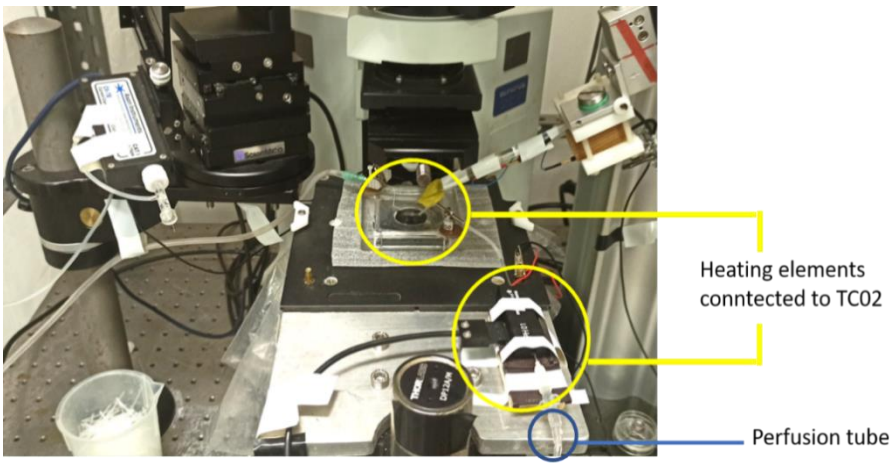

Fig. M.3. **Temperature control of the electrophysiological apparatus.** The perfused solution is heated up by the heater right before entering the recording chamber. Under this chamber, a second heater preserves the temperature during the recording.

Slices were visualized using an upright microscope (Olympus BX51WI) equipped with a 40X, 0.9 NA water immersion objective (LumplFl40XW, Olympus) and differential interference contrast (DIC) optics, using Infrared illumination (IR; excitation filter 750nm) and an IR CCD

camera (CV-A50IR, JAI).

Saline-containing borosilicate glass capillaries (patch-clamp pipettes) mounted on a micromanipulator (S-PS-7000C, Scientifica Ltd, UK) were manually driven to the target cell under visual control and were connected through a silver wire to a Multiclamp 700B amplifier (Molecular Devices, San José, California) for current and voltage recordings. Current and voltage were digitized with a Digidata 1440A Interface and sampled with the Clampex acquisition software (Molecular Devices, San José, California). The corner frequency for analogue filtering was 10 kHz, and the sampling frequency was 50 kHz.

The depth of the recorded cells below the slice surface was registered using the LinLab software (Scientifica Ltd, UK), measuring the vertical displacement of the micromanipulator.

7. Identification of Cortical Layers

The Prelimbic (PL) region of the mPFC was visually identified as the midline-aligned cortical region present from Bregma 4.2 mm to 2.7 mm, as outlined in The Rat Brain Atlas (Paxinos and Watson, 2009) (fig.M.4). The target layer was visualized directly in the microscope, in particular, L2 is the thinnest layer of the prefrontal cortex containing only a few "rows" of pyramidal neurons, while L3 is about 2–3 times wider than L2 (Van Eden and Uylings 1985; Gabbott et al. 1997, 2005). L3 is bordered directly by L5, where neurons are characterised by a larger soma with respect to L3. The border between L5 and L6 is expected to be approximately half of the distance between the border of L3–L5 and the border between L6 and the white matter. L6 neurons were distinguished by oblique, horizontally orientated or inverted main dendrite, in contrast to L5 pyramidal neurons that all present ascending apical dendrites pointing towards the pia (as described by Van Aerde & Feldmeyer, 2015).

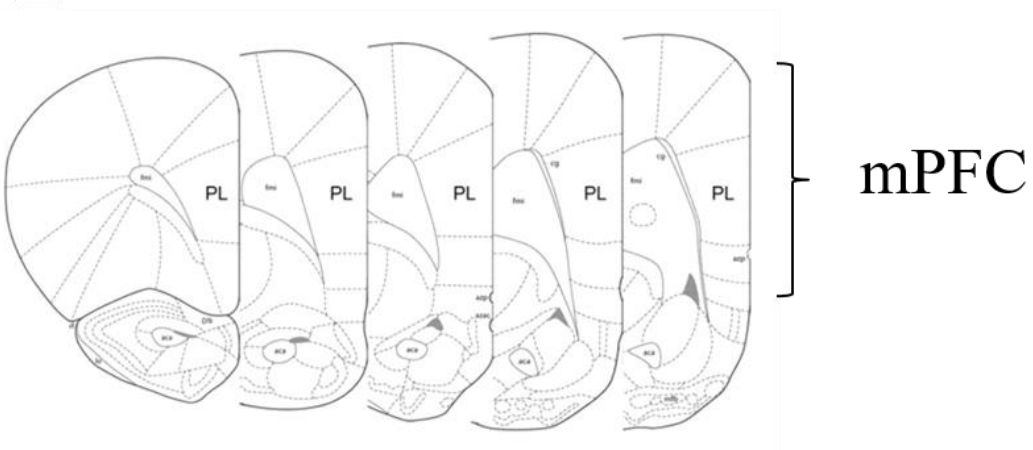

Fig. M.4. **Anatomical localization of rat PL area in the medial Prefrontal cortex (mPFC).** Adapted from Bloss et al, 2010.

8. Selection of pyramidal neurons

We aimed at restricting our analysis to pyramidal neurons (Pyrs), and putative Pyrs were chosen for recordings (in layer 2-3 or layer 5) according to the triangular shape of their cell body; we avoided small and round, oval, or spindle-like cell bodies and multipolar or bipolar dendrites, as seen under the microscope with infrared-differential interference contrast optics. For layer 5 Pyr, the presence of visible apical dendrite projecting to Layer II/III was also required (Van Aerde & Feldmeyer, 2015). However, the selection based upon the cell body shape may not exclude all interneurons. We also required that some electrophysiological criteria were met to further exclude potential non-pyramidal neurons, as follows. A correlation between the firing pattern produced upon current injection and neuronal morphology has been reported in the prelimbic area of the medial prefrontal cortex in rats, both in vivo (Dégenètais et al, 2002) and in vitro (van Aerde and Feldmeyer, 2015). Specifically, pyramidal cells may exhibit a variety of firing patterns, going from "regular spiking" (RS), with little adaptation of firing frequency during a protracted step current injection, to strongly adapting or bursting patterns; moreover, characteristically, pyramidal neurons (Pyrs) in layer 2-3 and 5 never present very high firing frequencies (firing rate increase < 15Hz/100pA, Table 3 in van Aerde and Feldmayer, 2015). Interneurons may exhibit different types of firing patterns, going from the characteristic "fast-spiking" pattern, with very high firing frequencies and large post-spike after-hyperpolarization, to low-threshold spiking or regular spiking (Wang and Gao, 2009). The latter pattern does not differ from patterns observed in Pyrs, and this would make difficult the identification of Pyrs only based on firing pattern. However, typically, the input resistance (R_{in}) of all interneuron types is large in the mPFC, with fast-spiking interneurons having R_{in} above 150 MOhms, and other interneurons having R_{in} well above 200 MOhms (in adult rats; Wang and Gao, 2009). Thus the combined classification of neurons upon their firing pattern and R_{in} offers an electrophysiological criterion to distinguish Pyrs from the interneurons.

Overall, pyramidal neurons were visually identified as big triangularly-shaped cells in the selected layer. To further exclude potential non-pyramidal neurons, only cells with an input resistance in the range 50 - 200 MΩ were accepted for analysis. Finally, neurons showing a firing rate increase > 15Hz/100pA, or a spike frequency >50Hz when injected with a squared 1s-long, 300pA depolarizing current pulse from a potential of -76 mV, were considered fast-spiking interneurons and therefore not included in the analysis.

9. Whole-Cell recordings

Borosilicate glass pipettes were micromanipulated under visual control towards a target pyramidal neuron while maintaining a small positive pressure to keep the pipette's tip clean. After contacting the cell soma membrane, a tight seal (1-3 GΩ) was obtained by applying negative pressure to the pipette. The membrane was disrupted with additional suction to obtain the whole-cell configuration.

The cell resting membrane potential (V_{rest}) was immediately evaluated by switching the amplifier to the current clamp configuration with 0 injected current and reading the membrane potential. Cells with V_{rest} >-60 mV were discarded. Typically, V_{rest} was more negative for L2-3 than for L5 cells (see Results).

For all cells recorded with an intracellular (pipette) solution based on K^+ as the main intracellular cation (K-Gluconate solution, see below, "Solutions and Drugs"), we evaluated the firing output *vs* injected current relation (f-I relation; see Results) in current clamp, before proceeding to synaptic current recordings in voltage clamp. We kept L5 cells around -70 mV and L3 cells around -80 mV (as detailed in the Results) by injecting an appropriate holding current (generally -60 pA for L5, +40 pA for L2-3) and we applied squared 1s-long depolarizing current pulses with variable amplitude, generally from 0 to 500 pA for L3 neurons and from 0 to 300 pA for L5 neurons; pulses were applied every 10s while recording the membrane voltage (V_m). To record V_m, the bridge balance protocol was operated through the automated "bridge balance" options of the Multiclamp to compensate the series resistance voltage drop.

After switching to the voltage-clamp configuration, the cell input resistance, R_{in}, and the series resistance R_s were evaluated after applying a 100ms-long, -10 mV voltage step, as the ratio between the applied voltage step and the steady-state or the peak transient membrane current, respectively (fig. M.5).

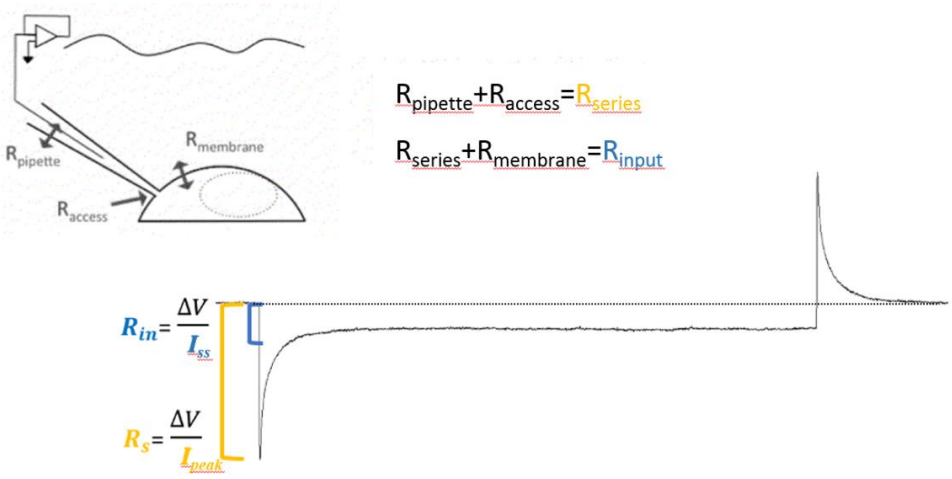

Fig. M.5. **Series and input resistance measurement**. Top: scheme of resistances in the whole-cell circuit. Bottom: current trace in response to a -10 mV, 100 ms voltage step applied in the voltage-clamp configuration. The series resistance was calculated by dividing the voltage step by the negative current peak (I_{peak}, in yellow). The ratio between the applied voltage and the current measured at steady-state (I_{ss}, in blue) is equal to the input resistance.

9.a) sEPSCs and mEPSCs recordings

We used pipettes with tip resistance ranging from 2 to 3 MΩ when filled with the K-Gluconate internal solution. After the measurement of the f-I relation in current-clamp mode, we switched to voltage clamp, holding the membrane potential at -60 mV, both for neurons in layer 5 and layer 2-3. Neurons with compensated series resistance (R_s) > 14 MΩ or with R_s changes > 30% during the analysed time window were discarded. L2-3 cells with negative basal current, or L5 cells with basal current < -200 pA, when recorded at -60mV, were excluded from the analysis. Recording of sEPSCs started around 5 min from the whole-cell break-in. To isolate mEPSCs, around 8-9 min after break-in we added to the ACSF a cocktail of inhibitors, in order to block action potential generation and inhibitory synaptic receptors. The cocktail included 500µM tetrodotoxin (TTX), 100µM picrotoxin and 1µM strychnine, to block respectively the fast voltage-dependent Na^+ channels responsible for action potential development, and $GABA_a$ and Glycine receptors. The recording of mEPSCs initiated around 16 min after the break-in, after checking for the absence of spikes during a suprathreshold current injection in current clamp. sEPSCs and mEPSCs were collected for analysis in time windows lasting ≤ 2 min.

9.b) E/I recordings.

We used pipettes with tip resistance ranging from 3 to 7 MΩ when filled with Cs-based solution (see below, par. 10.a). As this internal solution blocked Na+ and some voltage dependent K+

channels, inhibiting AP generation, we could not evaluate the firing pattern of neurons. Therefore pyramidal neurons were only visually identified by the morphological characteristics mentioned above. To isolate excitatory from inhibitory synaptic currents, the membrane potential was held at -58 mV, the average reversal potential (V_{rev}) of inhibitory currents, i.e. the potential where the IPSCs are zeroed, while to record inhibitory currents, the membrane potential was held at + 3mV, the average excitatory reversal potential.

The V_{rev} of inhibitory and excitatory currents was determined in separated whole-cell experiments using the Cs-based solution. For inhibitory currents, V_{rev} was found by varying the holding potential across the range -75 to -50 mV and checking for the zero-current potential, while excitatory currents were pharmacologically inhibited with NBQX (2 µM) and D-APV (50 µM). The average V_{rev} was 2.85±0.77 (n=2 cells). For excitatory currents, V_{rev} was measured by varying the holding potential across the range 0 to +20 mV and checking for the zero-current potential, in the presence of pharmacological inhibition of inhibitory currents with picrotoxin (100 µM) and strychnine (500 nM). The average excitatory V_{rev} was -58.24±1.52 (n=2 cells).

Neurons with compensated R_s > 20MΩ or with R_s changes > 30% during the recording session were discarded. Cells displaying a basal current < -200 pA when recorded at -58 mV were excluded from the analysis.

10. Solutions and Drugs

10.a) Solutions

During slicing and slice maintenance, the tissue was incubated in a "*Slicing solution*" containing (in mM): NaCl 83, KCl 2.5, NaH_2PO_4 1.25, $NaHCO_3$ 21, Sucrose 72, Glucose 25, Sodium Ascorbate 0.45, $CaCl_2$ 1, $MgCl_2$ 4; the pH was maintained at 7.4 by bubbling carbogen (5% CO_2, 95% O_2). Recordings were performed when slices were perfused with the "*ACSF*" solution, containing (in mM): NaCl 125, KCl 2.5, NaH_2PO_4 1.25, $NaHCO_3$ 26, Glucose 10, $CaCl_2$ 1.5, $MgCl_2$ 1, the pH was maintained at 7.4 by bubbling carbogen. This solution was prepared using Volvic water, which contains a known low number of divalent cations (Ca^{2+}, Mg^{2+}) which was taken into account for reaching the final desired concentration.

Internal solutions were prepared with variable composition depending on the experimental focus. To mimic physiological intracellular ionic concentrations, allowing the generation of action potentials, we used the "*K-Gluconate*" solution, containing (in mM): K-gluconate 140, EGTA 0.2, HEPES 10, $Na_2ATP*3H_2O$ 4, Na_3-GTP 0.3, Na_2-Phosphocreatine 5, $MgCl_2$ 4, pH 7.4.

For E/I recordings, we used the "*Cs-based*" internal solution, containing in mM: Cesium Methansulfonate 135, KCl 10, Hepes 10, $MgCl_2$ 1, EGTA 0.2, MgATP 4, Na_3GTP 0.3, Na_2-Phosphocreatine 20, pH 7.3. Lidocaine N-Ethyl Chloride (5mM) was freshly added in order to block voltage-dependent Na^+ channels in the recorded cell. This Cs-containing solution was chosen to enable the recording of IPSCs at a positive potential (+3 mV, see the previous paragraph), where many voltage-gated ion channels are open. In this condition, to favour cell stability for relatively long periods, it was important to inactivate K^+ and Na^+ channels with Cs^+ ions and lidocaine, respectively. Both internal solutions were prepared using MilliQ water.

10.b) Drugs

All drugs were bath-applied, with an in-flow maintained at 2 ml/min. Tetrodotoxin (TTX) was purchased from Latoxan, dissolved in 0.1M sodium citrate and stocked at -20°C. 2,3-Dioxo-6-nitro-1,2,3,4-tetrahydrobenzo[f]quinoxaline-7-sulfonamide (NBQX, Abcam), D-(-)-2-Amino-5-phosphonopentanoic acid (D-APV, Abcam) and strychnine (MerckLifeScience) were prepared in distilled water and stored at -20°C. Lidocaine (MerckLifeScience) was diluted in MilliQ water and stored at -20°C. Picrotoxin (Tocris) was prepared in boiled water and stored at +4°C, covered with an aluminium foil to be protected from light.

11. Data analysis

11.a) Detection of synaptic currents

In order to detect post-synaptic currents, we used the dedicated software Clampfit (MDS Analytical Technologies). Specifically, we used the "template search" routine in Clampfit, which is a detection algorithm based on finding segments of the current trace bearing a sufficiently large cross-correlation coefficient with a "template" trace, i.e. a coefficient exceeding a fixed "template match threshold". A template is a custom-defined waveform representing the prototypical post-synaptic current of interest. Clampfit includes a macro to design one or more templates based on the synaptic currents present in a customer-provided trace.

Excitatory synaptic currents (sEPSCs and mEPSCs) in L2-3 pyramidal neurons were detected using a single template, formed by averaging ~30 representative EPSCs from an exemplar cell(Exc template, Fig.M.6).

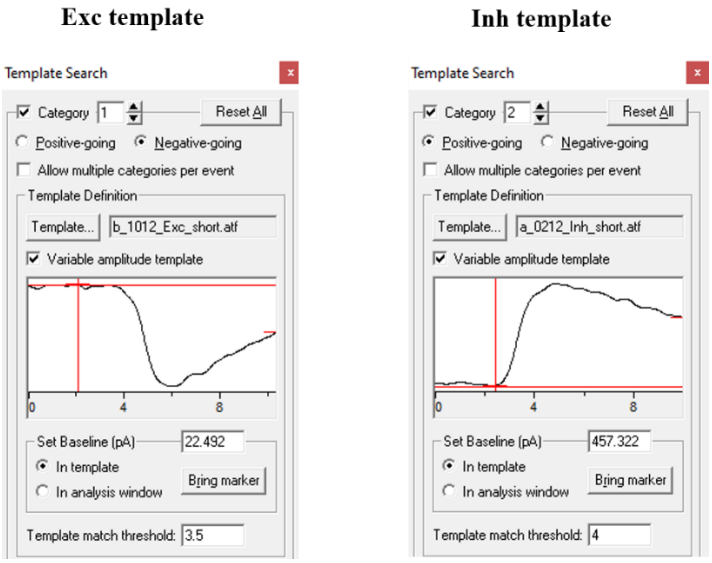

Fig M.6. **L2-3 templates**. Model of post-synaptic currents used for detection of events in neurons located in L2-3. Left: template for excitatory synaptic currents. Right: template for inhibitory synaptic currents. The templates were modelled with short duration, to detect superimposed events occurring in high-frequency clusters with a minimum number of lost events. The decay phase of the detected synaptic currents can not be studied with these templates.

For sEPSCs and mEPSCs recorded with the K-Gluconate internal solution, the template match threshold was chosen to be 4. Putative EPSCs were accepted only if they exceeded a threshold peak amplitude, taken as 10 pA for mEPSCs and 16pA for sEPSCs. Such high threshold values reflected the relatively large baseline noise (1.5 – 7 pA baseline standard deviation after filtering current traces with a digital Gaussian filter with -3dB cutoff at 1kHz) and consequently the low signal/noise ratio. Also, given the high number of superimposed EPSCs and a relative baseline instability, we found that to minimize the number of missed events, the template had to be only 7ms long (+3 ms of baseline preceding the event). This choice improved the estimate of sEPSC frequency, by increasing the number of detected events. However, the decay of sEPSCs was typically longer than 7 ms, so it was not possible to study the sEPSC decay using this template. Therefore we will present the analysis of sEPSC peak amplitude and rise time, but not of sEPSC decay and sEPSC area (= charge transfer). We also measured the intervals between consecutive sEPSCs (inter-event interval, or IEI).

For sEPSCs recorded with the Cs-based solution, the template match threshold was chosen as 3.5 and the peak amplitude threshold was 11 pA. For inhibitory synaptic currents recorded with the Cs-based solution, similar to the case of sEPSCs, we used a single template (Inh template,

Fig. M.6), with matching threshold 4 and threshold peak amplitude 10 pA.

Finally, sEPSCs and mEPSCs recorded in L5 pyramidal neurons were detected with the Template Search algorithm, using two templates with slower (Slow template, Fig.M.7) and faster (Fast template, Fig.M.7) decay kinetics, because of the presence, in some of the cells, of a significant proportion of very fast events. The threshold for detection with the Slow template was 10 pA for mEPSCs and 11 pA for sEPSCs, while the threshold for the Fast template was 15 pA.

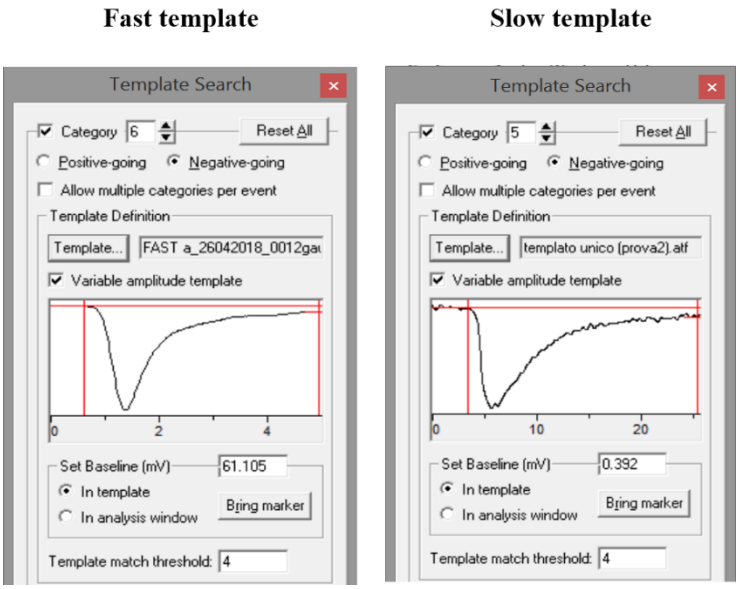

Fig.M.7. **L5 templates**. Model of post-synaptic currents used for detection of excitatory currents in L5 neurons. The Fast template (left) was used to detect events with fast kinetics (total duration around 5 ms), not detected by the Slow template (right), with a duration around 20 ms.

11.b) E/I ratio

The excitation/inhibition (E/I) ratio of synaptic conductance in each cell was calculated as the ratio of the total charge of sEPSCs over sIPSCs in a 2 min interval.

Indeed, the E/I ratio is the ratio of total average excitatory conductance over total average inhibitory conductance in a cell. In our conditions (excitatory conductance measured at reversal of inhibitory conductance, and vice versa), the driving force is the same for excitatory and inhibitory currents, so the E/I ratio coincides with the ratio of the total excitatory charge over total inhibitory charge transferred through the cell membrane:

$$\frac{\mathbf{E}}{\mathbf{I}} = \frac{\mathbf{G_{EPSC}}}{\mathbf{G_{IPSC}}} = \frac{\bar{G}_{\mathbf{EPSC}} \cdot |V_{\mathbf{EPSC}} - V_{\mathbf{rev,e}}|}{\bar{G}_{\mathbf{IPSC}} \cdot |V_{\mathbf{IPSC}} - V_{\mathbf{rev,i}}|} = \frac{\int \mathbf{I_{-58mV}(t)dt}}{\int \mathbf{I_{+3mV}(t)dt}} = \frac{\mathbf{Q_{tot,exc}}}{\mathbf{Q_{tot,inhib}}}$$

The total charge was calculated as the integral of the 120s-long current trace for the inhibitory charge, while, for the excitatory charge, it was generally measured in a shorter time window (never shorter than 20s) where the trace was stable and the signal/noise ratio was highest. We then scaled this value to the ratio of 120 s and the window's length, to obtain total charges over comparable time intervals at -58mV and +3mV in each cell. This procedure using integrals of long stretches of the current trace was preferred to the alternative procedure of detecting each individual event and measuring its area and summing them up. Indeed, in our case, given the high baseline noise and the frequent superposition of PSCs, it is hard to describe the waveform of individual PSCs, especially for the smaller ones, and this would have led to unpredictable errors. We also verified that the integration of baseline noise had a minimal impact on the charge results (not shown).

11.c) Histograms and statistical comparison of PSCs

After detection, normalized cumulative histograms of the inter-event intervals, peak amplitudes and rise times were calculated using IgorPro (Wavemetrics). For peak and inter-event interval histograms, data were logarithmically transformed to facilitate the representation of largely variable values. For each parameter, the histogram bin width was chosen so as to obtain 20 bins of equal width between the maximum and minimum value across all included cells. In the case of peak amplitudes and IEIs, bins of equal width for the logarithmic transform of data correspond to bins of increasing width for the original data. Histograms of each experimental group were averaged for display. In the graphs, average ± s.e.m. are plotted for each bin. Averages for all groups are superimposed in the same graph (e.g. see fig. R.4B-D).

For statistical comparison of histogram distributions, following the example of previous studies (Indersmitten et al, 2015; Dumetz et al, 2020), the original histogram values (without averaging inside groups) were compared with repeated measures two-way ANOVA using bin as repeated-measures factor (thus accounting for the non-independence of bins in cumulative histograms), and group as the other factor. This was followed by post-hoc Tukey's multiple comparison test. Comparisons were performed using GraphPad Prism 9.0 software (GraphPad Software, LLC). It can be argued that this may not be the optimal strategy because it is based on the assumption that fractional counts are normally distributed in each bin (however there is no assumption of normality for the observed variable *per se*). Generally speaking, this assumption is incorrect because counts in a bin should be distributed according to a Poisson distribution (Brandt, 1999). In our specific case, it is important to specify that, while for the sEPSCs peaks in the FS1h

group, counts in the central bins were not normally distributed due to the presence of a subgroup of cells displaying bursts of large sEPSCs, for other parameters (rise time, intervals) counts in the central bins of normalized histograms were indeed normally distributed. On the contrary, in bins at the limits of the parameter's range, counts were not normal. On the other hand, at the beginning of our study, we performed statistical testing using the non-parametric Kolmogorov-Smirnov (K-S) test for comparing two unbinned distributions. For each experimental group, we formed a single distribution by collecting an equal number of randomly chosen samples from each cell in the group. We then ordered samples in ascending order in each distribution and we computed the K-S statistics. We obtained the corresponding probability P for the null hypothesis of samples arising from a unique parent distribution. We rejected this hypothesis when $P<0.05$, after applying the Bonferroni-Holm correction (i.e. multiplying each P value by the number of comparisons performed) whenever more than one pair of sample distributions were compared.

At the end of this first round of analysis we noticed that the K-S test was very sensitive because it indicated the presence of significant differences between most of the distributions compared. We were suspicious about the meaning of these differences and, although being aware of the theoretical difficulties mentioned above, we turned to comparison of binned histograms with repeated-measures 2-way ANOVA. We verified in all cases that when significant differences across two or more groups were obtained with 2-way ANOVA, they were also obtained with the K-S test. The reversal was not true: differences obtained with the K-S test were not reproduced by 2-way ANOVA. Therefore, in our hands the 2-way ANOVA was a more stringent test, possibly having less statistical power, however we are confident that it should minimize detection of false differences.

For the mean values of peaks, rise times and IEI, they were statistically compared across groups using a parametric or non-parametric test, according to the results of the normality/lognormality check for the corresponding data. In detail, when the data in all groups passed the normality check, the statistical comparison was performed with 1-way ANOVA (or t-test in the case of only two groups); when the data did not pass the normality test but passed the lognormality test, the logarithmic transform of the data was compared with 1-way ANOVA or t-test; finally, when neither the normality nor the lognormality test was passed by at least one of the groups, the test of choice was the Kruskal-Wallis statistics (or the Mann-Whitney test in the case of only two groups). All the parametric tests have been performed assuming that the variances of the populations were different, applying the Welch's correction on the t-test and the Brown-

Forsythe and Welch's ANOVA test when 1-way ANOVA was required. Furthermore, the comparison of averages of the means of the various parameters yielded the same results (in terms of presence/absence of significant differences) as comparison of averages of median values. Data for medians are not reported in this thesis.

RESULTS

The aim of this work was to detect possible sustained effects of the acute foot-shock (FS) stress protocol in the prelimbic mPFC of adult rats. We studied with patch-clamp recordings the excitatory synaptic transmission in layer 2-3 and 5 of this region, both 1 and 24 hours after FS. We compared measurements in stressed animals undergoing FS and treated or not with systemic ketamine injection. Finally, in L2-3, we also recorded spontaneous inhibitory synaptic currents (sIPSCs), and we evaluated the ratio of the total excitatory to inhibitory conductance in individual pyramidal neurons (E/I ratio), which is an index of local network activation.

1. Foot-shock stress transiently increases plasma corticosterone levels

As an acute stressor, we decided to use unpredictable foot-shock stress, a protocol that involves both physical and emotional components and is considered an elite choice for studying PTSD. Adults male rats were randomly separated into groups, and some groups were subjected to the electric foot-shock protocol (see Methods).

As a read-out of the stress reaction, in a fraction of the animals, we measured the corticosterone (CORT) levels in the plasma isolated from blood gathered at the time of sacrifice. We analysed samples collected from animals not exposed to the stressor (CTR), and from rats exposed to the acute stress protocol, 1 hour (FS1h) or 24 hours (FS24h) before the sacrifice. As expected, CORT levels are enhanced in the FS1h group (364 ±112 ng/ml, n=9 animals), while later-on they return to control levels (FS24h: 42 ± 22 ng/ml, n=6 animals; CTR: 57 ± 22 ng/ml, n=13 animals). After confirming the lognormality of the values, we performed a statistical analysis on the logarithmic transform of the data which confirmed that CORT concentration averages are significantly different (one-way ANOVA, $p<0.05$), specifically the FS1h is different from the other two groups (post-hoc Tukey's multiple comparisons test: FS1h *vs* CTR, p=0.002 (**); FS1h vs FS24h, p=0.01(*)) (Fig.R.1).

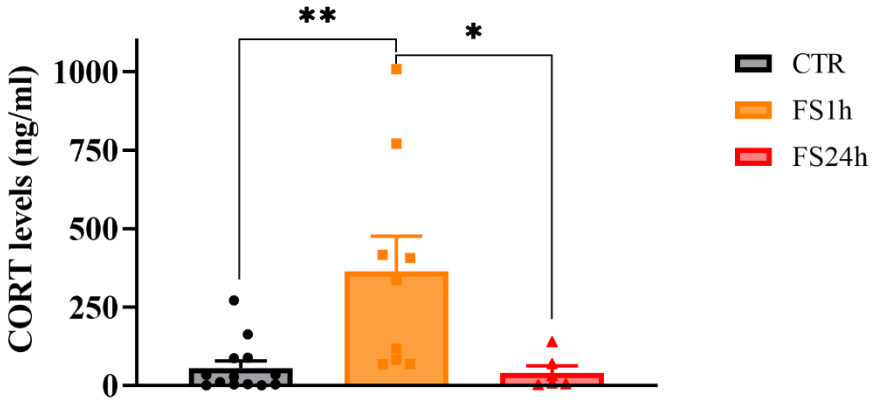

Fig.R.1. **Corticosterone levels are enhanced 1 hr after the foot-shock acute stress procedure.** Corticosterone levels were measured with the ELISA immunoassay on blood samples collected from rats trunk during the sacrifice. The graph displays the averages (bars; ± s.e.m.) and the individual values (symbols) of the corticosterone level (ng/ml) in 13 control animals (CTR), 9 animals sacrificed 1 hour after FS (FS1h) and 6 animals sacrificed 24 hours after FS (FS24h). The statistical comparisons were performed on the logarithmic transform of data, after assessing their lognormality. CORT averages are significantly different (one-way ANOVA, $p<0.05$). The post-hoc Tukey's multiple comparisons test shows a significant difference between FS1h and the other two groups (FS1h vs CTR, p=0.002 (**); FS1h vs FS24h, p=0.01(*)).

2. Firing patterns in layer 2-3 and layer 5 neurons of the prelimbic mPFC

We aimed at restricting our analysis to pyramidal neurons (Pyrs). As explained in Methods, putative Pyrs were chosen for recordings in layer 2-3 (L2-3) or layer 5 (L5) of the prelimbic mPFC according to their cell body shape. Their identity was further confirmed upon electrophysiological criteria. Specifically, cells accepted as Pyrs had input resistance in the range 50-200 MOhms (to exclude potential interneurons with non-*fast spiking* firing pattern, which typically have R_{in}>200 MOhm), and their firing pattern was required to be a "*regular spiking*" (RS) pattern, thus excluding fast-spiking interneurons, as well as other less frequent types of non-RS pyramidal neurons. To perform this selection, we routinely checked the firing pattern of all the recorded cells, using the *K-gluconate* internal solution (see Methods), both in L2-3 and L5. Immediately after break-in and establishment of the whole-cell configuration, we switched to current-clamp (CC) mode, we activated the bridge-balance series resistance correction and we injected a steady holding current to keep neurons around -80 mV (in L2-3) or around -70 mV (in L5). We next proceeded to record the firing response of each neuron to 1s-long step current injections with variable intensity.

We found three classes of neurons with different firing responses:

- fast-spiking neurons, a class of interneurons with low rheobase that could fire > 50 action potentials when injected with a 300 pA current stimulus (fig. R.2A);
- adapting neurons, characterised by long pauses and/or firing arrest (fig.R.2B);
- regular spiking (RS) neurons, presenting a tonic or very slowly adapting firing pattern (fig.R.2B). This cell type included around 80% of the cells patched in each experimental group.

In the rest of our analysis, we focused on RS cells with R_{in}<200 MOhm, which represent the largest subgroup of pyramidal neurons.

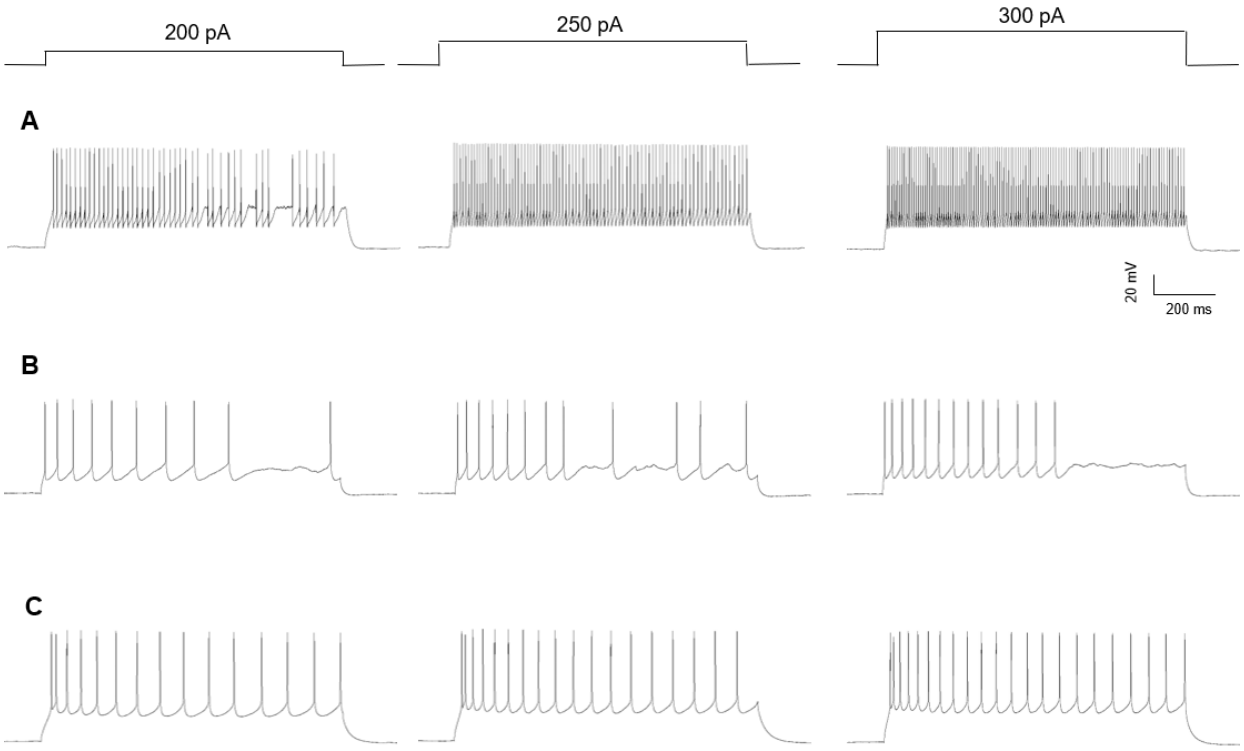

Fig.R.2 **Firing patterns in mPFC neurons**. Three different firing patterns found in L5 and L2-3 in the prelimbic mPFC. The firing pattern of each neuron was studied with step current injections of increasing intensity through the patch pipette (0 to 400/500 pA, 1 s duration) from a membrane potential of ~-80 mV (in L2-3) or ~-67mV (in L5). (A) Fast-spiking interneuron, showing a large after-hyperpolarization after each spike, and a frequency of 121 Hz at +300pA current injection. (B) A neuron with adapting firing, characterized by long irregular firing pauses, or firing arrest upon strong stimuli. (C) Regular spiking (RS) neuron, showing a fast doublet of spikes at the beginning of the response, followed by periodic firing, with frequency increasing with stimulus intensity. RS neurons were the most abundant neurons found in the mPFC. We restricted our post-synaptic current analysis to RS neurons.

3. Firing in RS cells of layer 2-3 is not affected by acute stress and ketamine

We analysed the excitability of the RS neurons, reporting the early (1 hour after foot-shock) and late (24 hours after foot-shock) effects of foot-shock onto the neuronal firing elicited by increasing current injections. We plotted the number of action potentials elicited in the 1s long current step, *vs* the current injection ("*f*-I curve") for each cell, averaged over each experimental group. We studied the *f*-I curve for CTR1h and FS1h cells (see Methods, fig. M.1 and par.1 for a detailed description of the experimental groups) recorded at a resting membrane potential of – 81± 1 mV (fig.R.3, left panel). When statistically compared with a 2-way ANOVA (factors: group, stimulus intensity) there was no significant main effect of group ($F(1,41)=0.136$, $p=0.7143$), nor significant interaction between group and stimulus ($F(8,305)=1.78$, $p=0.0806$), indicating no significant differences in excitability between the two groups. Likewise, we analysed the excitability of CTR24h, FS24h and FSKet cells recorded at a resting membrane potential of –79 ± 1 mV (fig.R.3, right panel), and according to a 2-way ANOVA analysis, we found that there were no significant differences among the three groups (main effect of group: $F(3,60)=0.407$, $p=0.407$; interaction group x stimulus, $F(36,711)=0.403$, $p=0.9994$), indicating that neither acute stress nor ketamine injection change RS Pyr excitability 24 hours after foot-shock.

Overall, neither early nor late effects of foot-shock on neuronal excitability could be found in our analysis.

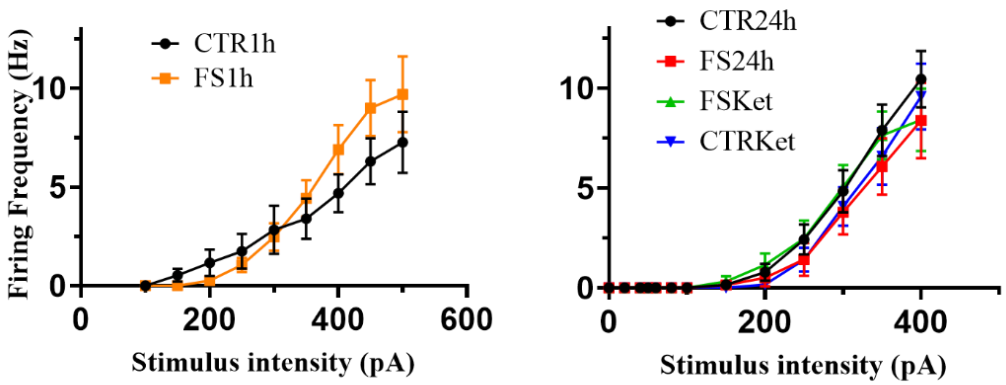

Fig.R.3 **Foot-shock stress does not significantly affect the excitability of L2-3 regular spiking neurons**. Spike frequency elicited by increasing current injections (f-I curve) was measured 1hr after the FS stress protocol (left), or 24 hrs after FS following saline or ketamine (10mg/kg) injection 6 hrs after FS (right). Average spike frequency vs injected current (±s.e.m.) from FS1h (20 cells from 8 animals) and CTR1h (24 cells from 11 animals) regular spiking neurons, recorded at – 81± 1 mV (*left*), and from CTR24h (20 cells from 9 animals), FS24h (14 cells from 7 animals), FSKet (21 cells from 9 animals) and CTRKet (12 cells from 4 animals) pyramidal neurons, recorded at – 79± 1 mV (*right*). Mixed-model or 2-way ANOVA analysis did not reveal any difference across groups.

4. Foot-shock and ketamine effects on synaptic transmission in L2-3 mPFC

4a) Miniature excitatory transmission: no early (1hr) nor late (24hrs) changes after foot-shock and ketamine

Miniature synaptic currents (mEPSCs), or minis, are produced by spontaneous vesicle release from presynaptic terminals in the absence of action potentials (AP-independent release). Morphological data have shown a larger density of axo-spinous and axo-shaft excitatory synapses in layer 2-3 of the prelimbic area of the mPFC of adult rats 1hr after FS (Nava et al., 2015). Consequently, one would expect a higher mEPSCs frequency in Pyrs after FS due to an increase in the actual number of synaptic contacts. No previously published work has addressed the early or late effects of foot-shock stress on mEPSCs in the mPFC of adult animals. We compared the amplitude, frequency and kinetics of mEPSCs 1 and 24 hours after foot-shock stress. We also describe the study of the late effects of ketamine post-stress systemic injection on mEPSCs.

We recorded mEPSCs from neurons with cell body located in the prelimbic L2-3, holding the membrane potential at -60mV. Exemplar current traces are shown in fig. R.4A. To isolate excitatory activity, we blocked inhibitory synaptic transmission by perfusing picrotoxin

(100μM) and strychnine (1μM), blockers of $GABA_A$ and glycine receptors, respectively. Isolation of miniature activity was obtained by adding the Na^+-channel blocker TTX (500 μM) in the ACSF solution. A few minutes after starting bath perfusion of the drugs, the efficacy of TTX action was confirmed by the disappearance of firing activity in response to a somatic current injection larger than the cell rheobase. After the recordings, we detected randomly occurring mEPSCs by checking similarity to a template EPSC waveform (see Methods). We excluded from analysis putative events with peak amplitude <10 pA. This relatively high threshold was required because a fraction of the recordings displayed a large baseline noise (s.d. of baseline current). This implies that smaller events could have been missed by our study. Of notice, the fraction of below-threshold detected events was small in the noisier experiments, and larger in experiments with smaller baseline noise, suggesting that our detection algorithm did not produce a relevant number of false events.

After detection, we formed normalized cumulative histograms of the three parameters peak amplitude, inter-event interval, and 10-90% rise time, with a fixed bin amplitude and number of bins in all cells. Histogram bins were then averaged, plotted for all groups (Fig. R.4B-D, R.5B-D), and statistically compared using repeated measures 2-way ANOVA with bin and group as factors. For the applicability of this statistical approach to our data, see the discussion in par.11.c of the Methods section. Moreover, we directly compared the means of peak amplitudes, inter-event intervals and 10-90% rise times of mEPSCs (insets in Fig. R.4B-D, Fig. R.5B-D). The grand average of each parameter (represented by the bars in the insets) was compared across groups with a non-parametric test for unpaired data (Mann-Whitney test; 95% confidence level; data reported as means ± s.e.m.).

When considering early stress effects (1 hour after FS; comparison of n=11 cells from 7 animals in CTR1h, and n=12 cells from 6 animals in FS1h), there were no significant differences between the histograms of peak amplitude, inter-event interval and 10-90% rise time of the CTR1h and FS1h group. Moreover, none of the means of mEPSCs parameters was significantly different between the CTR1h and the FS1h groups: not the mean of peak amplitudes (fig. R.4B; FS1h: 17.1±0.3 pA; CTR1h: 19.2±1.6 pA, p=0.8328), nor the mean of intervals (fig. R.4C; FS1h: 211±22 ms; CTR1h: 313±79 ms, p=0.4134), nor the mean of rise times (fig. R.4D; FS1h: 1.81±0.03 ms; CTR1h: 1.74±0.03 ms, p=0.2604).

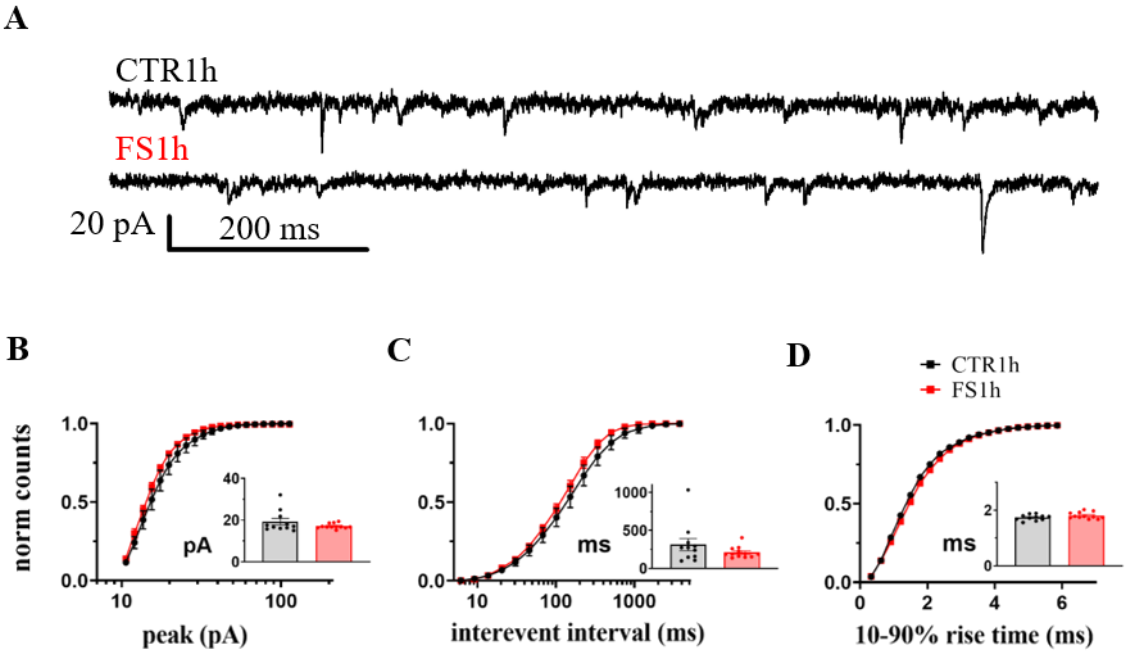

Fig. R.4. **No changes in L2-3 mEPSCs properties 1hour after FS stress**. Patch-clamp whole-cell recordings of miniature excitatory synaptic currents (mEPSCs) performed 1hr after foot-shock. Tetrodotoxin (TTX, 1µM), picrotoxin (PTX, 0.1 mM) and strychnine (Str, 1 µM) were present to block action potentials and inhibitory synaptic inputs through GABAa receptors. Holding potential: -60mV. (A) Representative current traces from CTR1h (*top*) and FS1h (*bottom*), showing mEPSCs as inward deflections. (B-D) Normalized cumulative histograms of mEPSC peak amplitude (left), inter-event interval (*centre*) and 10-90% rise time (*right*). Average (± s.e.m.) of histogram bins from 11 cells from 7 animals (CTR1h) and 12 cells from 6 animals (FS1h). Insets: individual values (dots) and group average (bars), for both groups, of the mean peak mEPSC amplitude (*left*), mean inter-event interval (*centre*) and mean 10-90% rise time (*right*). No significant differences between the two groups were present in histograms or mean values.

These results are in contrast with our initial hypothesis of an increase in the frequency (= a decrease in the inter-event interval) of mEPSCs. Possible explanations are presented in the Discussion, including the possibility that newly formed synapses are not active 1 hour after stress.

In order to verify if an increase could be detected 24 hours after foot-shock, we studied miniature transmission and a possible effect of ketamine at sub-anaesthetic dose, at this time point in stressed animals. In this experimental setting, animals were injected with saline (FS24h) or ketamine at sub-anaesthetic dose (10 mg/Kg) (FSKet) 6 hours after exposure to the stressor, while rats belonging to the control group (CTR24h) were injected with saline. We compared n=14 cells from 9 animals in CTR24h, n=11 cells from 8 animals in FS24h and n=9

cells from 6 animals in FSKet. mEPSCs recordings (fig.R.5A) were performed as specified above. The comparison of histograms with 2-way ANOVA shown that there were no significant differences among the histograms of peak amplitude, inter-event interval and 10-90% rise time of the CTR24h, FS24h and FSKet groups (fig. R.5B-D). Moreover, there were no differences in the means of peak amplitude (FSKet: 19.0±1.0 pA; FS24h: 16.7±0.8 pA; CTR: 17.6±1.0 pA, p=0.1531), the inter-event interval (FSKet: 319±45 ms; FS24h: 316±53 ms; CTR: 298±46 ms, p=0.8308) and the rise time 10-90% (FSKet: 1.58±0.06 ms; FS24h: 1.78 ± 0.06 ms; CTR: 1.65±0.07 ms, p= 0.0865) across the three studied groups.

Overall, the analysis of minis did not reveal any effect of acute stress on this synaptic transmission modality.

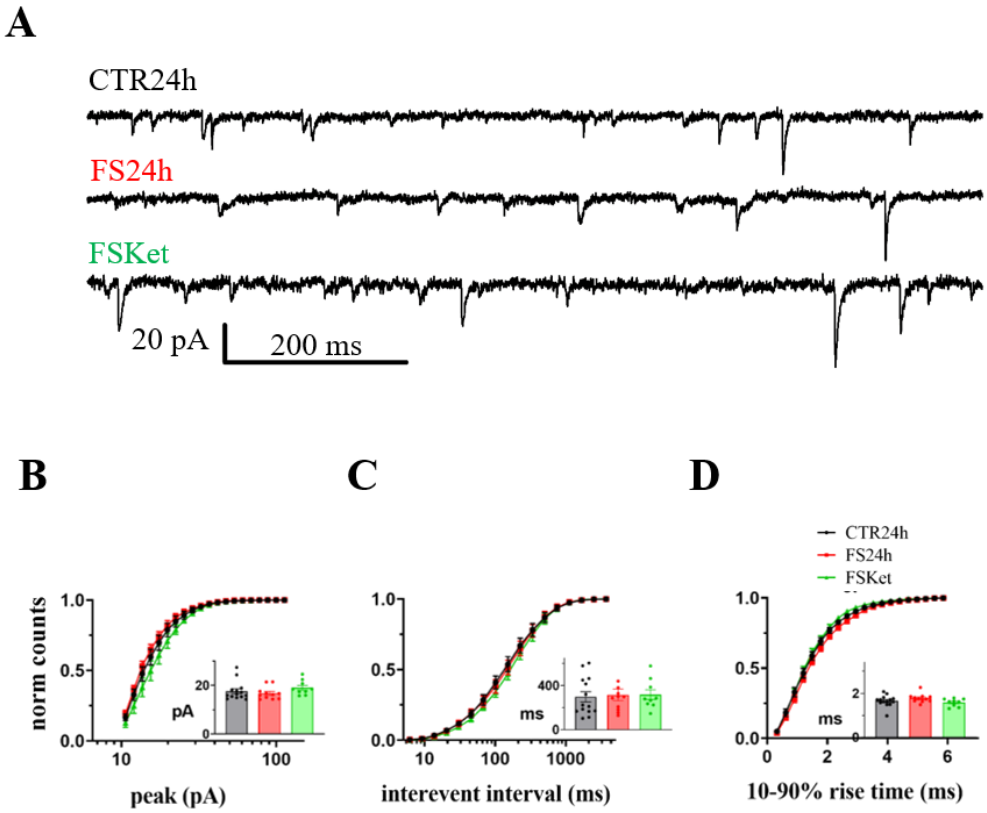

Fig.R.5. **Lack of sustained effects of acute stress or ketamine on L2-3 mEPSCs.** Patch-clamp whole-cell recordings of mEPSCs performed 24hrs after foot-shock, in animals that received an intraperitoneal (i.p.) injection of saline (FS24h) or ketamine (10mg/kg) (FSKet) 6hrs after FS. Tetrodotoxin (1µM), picrotoxin (0.1 mM) and strychnine (1 µM) present during the recording. Holding potential: -60mV. **(A)** Representative mEPSCs current traces from CTR24h (*top trace*), FS24h (*middle trace*) and FSKet (*bottom trace*) animals. **(B-D)** Normalized cumulative histograms of mEPSC peak amplitude (*left*), inter-event interval (*centre*) and 10-90% rise time (*right*). Average (± s.e.m.) of histogram bins from 14 cells from 9 animals (CTR24h), 11 cells from 8 animals (FS24h), and 9 cells from 6 animals (FSKet). Insets: individual values and group average, for CTR, FS 24h and FS Ket, of the mean peak mEPSC amplitude (*left*), mean inter-event interval (*centre*) and mean 10-90% rise time (*right*). No significant differences between the three groups were present in histograms or mean values.

4b) Spontaneous excitatory transmission: a subpopulation of large sEPSCs is activated 1hr after acute stress

A regulation affecting the probability of AP-evoked release could in principle leave unaffected the probability of spontaneous AP-independent vesicle fusion (Kaeser and Regehr, 2014). Moreover, it is unclear whether or not the molecular machinery giving rise to mEPSCs is at least partially molecularly distinct from the machinery governing AP-dependent release (Kavalali, 2015). These observations leave open the possibility that acute stress differently affects AP-dependent and AP-independent release mechanisms. To clarify this issue, we studied the spontaneous postsynaptic currents (sEPSCs; developing in the presence of spontaneous action potentials in the slice network) in L2-3 Pyrs in the prelimbic area.

It was previously shown an increase in the amplitude of sEPSCs 1 hour after FS in young adults animals (Musazzi et al, 2010; 170-200g Wistar rats), but it was not shown if a similar effect is also present in adult rats.

The sEPSCs were analysed in the FS1h (13 cells from 6 animals) and CTR1h (n=14 cells from 7 animals) groups recorded at -60mV in the whole-cell configuration, in slices bathed in ACSF in the absence of TTX. These recordings had higher baseline noise compared to the mEPSCs recordings because more membrane channels were overall activated and, to include a sufficient number of experiments in our analysis, we fixed the threshold for sEPSCs detection at 16 pA (see Methods). Interestingly, when analysing sEPSCs, some neurons from animals that underwent FS (5 cells from 4 animals, from a total of 13 cells recorded from 6 animals) were characterised by the intermittent appearance of clusters of large events (fig. R.6A). This was reflected in a significant right-shift of the average normalized cumulative histogram of peak amplitudes in the FS1h group, compared to CTR1h (fig. R.6B; 2-way ANOVA of binned peaks distributions: bin x group, $F(19, 475) = 1.65$, $P=0.0414$), indicating the presence of more events with larger amplitude in the stressed group. This cell sub-population is most likely responsible for the significantly larger variance, across experiments, of mean peak amplitudes (Fig.R.2B, inset; $F(12,13)=9.21$, $p=3\cdot10^{-4}$, unpaired t-test of the log of mean amplitudes) in the stressed *vs* control groups, while the difference of grand averages of mean peak amplitudes did not reach the significance ($p=0.069$, same test). In the effort to show that the large-amplitude sEPSCs were a unique effect induced by the acute stress protocol in a subpopulation of neurons, we also measured the CV of peak amplitudes (CV= standard deviation /mean) and we postulated that a CV larger than 0.71 indicates the presence of large-amplitude sEPSCs. We performed a chi-square statistical comparison of the number of cells presenting large ($\geq$0.71) versus small

(<0.71) peak CV, revealing that the relative chance of large peak CV in the CTR1h group was 0% (95% confidence interval: 0 – 0.6079%; P=0.0159, Fisher's exact test). This indicates that large amplitudes sEPSCs were more likely to occur 1 hour after the stress protocol than in control. No significant FS-induced changes were present in sEPSCs frequencies (Fig.R.2C; analysis of inter-event intervals) and 10-90% rise times (Fig.R.2D), as shown by 2-way ANOVA analyses of normalized cumulative histograms, and Mann-Whitney tests of mean values.

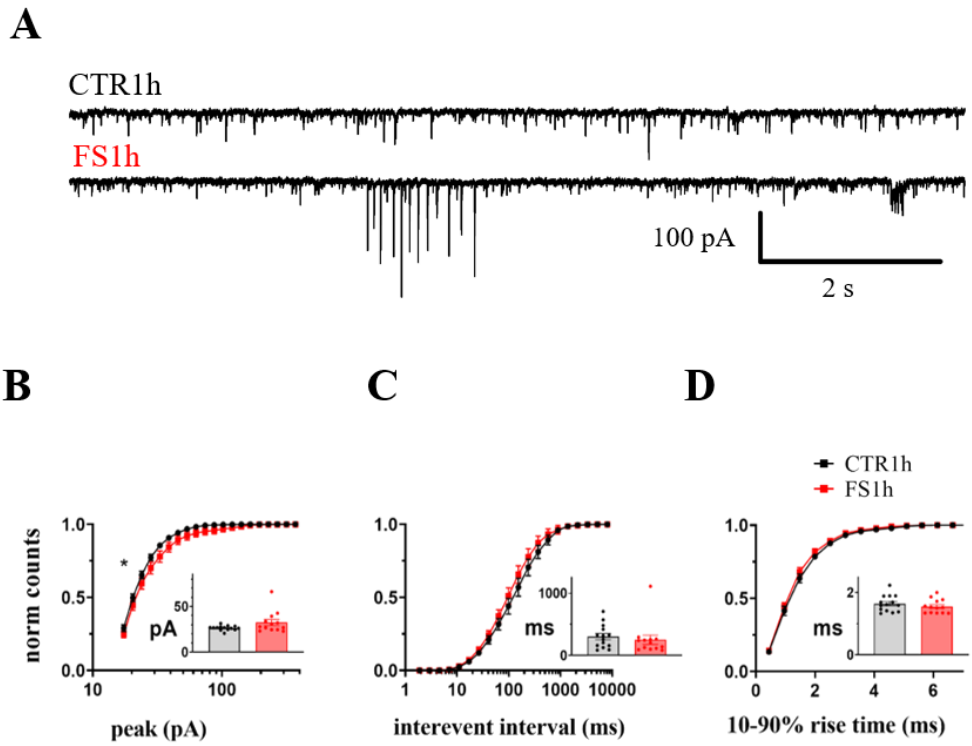

Fig.R.6. A large-amplitude sEPSCs subpopulation appears 1 hour after foot-shock in L2-3 neurons. Patch-clamp whole-cell recordings of spontaneously occurring excitatory synaptic currents (sEPSCs) performed 1 after FS. Holding potential: -60mV. **(A)** Current traces recorded from control (CTR1h, *top trace*), or stressed animals (FS1h, *bottom trace*). Notice the cluster of large (≥100pA) sEPSCs in the FS1h trace. **(B-D)** Normalized cumulative histograms of sEPSC peak amplitude (*left*), inter-event interval (*centre*) and 10-90% rise time (*right*). Average (±s.e.m.) of histogram bins from 14 cells from 7 animals (CTR1h) and 13 cells from 6 animals (FS1h). The peak histograms are significantly different (2-way ANOVA of binned peaks distributions, interaction of bin and group: F (19, 475) = 1.65, P=0.0414). *Insets*: individual values (dots) and group averages (bar) of the mean peak sEPSC amplitude (*left*), mean inter-event interval (*centre*) and mean 10-90% rise time (*right*) for the CTR 1h and FS1h groups. The mean peaks (b, inset) display a significantly larger variance in the FS *vs* CTR group ($F(12,13)=9.21$, $p=3\cdot10^{-4}$).

The clustered occurrence of large sEPSCs in the FS1h group is compatible with the presence of new strong synapses, which are activated intermittently. Alternatively, these clustered large

events could arise from higher excitability of the afferent neuronal network, which could produce bursts of APs, eliciting synchronous bursts of Glu release events. The latter could result in the summation of postsynaptic currents to produce the large amplitude sEPSCs.

4c) Ketamine injection after foot-shock induces a late increase in sEPSCs frequency

Previously published evidence suggests a prolonged enhancement of glutamate transmission after acute FS stress because high-K^+-evoked Glu release from synaptosomes prepared from frontal/prefrontal cortex of rats is boosted by FS, also 24 hours after stress (Musazzi et al., 2017). In the previous paragraph, we have shown an enhancement of sEPSC activity in L2-3 Pyrs shortly after FS stress. We decided to explore the late effect of FS stress on sEPSCs, as there is yet no available description of this phenomenon.

Whole-cell recordings of the spontaneous excitatory activity 24 hours after FS was performed as specified in the previous paragraph. We compared control (CTR24h; n=11 cells from 7 animals) and stressed (FS24h; n=12 cells from 7 animals) animals injected with saline, and stressed animals injected with ketamine (10mg/kg) (FSKet; n=9 cells from 6 animals). Injections occurred 18 hours before slice preparation for the sEPSCs recording. When comparing normalized cumulative histograms of sEPSCs amplitudes (fig.R.7B) in the three groups with 2-way ANOVA, there was no significant main effect of group ($p= 0.2945$), nor a significant interaction of group and bin ($p=0.0812$), although there was a tendency to increased amplitudes in ketamine-treated animals, as also suggested by significant multiple comparisons (Tukey's test; $p=0.036$, FSKet *vs* CTR24h; FSKet *vs* FS24h $p=0.037$). Concerning the frequency of sEPSCs, there was a significant difference among the three groups (main effect of group: $F(2,580)=10.4$, $p<10^{-4}$). Multiple comparisons revealed that this effect was due to shorter intervals in the FSKet group *vs* the other groups (FSKet *vs* FS24h $p<10^{-2}$; FSKet *vs* CTR24h $p<0.05$). The effect can be appreciated as a leftward shift of the FSKet histogram (in green) in fig.R.7C. Finally, when comparing the rise time histograms (fig.R.7D), there was a difference among groups (2-way ANOVA, main effect of group: $F(2,580)=17.8$, $p<0.0001$), which was due to an increase of 10-90% rise times in stressed *vs* control and ketamine-treated animals (Tukey's multiple comparisons: FS24h *vs* CTR24h $p<0.05$; FS24h *vs* FSKet $p<0.01$).

Although the mean values of analysed parameters (fig.R.7B-D, insets) did not display significant differences among groups (Kruskal-Wallis test: $p=0.1374$, peak amplitudes; $p=0.3184$, inter-event intervals; $p=0.0730$, rise times), it can be noticed that FSKet inter-event intervals and rise times values have a lower dispersion, across cells, compared to CTR and

FS24h values (coefficient of variation (CV) of intervals: FSKet 49%; FS24h 129%; CTR 81%; CV of rise times: FSKet 6.4%; FS24h 22.4%; CTR24h 23.4%). Dispersion was low for peak amplitudes in all groups (CV of peaks: 6.4%, FSKet; 19.9%, CTR24h; 20.2%, FS24h).

Overall, these data indicate that, contrary to our expectations, stress-induced alterations of sEPSCs were no more visible 24hrs after FS (fig.R.7A), except for a slight slowing of rise times. On the other hand, ketamine injection was able to shorten the inter-event interval of the sEPSCs, indicating an increase in the frequency of the events, which occurred rather homogeneously across cells. As will be discussed later, one possible explanation for this is that ketamine induces the activation or formation of a discrete number of synapses with shared characteristics.

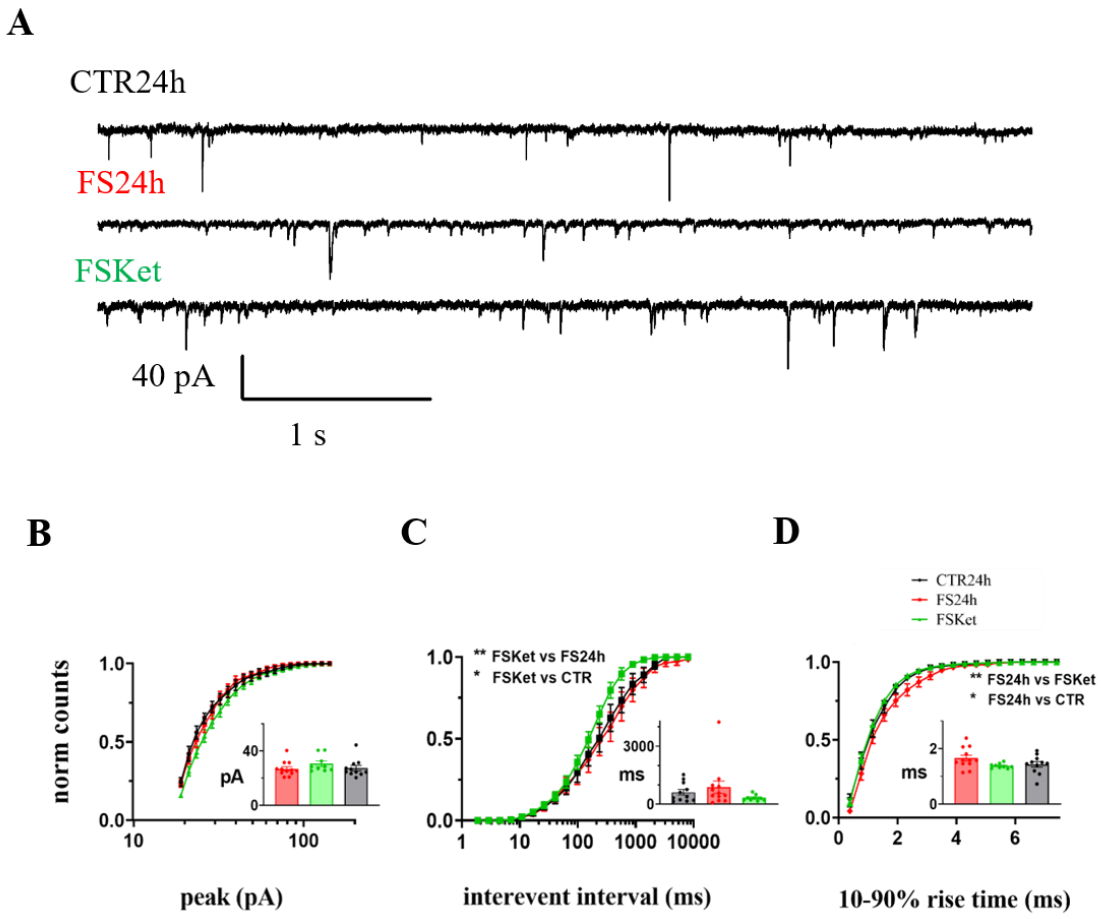

Fig. R.7. Effects of ketamine on sEPSCs 24hrs after stress in L2-3 neurons. Patch-clamp whole-cell recordings of sEPSCs performed 24hrs after FS. Holding potential: -60mV. **(A)** Representative current traces show sEPSCs from CTR24h (*top trace*), FS24h (*middle trace*) and FSKet (*bottom trace*) animals. **(B-D)** Normalized cumulative histograms of sEPSC peak amplitude (*left*), inter-event interval (*centre*) and 10-90% rise time (*right*). Average (±s.e.m.) of histogram bins from 11 cells from 7 animals (CTR24h), 12 cells from 7 animals (FS24h), and 9 cells from 6 animals (FSKet). The peak amplitudes are not significantly different, while the inter-event intervals are different (2-way ANOVA of binned inter-event intervals: there is a main effect of group, $F(2,580)=10.4$, $p<0.0001$; Tukey's multiple comparisons: FS-Ket vs CTR24h, $p<0.05$; FS-Ket vs FS24h, $p<0.01$), as well as the 10-90% rise times (2-way ANOVA, main effect of group, $F(2,580)=17.8$, $p<0.0001$; Tukey's multiple comparisons: FS-24h vs CTR24h, $p<0.05$; FS-24h vs FS-Ket, $p<0.01$). *Insets*: individual values (dots) of the sEPSCs mean peak amplitude (*left*), mean inter-event interval (*centre*) and mean 10-90% rise time (*right*) for CTR24h, FS24h and FSKet cells. Bars indicate the grand average ± s.e.m. of each parameter. The grand averages are not significantly different (Kruskal-Wallis test).

5. Measurement of the average excitatory and inhibitory charges in L2-3 neurons: the effect of acute stress

5a) The total excitatory and inhibitory conductances show a tendency to increase 1 hour after foot-shock

Interestingly, in 2019 a study of the Kash group demonstrated that 90 minutes after a stress protocol involving exposure of subjects to predator odour, there was an increase in the ratio between excitation and inhibition (E/I ratio) restricted to L2-3 in the prelimbic region of the mPFC in adult mice (Hwa et al, 2019). For this reason, having detected an early effect of FS stress on spontaneous excitatory transmission, we decided to evaluate its effects on inhibitory transmission and the balance of the excitatory and inhibitory transmission (E/I ratio).

To explore this aspect, animals were subjected to FS and sEPSCs and sIPSCs were recorded in the whole-cell configuration, using a Cs-based internal solution supplemented with lidocaine (see Methods), in order to block some Na^+- and K^+-channels, allowing to swiftly change holding potential without undermining cell vitality. This choice, however, prevented the description of cellular firing properties. After measuring the reversal potential of excitatory and inhibitory currents (see Methods), we analysed the two types of spontaneous current, recording sEPSCs at the reversal potential of the inhibitory currents (on average -58 mV), and sIPSCs at the zero-current potential of the excitatory transmission (on average + 3 mV). This strategy allowed to equal the excitatory to inhibitory charge ratio with the excitatory to inhibitory total conductance ratio (see Methods). Thanks to the block of K^+ and Na^+ channels, the baseline noise of the traces was relatively small, so we could use a detection threshold of 11 pA for sEPSC and 10 pA for sIPSCs.

Fig.R.8 displays the current traces obtained for sEPSCs and sIPSCs in two exemplar cells (panel A), and the normalized cumulative distributions of peak amplitude, inter-event intervals and 10-90% rise times of sEPSCs (panels B-D) and sIPSCs (panels E-G) obtained in the FS1h (n=12 cells, N=4 animals) and CTR1h groups (n=11 cells, N=4 animals). Statistical comparison of histograms, with 2-way ANOVA, and of the corresponding mean values with the Mann-Whitney test, of considered parameters did not reveal significant differences between the two groups (mean sEPSCs of: peak, CTR1h 20.2±0.8 pA and FS1h 22.61±1.3 pA; inter-event interval, CTR1h 121.3±10.5 ms and FS1h 129.7±14.8 ms; rise 10-90%, CTR1h 1.67±0.04 ms and FS1h 1.77±0.06 ms. Mean sIPSCs of: peak, CTR1h 30.0±1.1 pA and FS1h 33.8±5.8 pA; inter-event interval, CTR1h 87.2±14.5 ms and FS1h 64.8±10.6 ms; rise 10-90%, CTR1h 2.40±0.09 ms and FS1h 2.51±0.12 ms). The failure to reveal the previously reported changes

in sEPSCs with the Cs-based solution contrasts with the visual inspection of traces. Clusters of large sEPSCs were still selectively present in some FS1h cells (fig.R.8A, bottom pair of traces, recording at – 58mV), but their contribution to histograms and means fails to reach statistical significance. Nonetheless, a tendency to an increase of the excitatory transmission in FS1h cells can be appreciated when analysing total charges (fig. R.8H-I). The total charge of sEPSCs and sIPSCs is calculated as the area of a representative stable segment of the respective baseline-subtracted current recordings. The segment was 120s long for sIPSCs (at +3mV holding potential), while in the case of sEPSCs (at -58mV holding potential) in some cells only shorter intervals (always >20s long) were stable enough for integration, and results were multiplied by the appropriate scaling factor for calculating the E/I ratio. The excitatory charge (fig.R.8H) had a tendency to increase 1 hr after FS, although non-significant (CTR1h 368±43 pC, n=10 cells; FS1h 444±45 pC, n=11 cells, means ± s.e.m.; p=0.240, unpaired t-test). A similar tendency to a charge augmentation was visible in the inhibitory charges (fig.R.8I) of stressed animals *vs* controls (CTR1h 670±91 pC, n=11; FS1h 1065±266 pC, n=12, means ± s.e.m.; p=0.486, Mann-Whitney test). This enhancement of charges, however, did not affect the mean E/I ratio (fig.R.8J), that remained invariant in the two groups (CTR1h 0.57±0.07, n=10; FS1h 0.62±0.12, n=11; p=0.782, unpaired t-test), suggesting that the increased conductance of both excitation and inhibition could represent a compensatory mechanism to maintain the optimum E/I balance of the network.

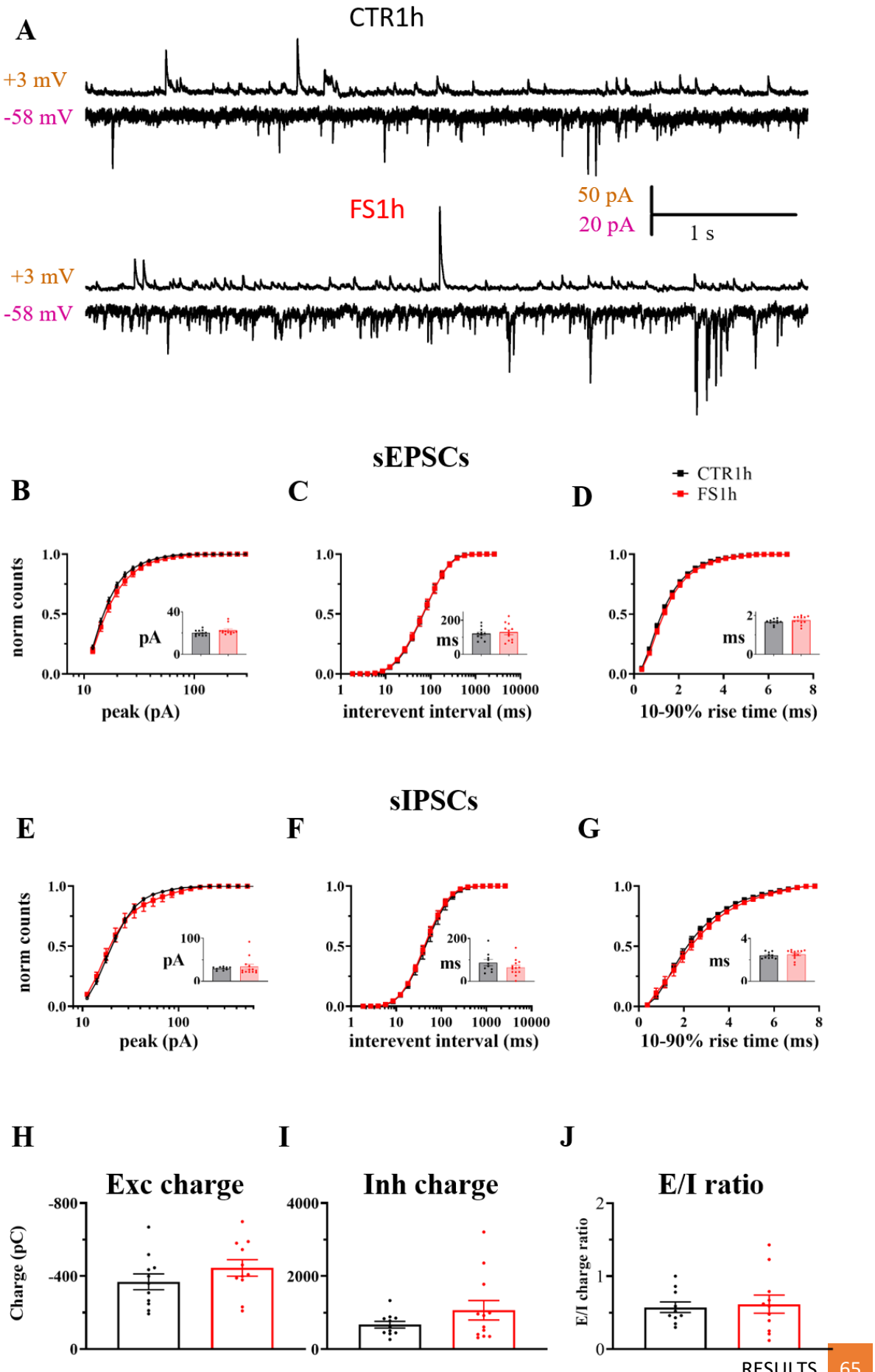
A
CTR1h
+3 mV
-58 mV
FS1h
50 pA
20 pA
1 s
+3 mV
-58 mV
sEPSCs
B
C
D
CTR1h
FS1h
norm counts
peak (pA)
interevent interval (ms)
10-90% rise time (ms)
pA
ms
sIPSCs
E
F
G
norm counts
peak (pA)
interevent interval (ms)
10-90% rise time (ms)
H
I
J
Exc charge
Inh charge
E/I ratio
Charge (pC)
E/I charge ratio

Fig. R.8 **Slight increase in excitatory and inhibitory charges 1h after foot-shock stress in L2-3 neurons**. sEPSCs and sIPSCs were recorded at -58 mV and +3 mV, respectively, with a Cs-Gluconate-based internal solution in each cell of the CTR1h (11 cells from 4 animals) and FS1h (12 cells from 4 animals) experimental groups. **(A)** Representative traces of inhibitory (outward) and excitatory (inward) synaptic currents from a CTR1h (top pair of traces) and an FS1h (bottom pair) cell. (**B, E**) Average (±s.e.m.) normalized cumulative histogram of peak amplitudes of sEPSCs (B) and sIPSCs (E). Amplitude threshold was 11 pA and 10 pA for sEPSCs and sIPSCs, respectively. Insets in B, E represent mean peaks in each cell (dots) and their grand average (bars) for CTR1h and FS1h. (**C, F**) Average (±s.e.m.) normalized cumulative histogram of inter-event intervals of sEPSCs (C) and sIPSCs (F). Insets: mean inter-event intervals in each cell (dots) and their grand average (bars). (**D, G**) Average (±s.e.m.) normalized cumulative histogram of 10-90% rise times of sEPSCs (D) and sIPSCs (G). Insets: mean rise time in each cell (dots) and their grand average (bars). Neither 2-way ANOVA comparison of binned distributions, nor t-test of mean values reported a significant difference between the two groups in B-G. (**I, J**) The total charge transfer of the excitatory (I) and inhibitory (J) conductance was evaluated as the total area of the respective baseline-subtracted current traces over a fixed time interval (20-120 s). There was a non-significant tendency to a slight increase of both charges in FS1h vs CTR1h (t-test excitatory charge, p=0.24; t-test inhibitory charge, p = 0.48). (**H**) E/I ratio (ratio of excitatory to inhibitory charge), in each cell (dots), and the E/I grand average (bars) in CTR1h and FS1h.

5b) Increase of the excitatory conductance and E/I ratio 24 hours after acute stress

We next evaluated the conductances and E/I ratio at later times. For this reason, we recorded sEPSCs and sIPSCs 24 hours after the foot-shock stress, with the same strategy as above. We compared recordings from 10 cells (9 animals) in the FS24h group and 7 cells (6 animals) in the CTR24h group.

The analysis of the normalized cumulative intervals distributions of sEPSCs (fig. R.9C) revealed a significant difference between the two groups (2-way ANOVA, interaction of group and bin, $F(19, 285)=2.19$, $p=0.0033$ (**)), with a leftward shift of the FS24h intervals histograms, indicating smaller intervals. The average of mean values of intervals had a non-significant tendency to decrease in the FS24h group (FS24h 161±18.5ms; CTR24h 235±39ms; means ± s.e.m.; p=0.081, unpaired t-test), suggesting, accordingly to the interval histograms, an increase in sEPSCs frequency in the FS24h group. Meanwhile, the analysis of means and distributions of the other parameters did not find any significant differences neither in the excitatory nor the inhibitory transmission (mean peak: FS24h 22.3 ± 1.8 pA; CTR24h 21.4 ± 2.1 pA; means ± s.e.m.; p=0.760, unpaired t-test; mean rise time: FS24h 1.70 ± 0.14ms; CTR24h 1.48±0.16ms; means ± s.e.m.; p=0.294, unpaired t-test). In summary, 24 hours after FS the only suggested change in spontaneous postsynaptic currents is the increase in the frequency of excitatory currents.

In parallel, we analysed the total excitatory and inhibitory charges 24 hours after stress, as above (fig. R9H-I). Interestingly, FS increased the excitatory charge (means ± s.e.m.: CTR24h 225±61 pC, n=6; FS24h 397±40 pC, n=9, p=0.0286 (*), unpaired t-test), as suggested by the sEPSC frequency change, while it did not induce any sustained change in the inhibitory charge (means ± s.e.m.: CTR24h 926±167 pC, n=6; FS24h 1139±245 pC, n=9, p=0.776, Mann-Whitney test). These combined effects result in a significant enhancement of the E/I ratio (0.24±0.03, n=6, CTR1h; 0.43±0.06, n=9, FS1h; p=0.0425 (*), unpaired t-test) (fig. R.9J), suggesting that the inability of the network to preserve the physiological balance of excitation and inhibition 1 day after FS could contribute to its maladaptive effects.

It should be also noticed that the measurement of postsynaptic currents and the total charge transfer with the Cs-based solution allowed us to detect sustained differences in spontaneous synaptic transmission that could not be detected in experiments using the K-Gluconate internal solution. This could be explained by the fact that recordings in the latter condition had a more noisy baseline, which prevented detection of a large fraction of sEPSC, hindering the observation of an increase in the frequency of sEPSCs 24 hours after stress. A further explanation could be offered by the possibility that the neuronal population sampled in these experiments includes not only RS Pyr neurons, but also other pyramidal (van Aerde and Feldmayer, 2015) and non-pyramidal (Wang and Gao, 2009) neuronal types, given that firing properties were not verified.

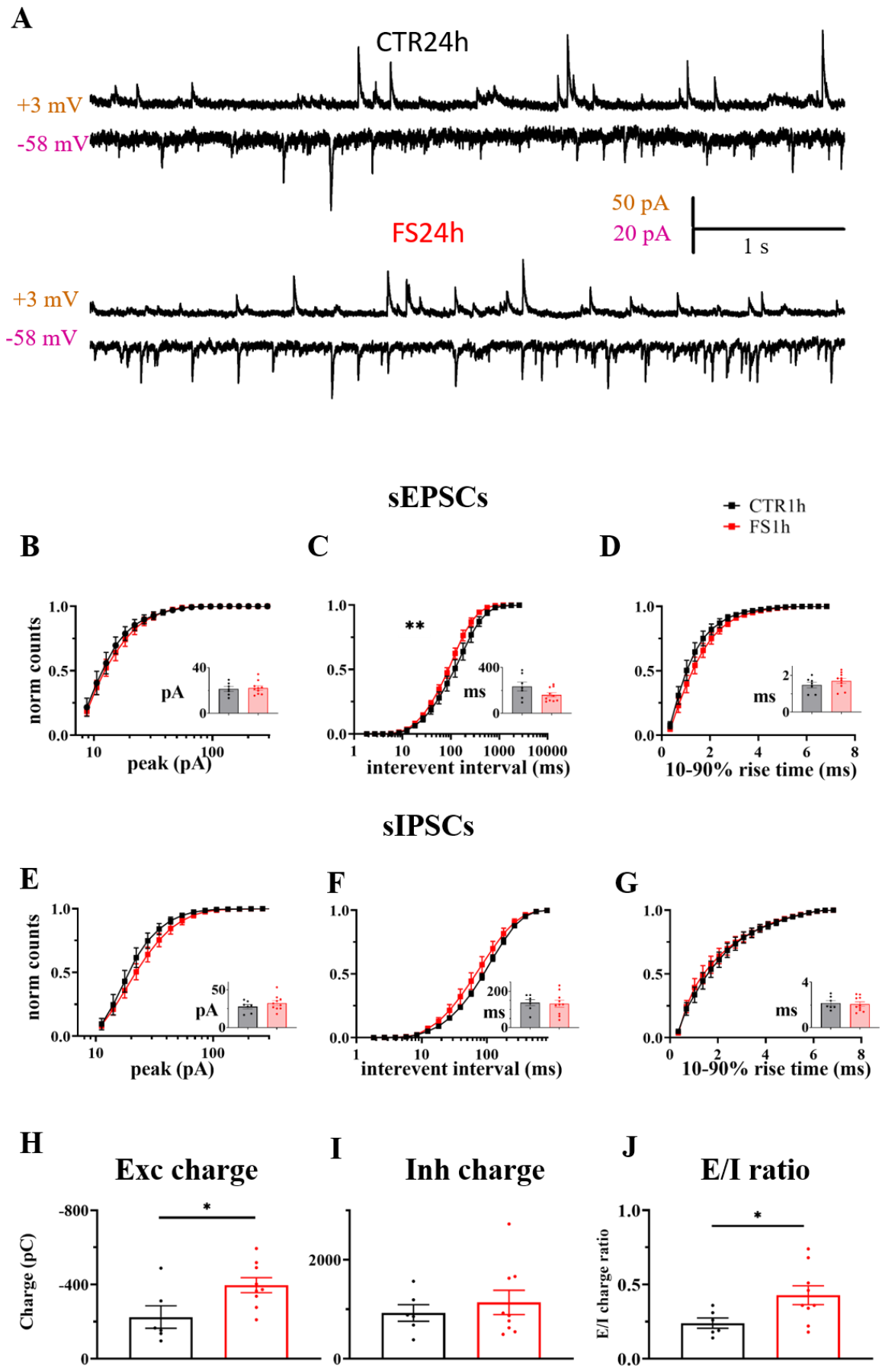
A
CTR24h
+3 mV
-58 mV
50 pA
20 pA
1 s
FS24h
+3 mV
-58 mV
sEPSCs
CTR1h
FS1h
B
C
D
norm counts
peak (pA)
interevent interval (ms)
10-90% rise time (ms)
pA
ms
**
sIPSCs
E
F
G
H
Exc charge
I
Inh charge
J
E/I ratio
Charge (pC)
E/I charge ratio
*

Fig. R.9 **Increase of excitatory conductance and E/I ratio 24 hrs after foot-shock stress in L2-3 neurons.** sEPSCs and sIPSCs were recorded at -58 mV and +3 mV, respectively, with a *Cs-based* internal solution in each cell of the CTR24h (7 cells from 6 animals) and FS24h (10 cells from 9 animals) experimental groups. (**A**) Representative traces of inhibitory (outward) and excitatory (inward) synaptic currents from a CTR24h (top pair of traces) and an FS24h (bottom pair) cell. (**B, E**) Average (±s.e.m.) normalized cumulative histogram of peak amplitudes of sEPSCs (B) and sIPSCs (E). Amplitude threshold was 11 pA and 10 pA for sEPSCs and sIPSCs, respectively. Insets in B, E represent mean peaks in each cell (dots) and their grand average (bars) for CTR24h and FS24h. (**C, F**) Average (±s.e.m.) normalized cumulative histogram of inter-event intervals of sEPSCs (C) and sIPSCs (F). 2-way ANOVA comparison of sEPSCs binned distributions reveals an interaction of group and bin in this experiment (F (19, 285)=2,19, p=0,0033), although Sidak's multiple comparisons test failed to reveal any point where the two curves were different. Insets: mean inter-event intervals in each cell (dots) and their grand average (bars). (**D, G**) Average (±s.e.m.) normalized cumulative histogram of 10-90% rise times of sEPSCs (D) and sIPSCs (G). Insets: mean rise time in each cell (dots) and their grand average (bars). Neither 2-way ANOVA comparison of binned distributions, nor t-test of mean values reported a significant difference between the two groups. (**I, J**) The total charge transfer of the excitatory (I) and inhibitory (J) conductances was evaluated as the total area of the respective baseline-subtracted current traces. t-test comparison of excitatory charges revealed a significant difference between the two groups (p= 0,0286 (*)). (**H**) E/I ratio, in each cell (dots), and the E/I grand average (bars) in CTR24h and FS24h (t-test, p-value= 0,0425 (*)).

6. Ketamine effects on L5 mPFC neurons: excitability and synaptic transmission

Several studies have shown that the mPFC is a key region for the therapeutic action of ketamine after chronic stress (see Introduction). For example, it has been shown that ketamine counteracts the morphological changes induced by chronic stress such as the loss of synaptic spines in the apical dendritic region, and the consequent synaptic transmission changes, in L5 Pyr neurons of the prelimbic and anterior cingulate area in the mPFC, 24 hours after the injection (Li et al, 2011; Liu et al., 2015). We speculated that the effects of severe trauma such as foot-shock stress might induce sustained effects comparable to chronic stress effects, and we decided to evaluate whether changes in the excitatory transmission (mEPSCs and sEPSCs) were detectable in L5 Pyrs 24 hours after FS and if ketamine treatment was able to reverse them.

Similar to our study of L2-3 Pyrs, we performed whole-cell recordings of RS neurons from animals randomly assigned to four different groups: rats undergoing foot-shock stress protocol and receiving an injection of saline (FS24h) or ketamine (10mg/kg) (FSKet) 6 hours after exposure to the stressor, and control animals injected 18 hours before the electrophysiological experiment with either saline (CTR24h) or ketamine (10mg/kg) (CTRKet). The results presented in this section should be considered as preliminary, as they are based on a small sample.

6a) Ketamine injection decreases excitability in stressed animals

As for the L2-3 Pyrs, we preliminarily investigated the excitability of the L5 RS neurons. After break-in, recordings were switched to CC mode, and cells were maintained around -65 to -70 mV (on average: -67 ± 2mV), close to the resting potential of L5 Pyrs. We proceeded to record the neuronal firing elicited by injections of current steps with increasing intensity, and we plotted the number of action potentials in 1s *vs* current injection, to reconstruct the *f*-I curve for each cell. The graph in fig.R.10 reports the superimposed average *f*-I curves of all groups (except the CTRKet group, not available). It can be visually appreciated that the average slope of the *f*-I curve is larger for cells in the FS24h group. When performing a statistical comparison with the 2-way ANOVA test, with group and stimulus intensity as factors, we found a significant difference among the three groups (interaction group x stimulus: $F(18,189)=1.70$, $p=0.0423$). Post-hoc Tukey's multiple comparisons test showed a significant difference between FS24h and FSKet in the range 60-200pA ($p=0.026$). This result indicates that the injection of a sub-anaesthetic ketamine dose opposes putative stress effects on the neuronal excitability. However, we were not able to prove a statistically significant increase of Pyrs excitability in stressed animals vs control (in FS24h *vs* CTR24h).

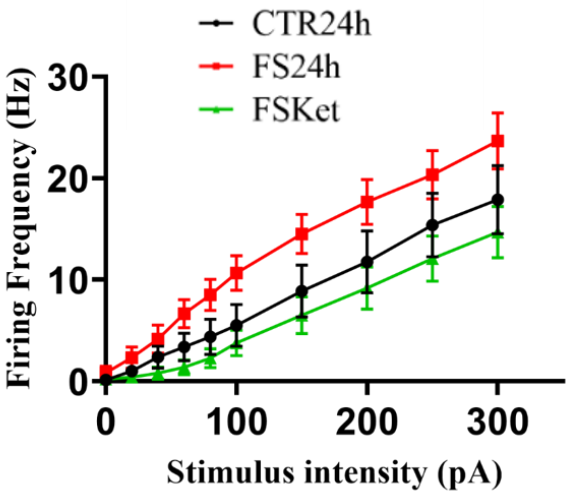

Fig.R.10 **Neuronal excitability in L5 RS neurons of stressed animals is decreased by ketamine**. Spike frequency elicited by increasing current injections (*f*-I curve) in mPFC L5 regular spiking neurons from animals sacrificed 24 hrs after FS and injected with saline (FS24h) or ketamine (10mg/kg; FSKet) 6 hrs after FS, or controls (CTR24h) injected with saline 18 hrs before recordings. The graph reports the average (±s.e.m.) firing frequency of CTR24h (10 cells from 8 animals), FS24h (6 cells from 5 animals) and FSKet (9 cells from 5 animals) neurons recorded at -67±2 mV, vs stimulus current. Two-way ANOVA analysis does not reveal a main effect of the experimental group (p=0.051), however, there is a significant interaction between stimulus intensity and group (F(18,189)=1,70, p=0,0423). The post-hoc Tukey's multiple comparisons test reveals a significant difference between FS24h and FSKet in the range 60-200pA (mean p=0.026).

6b) Modulation of mEPSCs in L5 Pyrs by acute stress and ketamine

Recordings of miniature currents (fig. R.11A) were performed as in L2-3, holding the cells at -60mV. After verifying the cell firing behaviour and passive properties in CC, we acquired for 2 minutes sEPSC activity (see next paragraph), and immediately after we started bath perfusion with a cocktail of blockers (Picrotoxin (100µM), Strychnine (1µM) and TTX (500 µM)) dissolved in the ACSF solution. After confirming disappearance of firing in CC, the recording was switched to voltage-clamp (VC) and current traces containing mEPSCs were recorded for 120s. The analysis of mEPSCs revealed the presence of fast events that were not detected by the template used in L2-3 analysis, forcing us to change the detection method. We used two templates ("fast" and "slow" templates, see Methods) for the simultaneous detection of faster and slower excitatory spontaneous currents. Statistical analysis of normalized cumulative histograms with 2-way ANOVA revealed that neither peak amplitudes, nor intervals nor rise times distributions were significantly different among the four groups analysed (CTR24h: n=10 cells, 6 animals; FS24h: n=9 cells, 5 animals; FSKet: n=7 cells, 5 animals; CTRKet: n=7 cells,

3 animals). Moreover, no differences were present among mean values of mEPSCs peak amplitude (mean peak±s.e.m., CTR: 19.6±1.6 pA; FS24h: 16.3±0.8 pA; FSKet: 16.1±0.7 pA; CTRKet: 16.4±1.6 pA), inter-event intervals (mean interval±s.e.m., CTR: 476.5±113.8 ms; FS24h: 602.1±105.7 ms; FSKet: 498.9±57.9 ms; CTRKet: 834.9±294.5 ms), and rise times (mean10-90% rise time±s.e.m., CTR: 2.2±0.1 ms; FS24h: 2.1±0.2 ms; FSKet: 1.9±0.1 ms; CTRKet: 2.2±0.3 ms) across the studied groups (fig.R.11B-D).

These data show that we could not confirm our initial hypothesis that acute stress produces sustained effects on miniature excitatory transmission in L5 Pyrs. Moreover, we could not prove that either ketamine per se or ketamine in stressed animals were able to modify mini transmission.

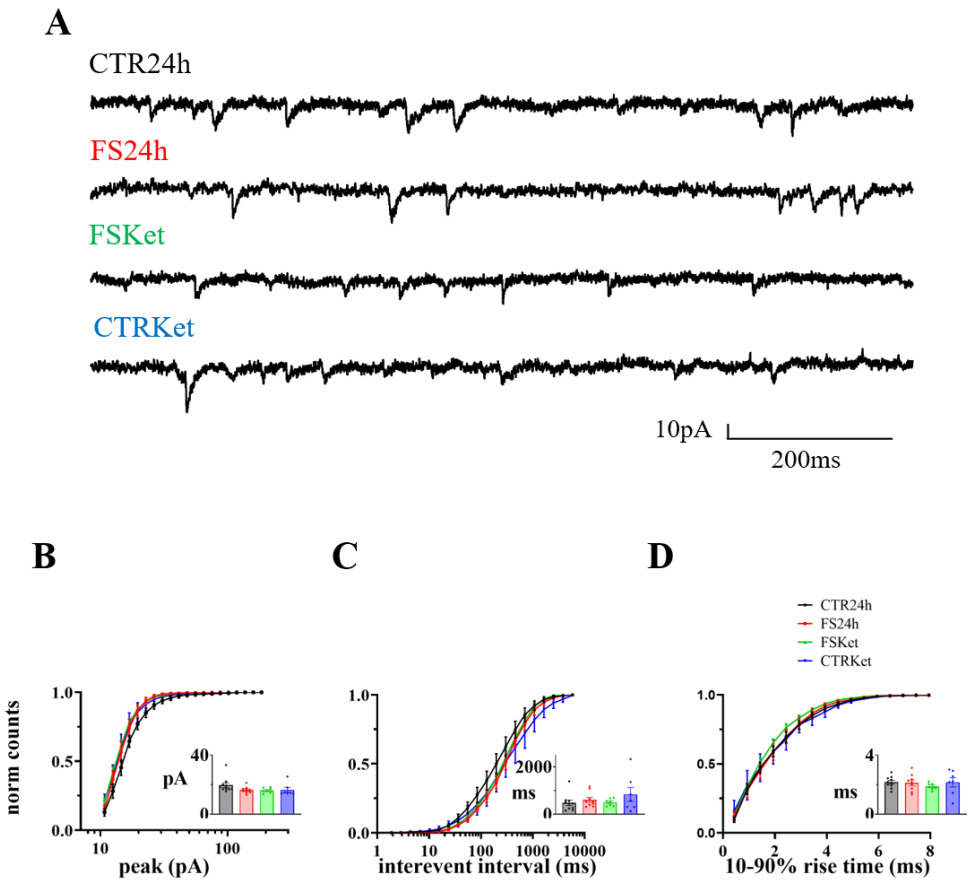

Fig.R.11. **No effects of acute stress and ketamine on miniature excitatory transmission 24 hours after foot-shock in L5 neurons**. Patch-clamp whole-cell recordings of mEPSCs performed 24hrs after foot-shock, from animals injected intraperitoneally (i.p.) with saline (FS24h) or ketamine (10mg/kg) (FSKet) 6hrs after FS, or from saline-injected (CTR24h) or ketamine-injected (CTRKet) controls. Tetrodotoxin (TTX, 1µM), picrotoxin (PTX, 0.1 mM) and strychnine (Str, 1 µM) present to block action potentials and inhibitory synaptic inputs through GABAa receptors. Holding potential: -60mV. (A) Representative mEPSCs traces from CTR24h (*top*), FS24h (*middle-up*), FSKet (*middle-down*) and CTRKet (*bottom*), showing mEPSCs as inward deflections. (B-D) Average (±s.e.m.) normalized cumulative histograms of mEPSC peak amplitude (*left*), inter-event interval (*centre*) and 10-90% rise time (*right*) from CTR24h (10 cells from 6 animals), FS24h (9 cells from 5 animals), FSKet (7 cells from 5 animals) and CTRKet (7 cells from 3 animals). Insets: individual values (dots) and group average (bar) for each group, of the mean peak mEPSC amplitude (*left*), mean inter-event interval (*centre*) and mean 10-90% rise time (*right*). No significant differences between the two groups were present in histograms or mean values.

6c) Modulation of sEPSCs in L5 Pyrs by acute stress and ketamine

We finally performed an initial analysis aimed at verifying the sustained effects of acute stress and sub-anaesthetic ketamine on sEPSCs. The following data are preliminary, as they are based on just a few experiments. The sEPSCs were recorded at -60mV in the whole-cell configuration in slices bathed in ACSF in the absence of TTX (fig. R.12A). Detection of sEPSCs was performed using the detection strategy explained above, using two templates (fast and slow template, see Methods). We analysed 6 cells from 3 animals for CTR, 7 cells from 2 animals for FS24h, 3 cells from 2 animals for FSKet and 8 cells from 3 animals for CTRKet, respectively. As for mEPSCs, statistical analysis of normalized cumulative histograms (fig.R.12B-D) with 2-way ANOVA did not reveal differences among groups in peak amplitudes, intervals or rise times distributions. Moreover, no differences were found among mean values of sEPSCs peak amplitude (mean peak±s.e.m., CTR: 19.2±1.6 pA; FS24h: 19.9±1.1 pA; FSKet: 24.4±6.6 pA; CTRKet: 21.6±3.1 pA), inter-event intervals (mean interval±s.e.m., CTR: 314±157 ms; FS24h: 278±65 ms; FSKet: 504±266 ms; CTRKet: 337±100 ms), and of rise times (mean10-90% rise time±s.e.m., CTR: 1.9±0.1 ms; FS24h: 2.1±0.2 ms; FSKet: 1.7±0.2 ms; CTRKet: 2.0±0.1 ms) across the studied groups (fig.R.11B-D).

The absence of foot-shock induced effect on both mEPSCs and sEPSCs in L5 Pyrs is in contrast with our working hypothesis that acute stress produces sustained effects on excitatory transmission in L5 Pyrs, and that ketamine could reverse these effects. However, the analysis presented is based on a very small sample and is therefore preliminary. Our sample should be increased in future experiments to reach more reliable conclusions.

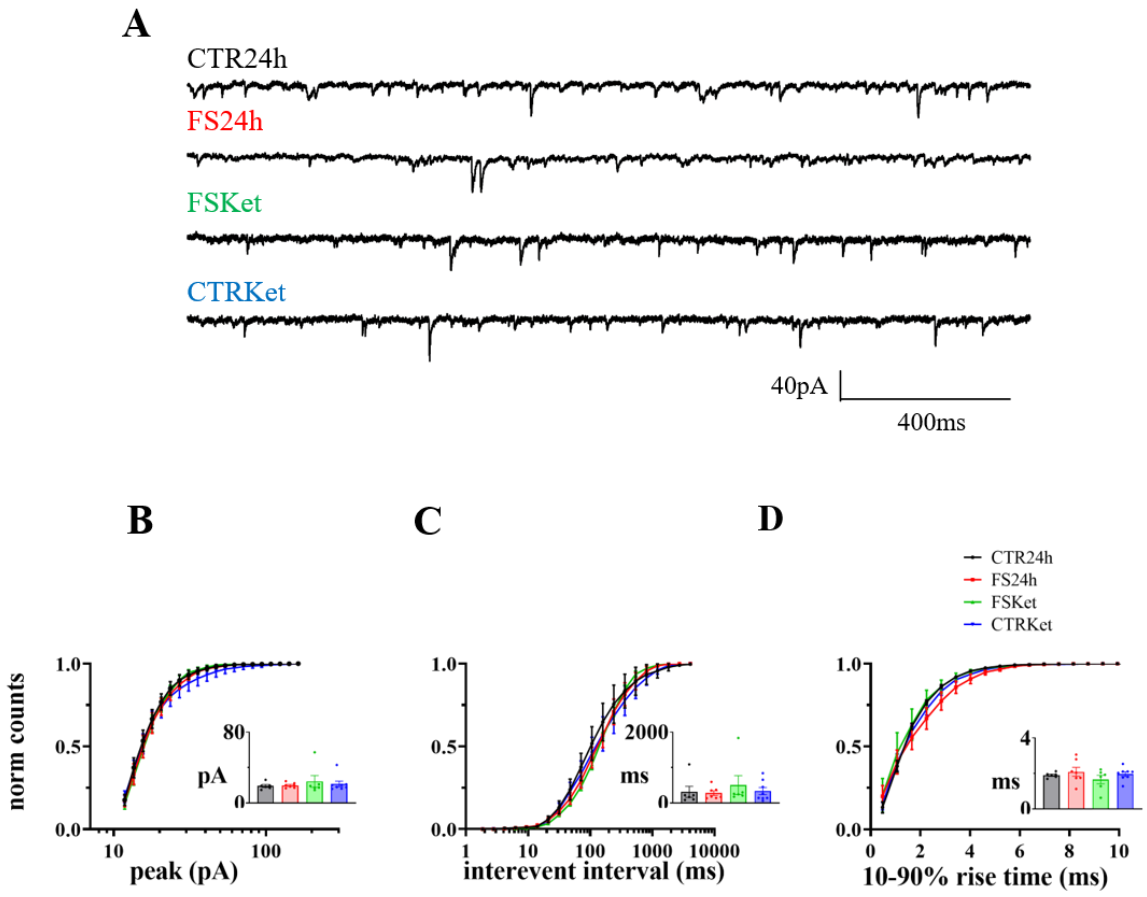

Fig.R.12. **Lack of sustained effects of foot-shock or ketamine on L5 sEPSCs.** Patch-clamp whole-cell recordings of sEPSCs currents performed 24hrs after foot-shock, from animals injected intraperitoneally (i.p.) with saline (FS24h) or ketamine (10mg/kg) (FSKet) 6hrs after FS, or from saline-injected (CTR24h) or ketamine-injected (CTRKet) controls. Holding potential: -60mV. (**A)** Current traces show sEPSCs from CTR24h (*top trace*), FS24h (*middle trace*), FSKet (*middle-down*) and CTRKet (*bottom*) animals. **(B- D)** Average (±s.e.m.) normalized cumulative histograms of sEPSC peak amplitude (*left*), inter-event interval (*centre*) and 10-90% rise time (*right*) from CTR24h (6 cells from 3 animals), FS24h (7 cells from 2 animals), FSKet (3 cells from 2 animals) and CTRKet (8 cells from 3 animals). Insets: individual values and group average, for CTR, FS 24h and FSKet, of the mean peak mEPSC amplitude (*left*), mean inter-event interval (*centre*) and mean 10-90% rise time (*right*). No significant differences between the three groups were present in histograms or mean values.

DISCUSSION

The mPFC plays a central role in many pathological conditions derived from stressor exposure. Our study aimed to characterise the putative alterations on local synaptic transmission in this region induced by a single session of unescapable foot-shock stress (FS), both at early and late time, in order to reveal possible maladaptive mechanisms that could lead to the development of psychopathological conditions. Given the presence of some common morphological characteristics between chronic stress and sustained effects of acute stress, such as dendritic retraction in the mPFC prelimbic (PL) area (Nava et al, 2017), we decided to investigate the alterations in synaptic transmission in the PL of the mPFC of adult rats, 1 day after exposure to the stressor. Moreover, given that in chronic stress models the NMDAR antagonist ketamine, used at low, anti-depressant doses, has already reached its peak 1 day after the injection (Li et al, 2011), this time point was also chosen to assess the possible effects of ketamine on acute stress-induced alterations. Intending to devise a rapid therapeutic intervention after acute stress, we examined the ketamine effect on synaptic transmission of stressed animals when injected 6 hours after the stress.

Focusing at first on layer 2-3 (L2-3) of the PL region in the mPFC, we have demonstrated that, in adult rats, foot-shock stress transiently induces the intermittent activation of strong excitatory synapses onto regular spiking (RS) pyramidal neurons (Pyrs), that could increase the amount of glutamate (Glu) released under action potential guidance, in accordance with the notion of an early increase in depolarization-evoked Glu release. Despite the fact that, 24 hours after acute stress, we could not demonstrate any acute stress-induced alteration in the spontaneous or miniature excitatory transmission (sEPSCs, mEPSCs) in RS Pyrs, we have shown that, in a mixed population of L2-3 neurons (E/I experiments, fig.R9), the total excitatory conductance increases, in parallel with a possible increase in the frequency of excitatory currents, as suggested by the difference in the inter-event interval distribution, that might contribute to the increased E/I ratio. Moreover, we have shown that ketamine injection increases the frequency of spontaneous excitatory inputs in RS Pyrs of stressed animals 1 day after the traumatic insult. Neither acute stress nor ketamine after stress could be confirmed to change either frequency or amplitude of miniature excitatory synaptic transmission in RS pyramidal neurons, contrary to previous shreds of evidence in other acute or chronic stress models (see below). Finally, a clear effect of ketamine at sub-anaesthetic doses on L5 neurons of the PL region of the mPFC from naïve or chronically stresses animals was reported by Liu et al. (2015), and for this reason, we started to explore the ketamine effects in this layer in the acute stress foot-shock model. In our

preliminary L5 analysis, we could not find yet any alteration provoked by FS and/or ketamine in the excitatory transmission recorded 1 day after the acute stress.

Acute stress effects on firing

Stress morphological and functional effects in the mPFC may vary according to the neuronal subcircuit affected (e.g., in chronic stress: Shansky et al., 2009; Liu et al., 2015; Liu et al., 2020). Prefrontal projection neurons characterised by different firing patterns may be involved in the activity of distinct local and long-range circuits in the mPFC, similarly to what happens in other cortical regions (somatosensory cortex: Hattox and Nelson, 2007; Le Be´ et al, 2007; frontal cortex: Morishima and Kawaguchi, 2006; Otsuka and Kawaguchi, 2008, 2011; visual cortex: Kasper et al., 1994; Christophe et al., 2005; Brown and Hestrin, 2009). Furthermore, it was reported that different firing patterns correspond to different morphological features of pyramidal neurons (van Aerde and Feldmeyer, 2015), including a different extension of the dendritic tree that could influence the number of synaptic connections and consequently the frequency of the post-synaptic current. For all these reasons, we aimed at selecting a uniform neuronal population, which in our hands was done by selecting neurons according to their firing pattern upon current injection, and to their input resistance (see Methods). By only allowing RS neurons with low input resistance in our sample, we could exclude the most prominent population of interneurons, the PV^+ fast-spiking interneurons, as well as other interneurons (Wang and Gao, 2009) and bursting or adapting pyramidal neurons.

Given the mPFC role as the hub of stress response coordination, a stress-induced firing alteration can be expected to regulate communication between the mPFC and other brain areas. There are very few published studies of neuronal excitability in the PL region after acute stress exposure. The work of Varela et al. (2012) suggests that deeper layers (L5-6) of this area are involved in the so-called behavioural immunization phenomenon, consisting in the individual perception of control over the stressor, that allows blunting of the behavioural and neurochemical stressor impact. This study reports a change in action potential dynamics, leading to an increase in neuronal excitability (gain of the *f*-I curve), only in rats exposed to acute escapable stress, but not to inescapable stress.

Our results suggest that immediately after foot-shock there is no alteration of the firing pattern of RS neurons in L2-3 of the prelimbic mPFC. This is in contrast with the reported dopamine D4R-dependent increase in spontaneous firing after acute mild restrain stress in adolescent animals (Yuen et al., 2013). It is also in contrast with the effect of acute mild stress used in the

study of working memory performance (Arnsten, 2015). Indeed the L2-3 layer is connected to the amygdala (Gabbot et al, 2005), which upon acute mild stress is thought to be disinhibited by the silencing of the mPFC. This would result from high levels of noradrenergic α1-adrenoceptor and dopaminergic D1 receptor stimulation, activating feedforward calcium–protein kinase C and cyclic AMP–protein kinase A signalling, which open HCN and KCNQ channels to weaken synaptic efficacy in spines and ultimately inhibiting neuronal firing (Arnsten, 2015). While foot-shock stress is known to acutely increase NA and DA release in the mPFC (Dazzi et al., 2001), the pattern of expression of adrenergic and dopaminergic receptor subtypes in the mPFC is complex (Santana and Artigas, 2017), and it is possible that the neurons analysed in our work were not endowed with the receptors required to participate in this pathway. Moreover, this modulation might not be preserved in the slice preparation.

Our analysis of neuronal excitability 1 day after foot-shock suggests on one side a lack of stress effects in L2-3 and on the other a stress-induced increase in the excitability of L5 principal neurons. These differences could mirror a different regulation of distinct neuronal microcircuits connecting the mPFC subregions to other areas (Gabbot et al, 2005). In particular, L5 neurons receive dopaminergic and glutamatergic connections from cells of the ventral tegmental area (VTA) (Gabbot et al, 2005; Douma and de Kloet, 2020), regions involved in stress adaptation. A study on $D1R^+$ and $D2R^+$ neurons in mice reported distinct changes in the firing activity of these neurons in L5 of PL after a chronic unpredictable stress paradigm (CUS; Anderson et al, 2019), with $D2R^+$ neurons displaying a decrease in the *f*-I gain, and $D1R^+$ neurons exhibiting an initial small gain increase followed by sudden firing arrest for more intense stimuli; overall in no case a gain increase for intense stimuli was reported, contrary to our results. This evidence suggests that 24 hours after acute stress the mPFC PL area is not affected in the same way as with chronic stress.

We found that injection of ketamine decreased the excitability of L5 neurons in stressed rats. This effect could be the consequence of the increased activity of interneurons, as suggested by a study of Ng et al. (2018), where it was demonstrated that ketamine under chronic stress conditions increased the excitability of PV^+ fast-spiking interneurons of the frontal cortex.

Acute stress effect on L2-3 miniature excitatory synaptic transmission

Miniature excitatory transmission is due to spontaneous, action potential (AP)-independent vesicle release. A change in mEPSCs can be taken as a clear indication of regulation of pre- or post-synaptic molecular mechanisms, while regulation of spontaneous EPSCs, occurring in the presence of spontaneous APs, might be secondary to an increase in neuronal firing. On the other

side, a regulation affecting the probability of AP-evoked release could in principle leave unaffected the probability of AP-independent vesicle fusion, i.e. miniature release (Kaeser and Regehr, 2014). It is also unclear whether or not the molecular machinery giving rise to mEPSCs is at least partially molecularly distinct from the machinery governing AP-dependent release (Kavalali, 2015). These considerations explain why it is not surprising that mEPSCs and sEPSCs might be distinctly regulated by stress.

In our study, we could not detect any acute stress-induced modulation of miniature transmission in L2-3 Pyrs, nor immediately (1 hour) after stress, or 1 day later. This is in contrast with the hypothesis suggested by morphological studies demonstrating a larger density of spines in L2-3 dendrites 1 hour after FS (Nava et al, 2014), as well as 1 day after FS (Nava et al., 2017), that should correlate with an increase in mEPSCs frequency. However, it is possible that the newly formed synapses reported in those studies were non-functional silent synapses, as they were mainly small, non-perforated, or axo-shaft synapses (Nava et al., 2014), or small volume spine synapses (Nava et al., 2017). It can be argued that an increase in mEPSCs frequency might go undetected if due to activity in newly formed synapses at the far end of distal dendrites, because of dendritic filtering. However, the possibility that our detection might not see these new synapses is challenged by the fact that the newly formed spines are distributed across the L2-3 (Nava et al, 2014), and should not be confined to the distal part of the dendritic tree.

Previous studies in mPFC L5 Pyrs of juvenile (3-4 weeks) male rats have shown that mEPSC amplitude is enhanced after mild acute stress, and depressed after chronic stress exposure, due to an increase or decrease in the expression of postsynaptic AMPA and NMDA receptors, respectively (Yuen et al, 2009, 2012). Several factors may explain the differences between the studies of Yuen and colleagues and our result, including the young age of the animals and the milder stressor. Of notice, improved performance of young, mildly stressed rats in mPFC-mediated tasks was demonstrated (Yuen et al, 2009), suggesting that the increase in mEPSCs amplitude could be a pro-adaptive mechanism. mEPSCs in our work do not seem to be altered 1 day after FS, neither in L2-3 nor in L5. This seems quite different from what happens in chronically stressed adult mice, where mEPSCs frequency is enhanced in a subpopulation of L5 neurons expressing D1 receptor, while it is reduced in L5 neurons expressing D2 receptor (Anderson et al, 2019). Our results could be reconciled with these chronic stress results in the hypothesis that our sample included both $D1R^{+}$ and $D2R^{+}$ cells, which are altered by stress in opposite ways.

Acute FS effects on spontaneous AP-dependent transmission

Coming to AP-dependent transmission, in the present study we observed, in L2-3 neurons at early times after exposure to the stressor, the appearance of intermittent clusters of large-amplitude sEPSCs. This is consistent with previous results obtained for sEPSCs in younger animals (Musazzi et al., 2010; 175-200g rats weight). This is also consistent with the demonstration of an increase in Glu release from synaptosomes prepared from the mPFC/FC, 1 hour after foot-shock (Musazzi et al, 2010), which was paralleled by the increase of the (functionally defined) readily releasable pool of synaptic vesicles, of vesicle docked to the presynaptic plasma membrane, and of phosphorylated-Ser^{9} synapsin 1 (Treccani et al, 2014). The clusters of large EPSCs might arise from an enhanced release probability at perforated spine synapses in L2-3, where it was shown that presynaptic compartments facing the perforated spine have an increased number of docked vesicles after FS (Nava et al, 2015). It is also possible that these events arise from randomly generated bursts of action potentials in the afferent neuronal network. This bursting could be secondary to synaptic changes elsewhere in the network and/or to a change of membrane excitability, possibly occurring in non-RS Pyrs or in interneurons since we could not detect this phenomenon in our analysis of firing. An increased firing of afferent neurons could synchronize release from multiple sites, explaining our detection of large amplitude sEPSCs. Currently we cannot distinguish between regulation of presynaptic release mechanisms, postsynaptic responsivity, or regulation of network excitability as causal mechanisms generating the stress-related clusters of large amplitude sEPSCs.

Since we showed an increase in the excitatory transmission in the prelimbic L2-3, we next investigated the presence of an increase in the ratio of average excitatory to inhibitory conductance (E/I ratio) in L2-3 neurons, inspired by a recent study in adult mice showing an increase in the E/I ratio selectively in L2-3 neurons of the PL area in animals exposed to acute stress (predator odour) 90 minutes before the recordings (Hwa et al, 2019). Even if we recorded from putative pyramidal neurons, as visually identifyed by their morphological aspect, we could not confirm the identity of the neurons in these experiments, which were performed with an Cs-based intracellular solution not allowing the recording of firing activity. In our hands, even if the clustered large events were still visible 1 hour after stress, the statistical comparison of sEPSC amplitudes did not confirm the peak increase observed with K-based internal solution. This might be related to a better resolution in the EPSC detection due to improved signal-to-

noise ratio, which might have increased the fraction of smaller amplitude EPSCs, lowering the statistical impact of FS-related large EPSCs.

It should be noticed that miniature currents are present in sEPSCs recordings because there is no way to isolate AP-dependent and AP-independent release. It is possible that minis account for a large proportion of the synaptic events in our recordings, as also observed in other studies (Malkin et al, 2014). This preponderance of minis is probably enhanced in the slice preparation, where the spontaneous firing of the local network tends to be down-regulated. If a specific stress effect on the mechanisms of AP-dependent release occurs, the "contamination" by minis in our recordings would decrease the ability to detect this effect, contributing to explain why the sEPSCs analysis failed to detect early amplitude increases. It could be argued that the recording of evoked EPSCs (eEPSCs) would avoid the difficulty of contamination by minis. In our study, we did not take the approach of studying eEPSCs for detecting stress effects, because experimental stimulation in our condition can only address a specific subgroup of axonal fibres and thus a subgroup of neuronal subtypes, which we could however not specifically control, in the absence of targeted approaches, such as optogenetic or chemogenetic tactics, allowing to precisely identify the stimulated afferent. Therefore, in the attempt to obtain a more balanced sampling of all possible neuronal afferents, allowing to identify any possible change in synaptic inputs, we decided to limit our study to sEPSC recordings.

Nevertheless, we observed a non-significant tendency to increase for the total excitatory charge, measured as the integral of current traces at the reversal potential of IPSCs (proportional to the average excitatory conductance). We observed a similar tendency also in the total inhibitory charge, (proportional to the average inhibitory conductance). There are no previous reports of acute stress effects on inhibitory GABA release in prelimbic neurons, neither in studies involving the early effect of FS in PFC/FC synaptosomes (Musazzi et al, 2010) nor of mild acute stress effects on inhibitory transmission in L5 PL neurons of juvenile rats (Yuen et al, 2009), while in the infralimbic mPFC of adult rats exposed to chronic stress, it was shown that inhibitory mini (mIPSC) frequency was selectively enhanced *vs* mEPSC frequency, in parallel with an increased number of inhibitory synaptic contacts (McKlveen et al., 2016). Whether or not FS increases inhibitory conductance in adult PL neurons should be explored in more detail. Interestingly, the E/I ratio was unaltered in stressed animals *vs* controls, suggesting that the local network was able to maintain an unaltered balance of excitation and inhibition immediately after the end of the stress protocol. Our result differs from the increased E/I ratio reported in the study of Hwa et al (2019) in the prelimbic L2-3. This could derive from the use

of different rodent species and/or from different acute stress protocols (the predator odour stress lacks physical component). Interestingly, our data show a significant FS-induced increase in the E/I ratio in L2-3 neurons, 24 hours after FS. This was due to a significant increase in the total excitatory charge, not accompanied by an increase in the total inhibitory charge. This result confirms the previously reported increase in the evoked Glu release 24 hours after FS from mPFC/FC synaptosomes of stressed animals (Musazzi et al, 2017). When separately comparing sEPSCs and sIPSCs in Cs-based recordings, we could only detect a tendency to increased sEPSC frequency, suggesting a lower statistical power of the analysis of individual EPSCs/IPSCs, which is subjected to errors deriving from missed events during detection. A similar consideration may explain the lack of stress effects, *vs* control, observed in sEPSCs recorded with the K-based intracellular solution 24 hours after FS (fig.R.7B-D).

Our data show that 24 hours after acute stress there is a significant increase in the rise times of the sEPSCs when using K-based internal solutions (fig.R.7D), and a tendency to increased rise times with Cs-based solutions (fig.R.9D), which is not present in recordings obtained 1 hour after stress. This kinetic change may arise from several factors, including differences in postsynaptic AMPA receptor composition, or in the shape of the postsynaptic spine, which may affect the propagation of electrical signals, or in the electrotonic distance of active synapses from the somatic recording electrode. It is interesting to notice that, whatever the underlying mechanism, this increase reflects a dynamical change in the excitatory transmission mechanisms occurring 1 day after a single traumatic event. This change might be related to a possible compensatory mechanism accompanying the dendritic retraction occurring 24 hours after FS (Nava et al, 2017).

<u>Ketamine effect on synaptic transmission of L2-3 and L5 neurons</u>

We found that the frequency of sEPSCs recorded in L2-3 Pyrs in stressed animals is enhanced after ketamine treatment. This is in accordance with the notion that, at this low dosage, ketamine systemic injection induces an increase in the density of synaptic spines in the prelimbic mPFC, as demonstrated ~1 day after injection in naïve (Li et al, 2010; Liu et al, 2015) and chronically stressed animals (Li et al., 2011; Liu et al, 2015; Moda-Sava et al, 2018; Ng et al, 2018), and up to 2 weeks after injection in naïve animals (Phoumthipphavong et al., 2016). Moreover, our data parallel results found for L5 principal neurons, where an enhancement by ketamine of 5-HT-evoked sEPSCs, both in naïve (Li et al., 2010; Aguilar-Valles et al., 2018) and chronically stressed (Li et al., 2011; Liu et al., 2015) animals, was reported. Moreover, we found that ketamine reverted the increase of sEPSC rise time induced by FS. One possible explanation for

this kinetic change is that ketamine activates synapses located near the soma, that disappeared or were inhibited by the acute stress reaction. Indeed, it was reported that ketamine induces re-formation of spines close to spines eliminated by previous chronic restraint stress (Ng et al, 2018) or chronic corticosterone treatment (Moda-Sava et al, 2018).

In our preliminary experiments, we could not show an effect of ketamine on sEPSCs in L5 neurons, contrary with previously published observations in naïve or chronically stressed animals (Li et al., 2010; Aguilar-Valles et al., 2018; Li et al., 2011; Liu et al., 2015). This could be determined by the fact that, in the latter studies, ketamine effects were demonstrated after intensely activating specific inputs by stimulation with various hormones (5-HT, hypocretin, CRF), while in our results we did not discriminate among specific subpopulations of neuronal afferents. Moreover, our results are based on a very small sample, and further investigations should address the ketamine effects on specific inputs to L5 Pyrs in the prelimbic mPFC of foot-shock stressed animals.

We were not able to detect any ketamine-related alteration of mEPSCs in L2-3 Pyr cells of acutely stressed animals (1 day after stress and 18 hours after ketamine treatment). Similarly, our preliminary analysis did not suggest a ketamine effect on minis in L5 Pyrs. As far as we know, it was never reported whether excitatory minis are affected by low-dose ketamine systemic injection in the mPFC or elsewhere, while it was reported that ketamine acute bath perfusion in slices or cultured neurons inhibits (hippocampal cultures, +40 mV; Autry et al., 2011) or has no effect (lateral habenula, slices, -60 mV; Yang et al., 2018) on mEPSCs.

Summarizing, these results suggest that ketamine systemic injection leads to an increase in the frequency of excitatory inputs to L2-3 pyramidal neurons in stressed animals, 1 day after exposure to the stressor, without changes in spontaneous AP-independent release.

In conclusion, our data confirm an early FS stress-induced enhancement of Glu transmission in L2-3 Pyr in the prelimbic mPFC. This enhancement is due to the activation of a few strong synaptic contacts and/or the synchronization of inputs from afferent neurons undergoing increased firing, and is not paralleled by a detectable increase in the E/I balance in single neurons. On the contrary, 1 day after FS, the excitatory Glu conductance is increased in parallel with an increase in the E/I balance. Ketamine at this time increases the frequency of sEPSCs, consistent with the synaptogenic effect reported in naïve and chronically stressed animals.

REFERENCES

Abdallah CG, Sanacora G, Duman RS, Krystal JH. Ketamine and rapid-acting antidepressants: a window into a new neurobiology for mood disorder therapeutics. Annu Rev Med. 2015;66:509-23. doi: 10.1146/annurev-med-053013-062946. Epub 2014 Oct 17. PMID: 25341010; PMCID: PMC4428310.

Aerni A, Traber R, Hock C, Roozendaal B, Schelling G, Papassotiropoulos A, Nitsch RM, Schnyder U, de Quervain DJ. Low-dose cortisol for symptoms of posttraumatic stress disorder. Am J Psychiatry. 2004 Aug;161(8):1488-90. doi: 10.1176/appi.ajp.161.8.1488. PMID: 15285979.

Aguilar-Valles A, Haji N, De Gregorio D, Matta-Camacho E, Eslamizade MJ, Popic J, Sharma V, Cao R, Rummel C, Tanti A, Wiebe S, Nuñez N, Comai S, Nadon R, Luheshi G, Mechawar N, Turecki G, Lacaille JC, Gobbi G, Sonenberg N. Translational control of depression-like behavior via phosphorylation of eukaryotic translation initiation factor 4E. Nat Commun. 2018 Jun 25;9(1):2459. doi: 10.1038/s41467-018-04883-5. PMID: 29941989; PMCID: PMC6018502.

Akana, S. F., Chu, A., Soriano, L. & Dallman, M. F. (2001) Corticosterone exerts site-specific and state dependent effects in prefrontal cortex and amygdala on regulation of adrenocorticotropic hormone, insulin and fat depots. J. Neuroendocrinol. 13, 625–637 (2001).

Alfarez, D.N., JoWls, M. and Krugers, H.J. (2003) Chronic unpredictable stress impairs Long-Term Potentiation in hippocampal CA1 area and dentate gyrus in vitro. Eur. J. Neurosci., 17: 1928-1934.

American Psychiatric Association. (2013). Anxiety Disorders. In Diagnostic and statistical manual of mental disorders (5th ed.). https://doi.org/10.1176/appi.books.9780890425596.dsm05

Anderson EM, Gomez D, Caccamise A, McPhail D, Hearing M. Chronic unpredictable stress promotes cell-specific plasticity in prefrontal cortex D1 and D2 pyramidal neurons. Neurobiol Stress. 2019 Mar 8;10:100152. doi: 10.1016/j.ynstr.2019.100152. PMID: 30937357; PMCID: PMC6430618.

Aoto J, Nam CI, Poon MM, Ting P, Chen L. (2008) Synaptic signaling by all-trans retinoic acid in homeostatic synaptic plasticity. Neuron 60: 308–320, 2008.

Arnsten A. F. (2009). Stress signalling pathways that impair prefrontal cortex structure and function. Nature reviews. Neuroscience, 10(6), 410–422. https://doi.org/10.1038/nrn2648.

Kumar A, Pareek V, Faiq MA, Ghosh SK, Kumari C. ADULT NEUROGENESIS IN HUMANS: A Review of Basic Concepts, History, Current Research, and Clinical Implications. Innov Clin Neurosci. 2019 May 1;16(5-6):30-37. PMID: 31440399; PMCID: PMC6659986.

Autry AE, Adachi M, Nosyreva E, Na ES, Los MF, Cheng PF, Kavalali ET, Monteggia LM. NMDA receptor blockade at rest triggers rapid behavioural antidepressant responses. Nature. 2011 Jun 15;475(7354):91-5. doi: 10.1038/nature10130. PMID: 21677641; PMCID: PMC3172695.

Bachen EA, Manuck SB, Marsland AL, Cohen S, Malkoff SB, Muldoon MF, Rabin BS. Lymphocyte subset and cellular immune responses to a brief experimental stressor. Psychosomatic Medicine. 1992;54:673– 679

Bae YS, Shin EC, Bae YS, Van Eden W. Editorial: Stress and Immunity. Front Immunol. 2019 Feb 14;10:245. doi: 10.3389/fimmu.2019.00245. PMID: 30837994; PMCID: PMC6383636. Bali A and Jaggi AS (2015) Electric foot shock stress adaptation: does it exist or not? Life Sci 130:97–102

Bennur S, Shankaranarayana Rao BS, Pawlak R, Strickland S, McEwen BS, Chattarji S. Stress-induced spine loss in the medial amygdala is mediated by tissue-plasminogen activator. Neuroscience. 2007 Jan 5;144(1):8-16. doi: 10.1016/j.neuroscience.2006.08.075. Epub 2006 Oct 16. PMID: 17049177.

Birnstiel, S., List, T.J. and Beck, S.G. (1995) Chronic corticosterone treatment maintains synaptic activity of CA1 hippocampal pyramidal cells: acute high corticosterone administration increases action potential number. Synapse, 20:117-124.

Bloss EB, Janssen WG, McEwen BS, Morrison JH. Interactive Effects of Stress and Aging on Structural Plasticity in the Prefrontal. Journal of Neuroscience 12 May 2010, 30 (19) 6726-6731; DOI: 10.1523/JNEUROSCI.0759-10.2010

Bonini D, Mora C, Tornese P, Sala N, Filippini A, La Via L, Milanese M, Calza S, Bonanno G, Racagni G, Gennarelli M, Popoli M, Musazzi L, Barbon A. Acute Footshock Stress Induces Time-Dependent Modifications of AMPA/NMDA Protein Expression and AMPA Phosphorylation. Neural Plast. 2016;2016:7267865. doi: 10.1155/2016/7267865. Epub 2016 Feb 4. PMID: 26966584; PMCID: PMC4757710.

Braga MF, Aroniadou-Anderjaska V, Manion ST, Hough CJ, Li H. Stress impairs alpha (1 A) adrenoceptor-mediated noradrenergic facilitation of GABAergic transmission in the basolateral amygdala. Neuropsychopharmacology 2004; 29:45–58.

Bremner JD, Randall P, Vermetten E, Staib L, Bronen RA, Mazure C, Capelli S, McCarthy G, Innis RB, Charney DS. Magnetic resonance imaging-based measurement of hippocampal volume in posttraumatic stress disorder related to childhood physical and sexual abuse--a preliminary report. Biol Psychiatry. 1997 Jan 1;41(1):23-32. doi: 10.1016/s0006-3223(96)00162-x. PMID: 8988792; PMCID: PMC3229101.

Berendse HW, Galis-de Graaf Y, Groenewegen HJ. Topographical organization and relationship with ventral striatal compartments of prefrontal corticostriatal projections in the rat. J Comp Neurol. 1992 Feb 15;316(3):314-47. doi: 10.1002/cne.903160305. PMID: 1577988.

Brandt, S. (1999). Data Analysis. Springer-Verlag, New York, p.163.

Brewin CR, Andrews B, Valentine JD. Meta-analysis of risk factors for post¬traumatic stress disorder in trauma-exposed adults. J Consult Clin Psychol 2000; 68:748-66.

Brown SP, Hestrin S (2009) Intracortical circuits of pyramidal neurons reflect their long-range axonal targets. Nature 457:1133–1136.

Brunson KL, Kramár E, Lin B, Chen Y, Colgin LL, Yanagihara TK, Lynch G, Baram TZ. Mechanisms of late-onset cognitive decline after early-life stress. J Neurosci. 2005 Oct 12;25(41):9328-38. doi: 10.1523/JNEUROSCI.2281-05.2005. PMID: 16221841; PMCID: PMC3100717.

Calabrese, F., Guidotti, G., Molteni, R., Racagni, G., Mancini, M., and Riva, M. A. (2012). Stress-induced changes of hippocampal NMDA receptors: modulation by duloxetine treatment. PLoS One 7:e37916. doi: 10.1371/journal.pone.0037916

Campioni MR, Xu M and McGehee DS. Stress-induced changes in nucleus accumbens glutamate synaptic plasticity. J Neurophysiol. 2009; 101:3192–3198. 91111.2008 [pii]. 10.1152/jn.91111.2008 [PubMed: 19357347]

Caudal D, Godsil BP, Mailliet F, Bergerot D and Jay TM. Acute stress induces contrasting changes in AMPA receptor subunit phosphorylation within the prefrontal cortex, amygdala and hippocampus. PLoS One. 2010 Dec 8;5(12):e15282. doi: 10.1371/journal.pone.0015282. PMID: 21170339; PMCID: PMC2999558.

Cerqueira JJ, Mailliet F, Almeida OF, Jay TM, Sousa N. The prefrontal cortex as a key target of the maladaptive response to stress. J Neurosci. 2007; 27:2781–2787. 27/11/2781 [pii]. 10.1523/ JNEUROSCI.4372-06.2007 [PubMed: 17360899]

Chourbaji, S., Zacher, C., Sanchis-Segura, C., Dormann, C., Vollmayr, B., and Gass, P. (2005). Learned helplessness: validity and reliability of depressive-like states in mice. Brain Res. Protoc. 16, 70–78.

Christian KM, Miracle AD, Wellman CL, Nakazawa K. Chronic stress-induced hippocampal dendritic retraction requires CA3 NMDA receptors. Neuroscience. 2011 Feb 3;174:26-36. doi: 10.1016/j.neuroscience.2010.11.033. Epub 2010 Nov 23. PMID: 21108993; PMCID: PMC3020251.

Christoffel DJ, Golden SA, Russo SJ. Structural and synaptic plasticity in stress-related disorders. Rev Neurosci. 2011;22(5):535-49. doi: 10.1515/RNS.2011.044. PMID: 21967517; PMCID: PMC3212803.

Christophe E, Doerflinger N, Lavery DJ, Molnár Z, Charpak S, Audinat E (2005) Two populations of layer V pyramidal cells of the mouse neocortex: development and sensitivity to anesthetics. J Neurophysiol 94:3357–3367

Chrousos GP, Gold PW. The concepts of stress and stress system disorders. Overview of physical and behavioral homeostasis. JAMA. 1992 Mar 4;267(9):1244-52. Erratum in: JAMA 1992 Jul 8;268(2):200. PMID: 1538563.

Chrousos GP. Stress and disorders of the stress system. Nat Rev Endocrinol. 2009 Jul;5(7):374-81. doi: 10.1038/nrendo.2009.106. Epub 2009 Jun 2. PMID: 19488073.

Citri A, Malenka RC. Synaptic plasticity: multiple forms, functions, and mechanisms. Neuropsychopharmacology. 2008 Jan;33(1):18-41. doi: 10.1038/sj.npp.1301559. Epub 2007 Aug 29. PMID: 17728696.

Cook SC and Wellman CL. Chronic stress alters dendritic morphology in rat medial prefrontal cortex. J Neurobiol. 2004 Aug;60(2):236-48. doi: 10.1002/neu.20025. PMID: 15266654.

Corcoran KA, Quirk GJ. Activity in prelimbic cortex is necessary for the expression of learned, but not innate, fears. J Neurosci. 2007 Jan 24;27(4):840-4. doi: 10.1523/JNEUROSCI.5327-06.2007. PMID: 17251424; PMCID: PMC6672908.

Cullinan,W.E., and Wolfe,T.J. (2000). Chronic stress regulates levels of mRNA transcripts encoding beta subunits of the GABA(A) receptor in the rat stress axis. Brain Res. 887,118–124.

Cunningham, E. T. Jr, Bohn, M. C. and Sawchenko, P. E. Organization of adrenergic inputs to the paraventricular and supraoptic nuclei of the hypothalamus in the rat. J. Comp. Neurol. 292, 651–667 (1990)

Daskalakis, N. P., Lehrner, A. and Yehuda, R. Endocrine aspects of post-traumatic stress disorder and implications for diagnosis and treatment. Endocrinol. Metab. Clin. North Am. 42, 503–513 (2013).

Dazzi L, Spiga F, Pira L, Ladu S, Vacca G, Rivano A, Jentsch JD, Biggio G. Inhibition of stress- or anxiogenic-drug-induced increases in dopamine release in the rat prefrontal cortex by long-term treatment with antidepressant drugs. J Neurochem. 2001 Feb;76(4):1212-20. doi: 10.1046/j.1471-4159.2001.00148.x. PMID: 11181840.

Dégenètais E, Thierry AM, Glowinski J, Gioanni Y. Electrophysiological properties of pyramidal neurons in the rat prefrontal cortex: an in vivo intracellular recording study. Cereb Cortex. 2002 Jan;12(1):1-16. doi: 10.1093/cercor/12.1.1. PMID: 11734528.

Dohrenwend BP, Turner JB, Turse NA, Adams BG, Koenen KC, Marshall R. The psychological risks of Vietnam for U.S. veterans: a revisit with new data and methods. Science. 2006 Aug 18;313(5789):979-82. doi: 10.1126/science.1128944. PMID: 16917066; PMCID: PMC1584215.

Douma EH, de Kloet ER. Stress-induced plasticity and functioning of ventral tegmental dopamine neurons. Neurosci Biobehav Rev. 2020 Jan;108:48-77. doi: 10.1016/j.neubiorev.2019.10.015. Epub 2019 Oct 27. PMID: 31666179.

Duman RS, Shinohara R, Fogaça MV, Hare B. Neurobiology of rapid-acting antidepressants: convergent effects on GluA1-synaptic function. Mol Psychiatry. 2019 Dec;24(12):1816-1832. doi: 10.1038/s41380-019-0400-x. Epub 2019 Mar 20. PMID: 30894661; PMCID: PMC6754322.

Dumetz F, Ginieis R, Bure C, Marie A, Alfos S, Pallet V, Bosch-Bouju C. Neuronal morphology and synaptic plasticity in the hippocampus of vitamin A deficient rats. Nutr Neurosci. 2020 Sep 12:1-12. doi: 10.1080/1028415X.2020.1809877. Epub ahead of print. PMID: 32924835.

Duncan EJ, Madonick SH, Parwani A, et al.Clinical and sensorimotor gating effects of ketaminein normals. Neuropsychopharmacology. 2001;25(1):72-83.

Feder A, Parides MK, Murrough JW, et al. Efficacy of Intravenous Ketamine for Treatment of Chronic Posttraumatic Stress Disorder: A Randomized Clinical Trial. JAMA Psychiatry. 2014;71(6):681–688. doi:10.1001/jamapsychiatry.2014.62

Feder A, Rutter SB, Schiller D, Charney DS. The emergence of ketamine as a novel treatment for posttraumatic stress disorder. Adv Pharmacol. 2020;89:261-286. doi: 10.1016/bs.apha.2020.05.004. Epub 2020 Jun 19. PMID: 32616209.

Fitzgerald JM, DiGangi JA, Phan KL. Functional Neuroanatomy of Emotion and Its Regulation in PTSD. Harv Rev Psychiatry. 2018 May/Jun;26(3):116-128. doi: 10.1097/HRP.0000000000000185. PMID: 29734226; PMCID: PMC5944863.

Flandreau EI, Toth M. Animal Models of PTSD: A Critical Review. Curr Top Behav Neurosci. 2018;38:47-68. doi: 10.1007/7854_2016_65. PMID: 28070873.

Foy, M.R., Stanton, M.E., Levine, S. and Thompson, R.F. (1987) Behavioral stress impairs long-term potentiation in rodent hippocampus. Behav. Neural. Biol., 48: 138-149.

Frank CA, Kennedy MJ, Goold CP, Marek KW, Davis GW. Mechanisms underlying the rapid induction and sustained expression of synaptic homeostasis. Neuron 52: 663–677, 2006.

Fukumoto K, Iijima M, Funakoshi T, Chaki S. 5-HT1A receptor stimulation in the medial prefrontal cortex mediates the antidepressant effects of mGlu2/3 receptor antagonist in mice. Neuropharmacology. 2018 Jul 15;137:96-103. doi: 10.1016/j.neuropharm.2018.05.001. Epub 2018 May 5. PMID: 29738849.

Gabbott PLA, Warner TA, Jays PRL, Salway P, Busby SJ. Prefrontal cortex in the rat: projections to subcortical autonomic, motor, and limbic centers. J Comp Neurol. 2005; 492(2):145–177. [PubMed: 16196030]

Galatzer-Levy, I. R. et al. Cortisol response to an experimental stress paradigm prospectively predicts long-term distress and resilience trajectories in response to active police service. J. Psychiatr. Res. 56, 36–42 (2014).

Galvez R, Mesches MH, McGaugh JL. Norepinephrine release in the amygdala inresponse to footshock stimulation.Neurobiol Learn Mem1996;66:253–257.

Garcia, R., Musleh, W., Tocco, G., Thompson, R.F. and Baudry, M. (1997) Time-dependent blockade of STP and LTP in hippocampal slices following acute stress in mice. Neurosci. Lett., 233: 41-44.

Geuze, E. et al. Reduced GABAA benzodiazepine receptor binding in veterans with post-traumatic stress disorder. Mol. Psychiatry 13, 74–83, 3 (2008).

Gilabert-Juan J, Castillo-Gomez E, Guirado R, Molto MD, Nacher J. Chronic stress alters inhibitory networks in the medial prefrontal cortex of adult mice. Brain Struct Funct. 2013; 218(6):1591–1605. [PubMed: 23179864]

Gilbertson MW, Shenton ME, Ciszewski A, Kasai K, Lasko NB, Orr SP, Pitman RK. Smaller hippocampal volume predicts pathologic vulnerability to psychological trauma. Nat Neurosci. 2002 Nov;5(11):1242-7. doi: 10.1038/nn958. PMID: 12379862; PMCID: PMC2819093.

Gold, P. W. The organization of the stress system and its dysregulation in depressive illness. Molecular Psychiatry, 20(1), 32–47. https://doi.org/10.1038/mp.2014.163

Goldstein, D. S., & Kopin, I. J. Adrenomedullary, adrenocortical, and sympathoneural responses to stressors: A meta-analysis. Endocrine Regulations, 42(1), 111–119. Retrieved from /pmc/articles/PMC5522726/?report=abstract

Goldwater DS, Pavlides C, Hunter RG, Bloss EB, Hof PR, McEwen BS, Morrison JH. Structural and functional alterations to rat medial prefrontal cortex following chronic restraint stress and recovery. Neuroscience. 2009 Dec 1;164(2):798-808. doi: 10.1016/j.neuroscience.2009.08.053. Epub 2009 Aug 29. PMID: 19723561; PMCID: PMC2762025.

Golier, J. A., Caramanica, K., Demaria, R. & Yehuda, R. A pilot study of mifepristone in combat- related PTSD. Depress Res. Treat. 2012, 393251 (2012).

Gourley SL, Kedves AT, Olausson P, Taylor JR. A history of corticosterone exposure regulates fear extinction and cortical NR2B, GluR2/3, and BDNF. Neuropsychopharmacology. 2009; 34(3):707–716. [PubMed: 18719621]

Grbesa, I., and Hakim, O. (2017). Genomic effects of glucocorticoids. Protoplasma 254, 1175–1185. doi: 10.1007/s00709-016-1063-y

Groeneweg, F. L., Karst, H., de Kloet, E. R., and Joëls, M. (2012). Mineralocorticoid and glucocorticoid receptors at the neuronal membrane, regulators of nongenomic corticosteroid signalling. Mol. Cell. Endocrinol. 350, 299–309. doi: 10.1016/j.mce.2011.06.020

Hammamieh R, Chakraborty N, De Lima TC, Meyerhoff J, Gautam A, Muhie S, D'Arpa P, Lumley L, Carroll E, Jett M (2012) Murine model of repeated exposures to conspecific trained aggressors simulates features of post-traumatic stress disorder. Behav Brain Res 235:55–66

Hare BD, Shinohara R, Liu RJ, Pothula S, DiLeone RJ, Duman RS. Optogenetic stimulation of medial prefrontal cortex Drd1 neurons produces rapid and long-lasting antidepressant effects. Nat Commun. 2019 Jan 15;10(1):223. doi: 10.1038/s41467-018-08168-9. PMID: 30644390; PMCID: PMC6333924.

Harris KM, Kater SB. Dendritic spines: cellular specializations imparting both stability and flexibility to synaptic function. Annu Rev Neurosci. 1994;17:341-371. doi:10.1146/annurev.ne.17.030194.002013

Hattox AM, Nelson SB (2007) Layer V neurons in mouse cortex projecting to different targets have distinct physiological properties. J Neurophysiol 98:3330–3340.

Heidbreder CA, Groenewegen HJ. The medial prefrontal cortex in the rat: evidence for a dorso-ventral distinction based upon functional and anatomical characteristics. Neurosci Biobehav Rev. 2003 Oct;27(6):555-79. doi: 10.1016/j.neubiorev.2003.09.003. PMID: 14599436.

Herman, J. P. & Mueller, N. K. Role of the ventral subiculum in stress integration. Behav. Brain Res. 174, 215–224 (2006).

Herman JP, McKlveen JM, Ghosal S, Kopp B, Wulsin A, Makinson R, Scheimann J, Myers B. Regulation of the Hypothalamic-Pituitary-Adrenocortical Stress Response. Compr Physiol. 2016 Mar 15;6(2):603-21. doi: 10.1002/cphy.c150015. PMID: 27065163; PMCID: PMC4867107.

Hill MN, McLaughlin RJ, Pan B, Fitzgerald ML, Roberts CJ, Lee TT-Y, et al. Recruitment of prefrontal cortical endocannabinoid signaling by glucocorticoids contributes to termination of the stress response. J Neurosci. 2011; 31(29):10506–10515. [PubMed: 21775596]

Holmes SE, Scheinost D, DellaGioia N, Davis MT, Matuskey D, Pietrzak RH, Hampson M, Krystal JH, Esterlis I. Cerebellar and prefrontal cortical alterations in PTSD: structural and functional evidence. Chronic Stress (Thousand Oaks). 2018 Jan-Dec;2:2470547018786390. doi: 10.1177/2470547018786390. Epub 2018 Jul 6. PMID: 30035247; PMCID: PMC6054445.

Horst NK, Laubach M. The role of rat dorsomedial prefrontal cortex in spatial working memory. Neuroscience. 2009 Dec 1;164(2):444-56. doi: 10.1016/j.neuroscience.2009.08.004. Epub 2009 Aug 7. PMID: 19665526; PMCID: PMC2761984.

Hwa, L. S., Neira, S., Pina, M. M., Pati, D., Calloway, R., & Kash, T. L. Predator odor increases avoidance and glutamatergic synaptic transmission in the prelimbic cortex via corticotropin-releasing factor receptor 1 signaling. Neuropsychopharmacology, 44(4), 766–775.

Indersmitten T, Tran CH, Cepeda C, Levine MS. Altered excitatory and inhibitory inputs to striatal medium-sized spiny neurons and cortical pyramidal neurons in the Q175 mouse model of Huntington's disease. J Neurophysiol. 2015 Apr 1;113(7):2953-66. doi: 10.1152/jn.01056.2014. Epub 2015 Feb 11. PMID: 25673747; PMCID: PMC4416625.

Joëls M, Krugers HJ, Verkuyl JM. Modulation of glutamatergic and GABAergic neurotransmission by corticosteroid hormones and stress- Techniques in the Behavioral and Neural Sciences, Chapter 4.7. https://doi.org/10.1016/S0921-0709(05)80029-X.

Joëls, M. and de Kloet, E.R. Corticosteroid actions on amino acid-mediated transmission in rat CA1 hippocampal cells. J. Neurosci., 13: 4082-4090.

Joëls M, Sarabdjitsingh RA, Karst H. Unraveling the time domains of corticosteroid hormone influences on brain activity: rapid, slow, and chronic modes. Pharmacol Rev. 2012 Oct;64(4):901-38. doi: 10.1124/pr.112.005892. PMID: 23023031.

Johnson, E. O., Kamilaris, T. C., Chrousos, G. P., & Gold, P. W. (1992). Mechanisms of stress: A dynamic overview of hormonal and behavioral homeostasis. Neuroscience and Biobehavioral Reviews, 16(2), 115–130. https://doi.org/10.1016/S0149-7634(05)80175-7

Jones, B.E.; Yang, T.Z. The efferent projections from the reticular formation and the locus coeruleus studied by anterograde and retrograde axonal transport in the rat. J. Comp. Neurol., 1985, 242(1), 56-92. [http://dx.doi.org/10.1002/cne.902420105] [PMID: 2416786]

Joseph L, Fink LM, Hauer-Jensen M. Cytokines in coagulationand thrombosis: a preclinical and clinical review. Blood Coagul Fibrinolysis 2002; 13: 105–116

Kaeser PS, Regehr WG. Molecular mechanisms for synchronous, asynchronous, and spontaneous neurotransmitter release. Annu Rev Physiol. 2014;76:333-63. doi: 10.1146/annurev-physiol-021113-170338. Epub 2013 Nov 21. PMID: 24274737; PMCID: PMC4503208.

Karsen, E. F., Watts, B. V. & Holtzheimer, P. E. Review of the effectiveness of transcranial magnetic stimulation for post-traumatic stress disorder. Brain Stimul. 7, 151–157 (2014).

Karst H, Berger S, Turiault M, Tronche F, Schütz G, Joëls M. Mineralocorticoid receptors are indispensable for nongenomic modulation of hippocampal glutamate transmission by corticosterone. Proc Natl Acad Sci U S A. 2005 Dec 27;102(52):19204-7. doi: 10.1073/pnas.0507572102. Epub 2005 Dec 16. PMID: 16361444; PMCID: PMC1323174.

Karst H, Joëls M. Effect of chronic stress on synaptic currents in rat hippocampal dentate gyrus neurons. J Neurophysiol. 2003 Jan;89(1):625-33. doi: 10.1152/jn.00691.2002. PMID: 12522207.

Karst H, Joels M. Corticosterone slowly enhances miniature excitatory postsynaptic current amplitude in mice CA1 hippocampal cells. J Neurophysiol. 2005; 94:3479–3486. 00143.2005[pii]. 10.1152/jn.00143.2005 [PubMed: 16033944]

Kasper EM, Larkman AU, Lübke J, Blakemore C. Pyramidal neurons in layer 5 of the rat visual cortex. I. Correlation among cell morphology, intrinsic electrophysiological properties, and axon targets. J Comp Neurol 339:459–474

Kavalali ET. The mechanisms and functions of spontaneous neurotransmitter release. Nat Rev Neurosci. 2015 Jan;16(1):5-16. doi: 10.1038/nrn3875. PMID: 25524119.

Kavushansky A, Richter-Levin G. Effects of stress and corticosterone on activityand plasticity in the amygdala.J Neurosci Res 2006;84:1580–1587

Kim, J.J., Foy, M.R. and Thompson, R.F. Behavioral stress modifies hippocampal plasticity through N-methyl-Daspartate receptor activation. Proc. Natl. Acad. Sci. U.S.A., 93: 4750-4753.

Kitayama N, Quinn S, Bremner JD. Smaller volume of anterior cingulate cortex in abuse-related posttraumatic stress disorder. J Affect Disord 2006;90:171-4.

Koenigs M, Grafman J. Posttraumatic Stress Disorder: The Role of Medial Prefrontal Cortex and Amygdala. The Neuroscientist. 2009;15(5):540-548. doi:10.1177/1073858409333072

Krystal JH, Karper LP, Seibyl JP, et al.Subanesthetic effects of the noncompetitive NMDAantagonist, ketamine, in humans. Psychotomimetic,perceptual, cognitive, and neuroendocrineresponses.Arch Gen Psychiatry. 1994;51(3):199-214

Kumar A, Pareek V, Faiq MA, Ghosh SK, Kumari C. ADULT NEUROGENESIS IN HUMANS: A Review of Basic Concepts, History, Current Research, and Clinical Implications. Innov Clin Neurosci. 2019 May 1;16(5-6):30-37. PMID: 31440399; PMCID: PMC6659986.

Lanius RA, Vermetten E, Loewenstein RJ, Brand B, Schmahl C, Bremner JD, Spiegel D. Emotion modulation in PTSD: Clinical and neurobiological evidence for a dissociative

subtype. Am J Psychiatry. 2010 Jun;167(6):640-7. doi: 10.1176/appi.ajp.2009.09081168. Epub 2010 Apr 1. PMID: 20360318; PMCID: PMC3226703.

Le Bé JV, Silberberg G, Wang Y, Markram H. Morphological, electrophysiological, and synaptic properties of corticocallosal pyramidal cells in the neonatal rat neocortex. Cereb Cortex. 2007 Sep;17(9):2204-13. doi: 10.1093/cercor/bhl127. Epub 2006 Nov 23. PMID: 17124287.

Lee MC, Yasuda R, Ehlers MD. Metaplasticity at single glutamatergic synapses. Neuron 66: 859–870, 2010.

Leon WC, Bruno MA, Allard S, Nader K, Cuello AC. Engagement of the PFC in consolidation and recall of recent spatial memory. Learn Mem. 2010 Jun;17(6):297-305. doi: 10.1101/lm.1804410. PMID: 20508034.

Lewis, D.I.; Coote, J.H. Excitation and inhibition of rat sympathetic preganglionic neurones by catecholamines. Brain Res., 1990, 530(2), 229-234. [http://dx.doi.org/10.1016/0006-8993(90)91287-Q] [PMID: 2265354

Lowy MT, Wittenberg L, Yamamoto BK. Effect of acute stress on hippocampal glutamate levels and spectrin proteolysis in young and aged rats. J Neurochem. 1995 Jul;65(1):268-74. doi: 10.1046/j.1471-4159.1995.65010268.x. PMID: 7790870.

Li N, Lee B, Liu RJ, Banasr M, Dwyer JM, Iwata M, Li XY, Aghajanian G, Duman RS. mTOR-dependent synapse formation underlies the rapid antidepressant effects of NMDA antagonists. Science. 2010 Aug 20;329(5994):959-64. doi: 10.1126/science.1190287. PMID: 20724638; PMCID: PMC3116441.

Li N, Liu RJ, Dwyer JM, Banasr M, Lee B, Son H, Li XY, Aghajanian G, Duman RS. Glutamate N-methyl-D-aspartate receptor antagonists rapidly reverse behavioral and synaptic deficits caused by chronic stress exposure. Biol Psychiatry. 2011 Apr 15;69(8):754-61. doi: 10.1016/j.biopsych.2010.12.015. Epub 2011 Feb 3. PMID: 21292242; PMCID: PMC3068225.

Liu RJ, Ota KT, Dutheil S, Duman RS, Aghajanian GK. Ketamine Strengthens CRF-Activated Amygdala Inputs to Basal Dendrites in mPFC Layer V Pyramidal Cells in the Prelimbic but not Infralimbic Subregion, A Key Suppressor of Stress Responses. Neuropsychopharmacology. 2015 Aug;40(9):2066-75. doi: 10.1038/npp.2015.70. Epub 2015 Mar 11. PMID: 25759300; PMCID: PMC4613616.

Liu WZ, Zhang WH, Zheng ZH, Zou JX, Liu XX, Huang SH, You WJ, He Y, Zhang JY, Wang XD, Pan BX. Identification of a prefrontal cortex-to-amygdala pathway for chronic stress-induced anxiety. Nat Commun. 2020 May 6;11(1):2221. doi: 10.1038/s41467-020-15920-7. PMID: 32376858; PMCID: PMC7203160.

Lowy MT, Wittenberg L, Yamamoto BK. Effect of acute stress on hippocampal glutamate levels and spectrin proteolysis in young and aged rats. Journal of Neurochemistry. 1995; 65:268–274. [PubMed: 7790870]

Lüscher C, Malenka RC. NMDA receptor-dependent long-term potentiation and long-term depression (LTP/LTD). Cold Spring Harb Perspect Biol. 2012 Jun 1;4(6):a005710. doi: 10.1101/cshperspect.a005710. PMID: 22510460; PMCID: PMC3367554.

Magariños AM, McEwen BS, Flügge G, Fuchs E. Chronic psychosocial stress causes apical dendritic atrophy of hippocampal CA3 pyramidal neurons in subordinate tree shrews. J Neurosci. 1996 May 15;16(10):3534-40. doi: 10.1523/JNEUROSCI.16-10-03534.1996. PMID: 8627386; PMCID: PMC6579123.

Magariños AM, Verdugo JM, McEwen BS. Chronic stress alters synaptic terminal structure in hippocampus. Proc Natl Acad Sci U S A. 1997 Dec 9;94(25):14002-8. doi: 10.1073/pnas.94.25.14002. PMID: 9391142; PMCID: PMC28422.

Malkin SL, Kim KKh, Tikhonov DB, Zaitsev AV. [Properties of spontaneous and miniature excitatory postsynaptic currents of rat prefrontal cortex neurons]. Zh Evol Biokhim Fiziol. 2014 Nov-Dec;50(6):440-6. Russian. PMID: 25782285.

Manahan-Vaughan, D. and Braunewell, H.-K. (1999) Novelty acquisition is associated with induction of hippocampal longterm depression. Proc. Natl. Acad. Sci. USA, 96: 8739-8744.

Manuck SB, Cohen S, Rabin BS, Muldoon MF, Bachen EA. Individual differences in cellular immune response to stress. Psychological Science. 1991;2:111–115.

Maroun M, Richter-Levin G. Exposure to acute stress blocks the induction of long-term potentiation of the amygdala-prefrontal cortex pathway in vivo. J Neurosci. 2003; 23:4406–4409. 23/11/4406 [pii]. [PubMed: 12805280]

Mathew SJ, Shah A, Lapidus K, Clark C, Jarun N, Ostermeyer B, Murrough JW. Ketamine for treatment-resistant unipolar depression: current evidence. CNS Drugs. 2012 Mar 1;26(3):189-204. doi: 10.2165/11599770-000000000-00000. PMID: 22303887; PMCID: PMC3677048.

Mathew SS, Pozzo-Miller L, Hablitz JJ. Kainate modulates presynaptic GABA release from two vesicle pools. J Neurosci. 2008 Jan 16;28(3):725-31. doi: 10.1523/JNEUROSCI.3625-07.2008. PMID: 18199771; PMCID: PMC2806850.

Mayanagi T, Sobue K. Social Stress-Induced Postsynaptic Hyporesponsiveness in Glutamatergic Synapses Is Mediated by PSD-Zip70-Rap2 Pathway and Relates to Anxiety-Like Behaviors. Front Cell Neurosci. 2020 Jan 8;13:564. doi: 10.3389/fncel.2019.00564. PMID: 31969804; PMCID: PMC6960224.

McEwen BS, Bowles NP, Gray JD, Hill MN, Hunter RG, Karatsoreos IN, Nasca C. Mechanisms of stress in the brain. Nat Neurosci. 2015 Oct;18(10):1353-63. doi: 10.1038/nn.4086. Epub 2015 Sep 25. PMID: 26404710; PMCID: PMC4933289.

McGaugh JL. The amygdala modulates the consolidation of memories of emotionally arousing experiences. Annu Rev Neurosci. 2004;27:1-28. doi: 10.1146/annurev.neuro.27.070203.144157. PMID: 15217324.

McGhee LL, Maani CV, Garza TH, Gaylord KM, Black IH. The correlation between ketamine and posttraumatic stress disorder in burned service members. J Trauma. 2008

Feb;64(2 Suppl):S195-8; Discussion S197-8. doi: 10.1097/TA.0b013e318160ba1d. PMID: 18376165.

McKinney RA, Capogna M, Durr R, Gahwiler BH, Thompson SM. Miniature synaptic events maintain dendritic spines via AMPA receptor activation. Nat Neurosci 2: 44–49, 1999.

McKlveen JM, Myers B, Herman JP. The medial prefrontal cortex: coordinator of autonomic, neuroendocrine and behavioural responses to stress. Journal of Neuroendocrinology. 2015 Jun;27(6):446-456. DOI: 10.1111/jne.12272.

McKlveen, J. M., Morano, R. L., Fitzgerald, M., Zoubovsky, S., Cassella, S. N., Scheimann, J. R., … Herman, J. P. (2016a). Chronic Stress Increases Prefrontal Inhibition: A Mechanism for Stress-Induced Prefrontal Dysfunction. Biological Psychiatry, 80(10), 754–764. https://doi.org/10.1016/j.biopsych.2016.03.2101

McKlveen, J. M., Morano, R. L., Fitzgerald, M., Zoubovsky, S., Cassella, S. N., Scheimann, J. R., … Herman, J. P. (2016b). Chronic Stress Increases Prefrontal Inhibition: A Mechanism for Stress-Induced Prefrontal Dysfunction. Biological Psychiatry, 80(10), 754–764. https://doi.org/10.1016/j.biopsych.2016.03.2101

Meunier D, Stamatakis EA, Tyler LK. Age-related functional reorganization, structural changes, and preserved cognition. Neurobiol Aging. 2014 Jan;35(1):42-54. doi: 10.1016/j.neurobiolaging.2013.07.003. Epub 2013 Aug 12. PMID: 23942392.

Mitra R, Jadhav S, McEwen BS, Vyas A, Chattarji S. Stress duration modulates the spatiotemporal patterns of spine formation in the basolateral amygdala. Proc Natl Acad Sci U S A. 2005 Jun 28;102(26):9371-6. doi: 10.1073/pnas.0504011102. Epub 2005 Jun 20. PMID: 15967994; PMCID: PMC1166638.

Moda-Sava RN, Murdock MH, Parekh PK, Fetcho RN, Huang BS, Huynh TN, Witztum J, Shaver DC, Rosenthal DL, Alway EJ, Lopez K, Meng Y, Nellissen L, Grosenick L, Milner TA, Deisseroth K, Bito H, Kasai H, Liston C. Sustained rescue of prefrontal circuit dysfunction by antidepressant-induced spine formation. Science. 2019 Apr 12;364(6436):eaat8078. doi: 10.1126/science.aat8078. PMID: 30975859; PMCID: PMC6785189.

Moghaddam B, Adams B, Verma A, Daly D. Activation of glutamatergic neurotransmission by ketamine: a novel step in the pathway from NMDA receptor blockade to dopaminergic and cognitive disruptions associated with the prefrontal cortex. J Neurosci. 1997 Apr 15;17(8):2921-7. doi: 10.1523/JNEUROSCI.17-08-02921.1997. PMID: 9092613; PMCID: PMC6573099.

Morishima M, Kawaguchi Y. Recurrent connection patterns of corticostriatal pyramidal cells in frontal cortex. J Neurosci. 2006 Apr 19;26(16):4394-405. doi: 10.1523/JNEUROSCI.0252-06.2006. PMID: 16624959; PMCID: PMC6674016.

Murrough JW, Perez AM, Pillemer S, Stern J, Parides MK, aan het Rot M, Collins KA, Mathew SJ, Charney DS, Iosifescu DV. Rapid and longer-term antidepressant effects of repeated ketamine infusions in treatment-resistant major depression. Biol Psychiatry. 2013 Aug 15;74(4):250-6. doi: 10.1016/j.biopsych.2012.06.022. Epub 2012 Jul 27. PMID: 22840761; PMCID: PMC3725185.

Musazzi L, Milanese M, Farisello P, Zappettini S, Tardito D, Barbiero VS, et al. Acute stress increases depolarization-evoked glutamate release in the rat prefrontal/frontal cortex: the dampening action of antidepressants. PLoS One. 2010; 5(1):e8566. [PubMed: 20052403]

Musazzi L, Tornese P, Sala N, Popoli M. Acute stress is not acute: sustained enhancement of glutamate release after acute stress involves readily releasable pool size and synapsin I activation. Mol Psychiatry. 2017 Sep;22(9):1226-1227. doi: 10.1038/mp.2016.175. Epub 2016 Oct 4. PMID: 27698433.

Musazzi L, Tornese P, Sala N, Popoli M. Acute or Chronic? A Stressful Question. Trends Neurosci. 2017 Sep;40(9):525-535. doi: 10.1016/j.tins.2017.07.002. Epub 2017 Aug 1. PMID: 28778394.

Musazzi L, Tornese P, Sala N, Popoli M. What Acute Stress Protocols Can Tell Us About PTSD and Stress-Related Neuropsychiatric Disorders. Front Pharmacol. 2018 Jul 12;9:758. doi: 10.3389/fphar.2018.00758. PMID: 30050444; PMCID: PMC6052084.

Musazzi L, Treccani G, Popoli M. Functional and structural remodeling of glutamate synapses in prefrontal and frontal cortex induced by behavioral stress. Front Psychiatry. 2015 Apr 27;6:60. doi: 10.3389/fpsyt.2015.00060. PMID: 25964763; PMCID: PMC4410487.

Nahar J, Rainville JR, Dohanich GP, Tasker JG. Further evidence for a membrane receptor that binds glucocorticoids in the rodent hypothalamus. Steroids. 2016 Oct;114:33-40. doi: 10.1016/j.steroids.2016.05.013. Epub 2016 Jun 18. PMID: 27327842; PMCID: PMC5053862.

Nava N, Chen F, Wegener G, Popoli M, Nyengaard JR. A new efficient method for synaptic vesicle quantification reveals differences between medial prefrontal cortex perforated and nonperforated synapses. J Comp Neurol. 2014 Feb 1;522(2):284-97. doi: 10.1002/cne.23482. PMID: 24127135.

Nava N, Treccani G, Alabsi A, Kaastrup Mueller H, Elfving B, Popoli M, Wegener G, Nyengaard JR. Temporal Dynamics of Acute Stress-Induced Dendritic Remodeling in Medial Prefrontal Cortex and the Protective Effect of Desipramine. Cereb Cortex. 2017 Jan 1;27(1):694-705. doi: 10.1093/cercor/bhv254. PMID: 26523035.

Nava N, Treccani G, Liebenberg N, Chen F, Popoli M, Wegener G, Nyengaard JR. Chronic desipramine prevents acute stress-induced reorganization of medial prefrontal cortex architecture by blocking glutamate vesicle accumulation and excitatory synapse increase. Int J Neuropsychopharmacol. 2014 Dec 13;18(3):pyu085. doi: 10.1093/ijnp/pyu085. PMID: 25522419; PMCID: PMC4360240.

Neumeister A, Normandin MD, Pietrzak RH, Piomelli D, Zheng MQ, Gujarro-Anton A, Potenza MN, Bailey CR, Lin SF, Najafzadeh S, Ropchan J, Henry S, Corsi-Travali S, Carson RE, Huang Y. Elevated brain cannabinoid CB1 receptor availability in post-traumatic stress disorder: a positron emission tomography study. Mol Psychiatry. 2013 Sep;18(9):1034-40. doi: 10.1038/mp.2013.61. Epub 2013 May 14. PMID: 23670490; PMCID: PMC3752332.

Ng LHL, Huang Y, Han L, Chang RC, Chan YS, Lai CSW. Ketamine and selective activation of parvalbumin interneurons inhibit stress-induced dendritic spine elimination. Transl Psychiatry. 2018 Dec 10;8(1):272. doi: 10.1038/s41398-018-0321-5. PMID: 30531859; PMCID: PMC6288154.

Novakovic V, Sher L, Lapidus KA, Mindes J, A Golier J, Yehuda R. Brain stimulation in posttraumatic stress disorder. Eur J Psychotraumatol. 2011;2. doi: 10.3402/ejpt.v2i0.5609. Epub 2011 Oct 17. PMID: 22893803; PMCID: PMC3402102.

Otsuka T, Kawaguchi Y. Firing-pattern-dependent specificity of cortical excitatory feed-forward subnetworks. J Neurosci. 2008 Oct 29;28(44):11186-95. doi: 10.1523/JNEUROSCI.1921-08.2008. PMID: 18971461; PMCID: PMC6671518.

Otsuka T, Kawaguchi Y. Cell diversity and connection specificity between callosal projection neurons in the frontal cortex. J Neurosci. 2011 Mar 9;31(10):3862-70. doi: 10.1523/JNEUROSCI.5795-10.2011. PMID: 21389241; PMCID: PMC6622807.

Pacheco A, Aguayo FI, Aliaga E, Muñoz M, García-Rojo G, Olave FA, Parra-Fiedler NA, García-Pérez A, Tejos-Bravo M, Rojas PS, Parra CS, Fiedler JL. Chronic Stress Triggers Expression of Immediate Early Genes and Differentially Affects the Expression of AMPA and NMDA Subunits in Dorsal and Ventral Hippocampus of Rats. Front Mol Neurosci. 2017 Aug 10;10:244. doi: 10.3389/fnmol.2017.00244. PMID: 28848384; PMCID: PMC5554379.

Papanicolaou DA, Petrides JS, Tsigos C, Bina S, Kalogeras KT, Wilder R et al. Exercise stimulates interleukin-6 secretion: inhibition by glucocorticoids and correlation with catecholamines. Am J Physiol 1996; 271:E601–E605.

Paré D, Lebel E, Lang EJ. Differential impact of miniature synaptic potentials on the soma and dendrites of pyramidal neurons in vivo. J Neurophysiol 78: 1735–1739, 1997.

Paré D, Shink E, Gaudreau H, Destexhe A, Lang EJ. Impact of spontaneous synaptic activity on the resting properties of cat neocortical pyramidal neurons In vivo. J Neurophysiol 79: 1450–1460, 1998.

Patel R, Spreng RN, Shin LM, Girard TA. Neurocircuitry models of posttraumatic stress disorder and beyond: a meta-analysis of functional neuroimaging studies. Neurosci Biobehav Rev. 2012 Oct;36(9):2130-42. doi: 10.1016/j.neubiorev.2012.06.003. Epub 2012 Jul 2. PMID: 22766141.

Pavlides C, McEwen BS. Effects of mineralocorticoid and glucocorticoid receptors on long-term potentiation in the CA3 hippocampal field. Brain Res. 1999 Dec 18;851(1-2):204-14. doi: 10.1016/s0006-8993(99)02188-5. PMID: 10642845.

Pavlides C, Nivón LG, McEwen BS. Effects of chronic stress on hippocampal long-term potentiation. Hippocampus. 2002;12(2):245-57. doi: 10.1002/hipo.1116. PMID: 12000121.

Pawlak V, Jensen V, Schupp BJ, Kvello A, Hvalby Ø, Seeburg PH, Köhr G. Frequency-dependent impairment of hippocampal LTP from NMDA receptors with reduced calcium permeability. Eur J Neurosci. 2005 Jul;22(2):476-84. doi: 10.1111/j.1460-9568.2005.04226.x. PMID: 16045500.

Paxinos G and Watson C. The rat brain in stereotaxic coordinates (Academic, San Diego), Ed 6 (2007)

Petrak LJ, Harris KM, Kirov SA. Synaptogenesis on mature hippocampal dendrites occurs via filopodia and immature spines during blocked synaptic transmission. J Comp Neurol. 2005 Apr 4;484(2):183-90. doi: 10.1002/cne.20468. PMID: 15736233.

Phoumthipphavong, V., Barthas, F., Hassett, S., & Kwan, A. C. Longitudinal Effects of Ketamine on Dendritic Architecture In Vivo in the Mouse Medial Frontal Cortex. eNeuro, 3(2), ENEURO.0133-15.2016. https://doi.org/10.1523/ENEURO.0133-15.2016

Pitman RK, Sanders KM, Zusman RM, Healy AR, Cheema F, Lasko NB, Cahill L, Orr SP. Pilot study of secondary prevention of posttraumatic stress disorder with propranolol. Biol Psychiatry. 2002 Jan 15;51(2):189-92. doi: 10.1016/s0006-3223(01)01279-3. PMID: 11822998.

Pitman RK, Rasmusson AM, Koenen KC, Shin LM, Orr SP, Gilbertson MW, Milad MR, Liberzon I. Biological studies of post-traumatic stress disorder. Nat Rev Neurosci. 2012 Nov;13(11):769-87. doi: 10.1038/nrn3339. Epub 2012 Oct 10. PMID: 23047775; PMCID: PMC4951157.

Powell DA, Maxwell B, Penney J. Neuronal activity in the medial prefrontal cortex during Pavlovian eyeblink and nictitating membrane conditioning. J Neurosci. 1996; 16(19):6296–6306. [PubMed: 8815909]

Quan M, Zheng C, Zhang N, Han D, Tian Y, Zhang T, Yang Z. Impairments of behavior, information flow between thalamus and cortex, and prefrontal cortical synaptic plasticity in an animal model of depression. Brain Res Bull. 2011 May 30;85(3-4):109-16. doi: 10.1016/j.brainresbull.2011.03.002. Epub 2011 Mar 9. PMID: 21396989.

Radley JJ, Rocher AB, Rodriguez A, Ehlenberger DB, Dammann M, McEwen BS, Morrison JH, Wearne SL, Hof PR. Repeated stress alters dendritic spine morphology in the rat medial prefrontal cortex. J Comp Neurol. 2008 Mar 1;507(1):1141-50. doi: 10.1002/cne.21588. PMID: 18157834; PMCID: PMC2796421.

Radley JJ, Gosselink KL, Sawchenko PE. A discrete GABAergic relay mediates medial prefrontal cortical inhibition of the neuroendocrine stress response. J Neurosci. 2009; 29(22):7330–7340. [PubMed: 19494154]

Radley JJ, Rocher AB, Miller M, Janssen WG, Liston C, Hof PR, McEwen BS, Morrison JH.(2006a) Repeated stress induces dendritic spine loss in the rat medial prefrontal cortex. Cereb Cortex. 2006 Mar;16(3):313-20. doi: 10.1093/cercor/bhi104. Epub 2005 May 18. PMID: 15901656.

Radley, J. J., Arias, C. M. & Sawchenko, P. E. Regional differentiation of the medial prefrontal cortex in regulating adaptive responses to acute emotional stress. J. Neurosci. 26, 12967–12976 (2006).

Radley JJ, Morrison JH. Repeated stress and structural plasticity in the brain. Ageing Res Rev. 2005 May;4(2):271-87. doi: 10.1016/j.arr.2005.03.004. PMID: 15993654.

Raskind MA, Peskind ER, Hoff DJ, Hart KL, Holmes HA, Warren D, Shofer J, O'Connell J, Taylor F, Gross C, Rohde K, McFall ME. A parallel group placebo controlled study of prazosin for trauma nightmares and sleep disturbance in combat veterans with post-traumatic stress disorder. Biol Psychiatry. 2007 Apr 15;61(8):928-34. doi: 10.1016/j.biopsych.2006.06.032. Epub 2006 Oct 25. PMID: 17069768.

Regehr WG. Short-term presynaptic plasticity. Cold Spring Harb Perspect Biol. 2012 Jul 1;4(7):a005702. doi: 10.1101/cshperspect.a005702. PMID: 22751149; PMCID: PMC3385958.

Resstel LBM, Correa FMA. Medial prefrontal cortex NMDA receptors and nitric oxide modulate the parasympathetic component of the baroreflex. Eur J Neurosci. 2006; 23(2):481–488. [PubMed: 16420454]

Resstel LBM, Fernandes KBP, Correa FMA. Medial prefrontal cortex modulation of the baroreflex parasympathetic component in the rat. Brain Res. 2004; 1015(1–2):136–144. [PubMed: 15223377]

Riaza Bermudo-Soriano C, Perez-Rodriguez MM,Vaquero-Lorenzo C, Baca-Garcia E. Newperspectives in glutamate and anxiety.PharmacolBiochem Behav. 2012;100(4):752-774.

Richter-Levin G (1998) Acute and long-term behavioral correlates of underwater trauma – potential relevance to stress and post-stress syndromes. Psychiatry Res 79:73–83

Rocher C, Spedding M, Munoz C, Jay TM. Acute stress-induced changes in hippocampal/ prefrontal circuits in rats: effects of antidepressants. Cereb Cortex. 2004; 14:224–229. [PubMed: 14704220]

Saal D, Dong Y, Bonci A, Malenka RC. Drugs of abuse and stress trigger a common synaptic adaptation in dopamine neurons. Neuron. 2003; 37:577–582. S0896627303000217 [pii]. [PubMed:12597856]

Sandi C, Davies HA, Cordero MI, Rodriguez JJ, Popov VI, Stewart MG. Rapid reversal of stress induced loss of synapses in CA3 of rat hippocampus following water maze training. Eur J Neurosci. 2003 Jun;17(11):2447-56. doi: 10.1046/j.1460-9568.2003.02675.x. PMID: 12814376.

Santana N, Artigas F. Laminar and Cellular Distribution of Monoamine Receptors in Rat Medial Prefrontal Cortex. Front Neuroanat. 2017 Sep 28;11:87. doi: 10.3389/fnana.2017.00087. PMID: 29033796; PMCID: PMC5625028.

Sarabdjitsingh RA, Kofink D, Karst H, de Kloet ER, Joels M. Stress-inducedenhancement of mouse amygdalar synaptic plasticity depends on glucocorti-coid andβ-adrenergic activity.PLoS ONE2012;7: e42143.

Sceniak, M. P., Lang, M., Enomoto, A. C., James Howell, C., Hermes, D. J., & Katz, D. M. (2016). Mechanisms of Functional Hypoconnectivity in the Medial Prefrontal Cortex of Mecp2 Null Mice. Cerebral Cortex, 26(5), 1938–1956. https://doi.org/10.1093/cercor/bhv002

Schottenbauer, M. A., Glass, C. R., Arnkoff, D. B. & Gray, S. H. Contributions of psychodynamic approaches to treatment of PTSD and trauma: a review of the empirical treatment and psychopathology literature. Psychiatry 71, 13–34 (2008)

Seamans JK, Floresco SB, Phillips AG. Functional differences between the prelimbic and anterior cingulate regions of the rat prefrontal cortex. Behav Neurosci. 1995 Dec;109(6):1063-73. doi: 10.1037//0735-7044.109.6.1063. PMID: 8748957.

Shansky RM, Hamo C, Hof PR, McEwen BS, Morrison JH. Stress-induced dendritic remodeling in the prefrontal cortex is circuit specific. Cereb Cortex. 2009 Oct;19(10):2479-84. doi: 10.1093/cercor/bhp003. Epub 2009 Feb 4. PMID: 19193712; PMCID: PMC2742599.

Shansky RM, Morrison JH. Stress-induced dendritic remodeling in the medial prefrontal cortex: effects of circuit, hormones and rest. Brain Res. 2009 Oct 13;1293:108-13. doi: 10.1016/j.brainres.2009.03.062. Epub 2009 Apr 8. PMID: 19361488; PMCID: PMC2748148.gi

Shephard B. A war of nerves: soldiers and psychiatrists in the twentieth century. London: Cape, 2000.

Shin, S.Y.,Han,T.H.,Lee,S.Y., Han,S.K.,Park,J.B.,Erdelyi,F., Szabo,G.,andRyu,P.D.(2011). Direct corticosteroid modulation of GABAergic neurons in the anterior hypothalamic area of GAD65-eGFP mice. Korean J. Physiol. Pharmacol. 15, 163–169.

Schlichting ML, Mumford JA, Preston AR. Learning-related representational changes reveal dissociable integration and separation signatures in the hippocampus and prefrontal cortex. Nat Commun. 2015 Aug 25;6:8151. doi: 10.1038/ncomms9151. PMID: 26303198; PMCID: PMC4560815.

Schlichting ML, Preston AR. Hippocampal-medial prefrontal circuit supports memory updating during learning and post-encoding rest. Neurobiol Learn Mem. 2016 Oct;134 Pt A(Pt A):91-106. doi: 10.1016/j.nlm.2015.11.005. Epub 2015 Nov 25. PMID: 26608407; PMCID: PMC4879117.

Shors, T.J., Seib, T.B., Levine, S. and Thompson, R.F. (1989) Inescapable versus escapable shock modulates long-term potentiation in the rat hippocampus. Science, 244: 224-226.

Shors, T.J. and Thompson, R.F. (1992) Acute stress impairs (or induces) synaptic long-term potentiation (LTP) but does not affect paired-pulse facilitation in the stratum radiatum of rat hippocampus. Synapse, 11: 262-265.

Shors, T.J., Levine, S. and Thompson, R.F. (1990a) Opioid antagonist eliminates the stress-induced impairment of longterm potentiation (LTP). Brain Res., 506: 316-318.

Shors, T.J., Levine, S. and Thompson, R.F. (1990b) Effect of adrenalectomy and demedullation on the stress-induced impairment of long-term potentiation. Neuroendocrinology, 51: 70-75.

Smith ME. Bilateral hippocampal volume reduction in adults with post-traumatic stress disorder: a meta-analysis of structural MRI studies. Hip¬pocampus 2005;15:798-807.

Spinedi E, Hadid R, Daneva T, Gaillard RC. Cytokines stimulate the CRH but not the vasopressin neuronal system: evidence for a median eminence site of interleukin- 6 action. Neuroendocrinology 1992; 56:46–53.

Steptoe, A., Hamer, M., & Chida, Y. (2007, October). The effects of acute psychological stress on circulating inflammatory factors in humans: A review and meta-analysis. Brain, Behavior, and Immunity. Brain Behav Immun. https://doi.org/10.1016/j.bbi.2007.03.011

Stewart MG, Davies HA, Sandi C, Kraev IV, Rogachevsky VV, Peddie CJ, Rodriguez JJ, Cordero MI, Donohue HS, Gabbott PL, Popov VI. Stress suppresses and learning induces plasticity in CA3 of rat hippocampus: a three-dimensional ultrastructural study of thorny excrescences and their postsynaptic densities. Neuroscience. 2005;131(1):43-54. doi: 10.1016/j.neuroscience.2004.10.031. PMID: 15680690.

Suris, A., North, C., Adinoff, B., Powell, C. M. & Greene, R. Effects of exogenous glucocorticoid on combat-related PTSD symptoms. Ann. Clin. Psychiatry 22, 22, 274–279 (2010).

Sutanto, W., & de Kloet, E. R. (1994). The use of various animal models in the study of stress and stress-related phenomena. Laboratory Animals, 28(4), 293–306. https://doi.org/10.1258/002367794780745092

Sutton MA, Ito HT, Cressy P, Kempf C, Woo JC, Schuman EM. Miniature neurotransmission stabilizes synaptic function via tonic suppression of local dendritic protein synthesis. Cell 125: 785–799, 2006.

Sutton MA, Wall NR, Aakalu GN, Schuman EM. Regulation of dendritic protein synthesis by miniature synaptic events. Science 304: 1979–1983, 2004.

Tavares RF, Correa FMA, Resstel LBM. Opposite role of infralimbic and prelimbic cortex in the tachycardiac response evoked by acute restraint stress in rats. J Neurosci Res. 2009; 87(11):2601–2607. [PubMed: 19326445]

Taylor FB, Lowe K, Thompson C et al. Daytime prazosin reduces psycho¬logical distress to trauma specific cues in civilian trauma posttraumatic stress disorder. Biol Psychiatry 2006;59:577-81.

Treccani G, Musazzi L, Perego C, Milanese M, Nava N, Bonifacino T, Lamanna J, Malgaroli A, Drago F, Racagni G, Nyengaard JR, Wegener G, Bonanno G, Popoli M. (2014a) Acute stress rapidly increases the readily releasable pool of glutamate vesicles in prefrontal and frontal cortex through non-genomic action of corticosterone. Mol Psychiatry. 2014 Apr;19(4):401. doi: 10.1038/mp.2014.20. PMID: 24658610.

Treccani G, Musazzi L, Perego C, Milanese M, Nava N, Bonifacino T, Lamanna J, Malgaroli A, Drago F, Racagni G, Nyengaard JR, Wegener G, Bonanno G, Popoli M. (2014b) Stress and corticosterone increase the readily releasable pool of glutamate vesicles in synaptic terminals of prefrontal and frontal cortex. Mol Psychiatry. 2014 Apr;19(4):433-43. doi: 10.1038/mp.2014.5. Epub 2014 Feb 18. PMID: 24535456.

Tronel S, Sara SJ. Blockade of NMDA receptors in prelimbic cortex induces an enduring amnesia for odor-reward associative learning. J Neurosci. 2003 Jul 2;23(13):5472-6. doi: 10.1523/JNEUROSCI.23-13-05472.2003. PMID: 12843246; PMCID: PMC6741223.

Turrigiano G. Homeostatic synaptic plasticity: local and global mechanisms for stabilizing neuronal function. Cold Spring Harb Perspect Biol. 2012 Jan 1;4(1):a005736. doi: 10.1101/cshperspect.a005736. PMID: 22086977; PMCID: PMC3249629.Verhae

Tyler WJ, Pozzo-Miller L. Miniature synaptic transmission and BDNF modulate dendritic spine

growth and form in rat CA1 neurones. J Physiol 553: 497–509, 2003.

Ulrich-Lai YM, Herman JP. Neural regulation of endocrine and autonomic stress responses. Nat Rev Neurosci. 2009; 10(6):397–409. [PubMed: 19469025]

van Aerde KJ and Feldmeyer D. Morphological and Physiological Characterization of Pyramidal Neuron Subtypes in Rat Medial Prefrontal Cortex, Cerebral Cortex, Volume 25, Issue 3, March 2015, Pages 788–805, https://doi.org/10.1093/cercor/bht278

van Rooij, S. J. et al. Smaller hippocampal volume as a vulnerability factor for the persistence of post-traumatic stress disorder. Psychol. Med. 45, 2737–2746 (2015).

van Zuiden, M. et al. Pre-existing high glucocorticoid receptor number predicting development of posttraumatic stress symptoms after military deployment. Am. J. Psychiatry 168, 89–96 (2011).

Varela JA, Wang J, Christianson JP, Maier SF, Cooper DC. Control over stress, but not stress per se increases prefrontal cortical pyramidal neuron excitability. J Neurosci. 2012 Sep 12;32(37):12848-53. doi: 10.1523/JNEUROSCI.2669-12.2012. PMID: 22973008; PMCID: PMC3732060.

Venero C, Borrell J. Rapid glucocorticoid effects on excitatory amino acid levels in the hippocampus: a microdialysis study in freely moving rats. Eur J Neurosci. 1999; 11:2465–2473. [PubMed: 10383636]

Verberne AJ, Lam W, Owens NC, Sartor D. Supramedullary modulation of sympathetic vasomotor function. Clin Exp Pharmacol Physiol. 1997; 24(9–10):748–754. [PubMed: 9315383]

Verhage M, Maia AS, Plomp JJ, Brussaard AB, Heeroma JH, Vermeer H, Toonen RF, Hammer RE, van den Berg TK, Missler M, Geuze HJ, Sudhof TC. Synaptic assembly of the brain in the absence of neurotransmitter secretion. Science 287: 864–869, 2000.

Verkuyl ,J.M., Hemby,S.E., and Joels,M. (2004).Chronic stress attenuates GABAergic inhibition and alters gene expression of parvocellular neurons in rat hypothalamus. Eur.J.Neurosci. 20, 1665–1673.

Vertes RP. Differential projections of the infralimbic and prelimbic cortex in the rat. Synapse. 2004; 51(1):32–58. [PubMed: 14579424]

Vogt, BA.; Vogt, JL.; Farber, NB. Cingulate Cortex and models of disease. In: Paxinos, G., editor. The Rat Nervous System. 3rd. New York, NY: Oxford Univeristy Press; 2004. p. 705-727.

Vyas A, Bernal S, Chattarji S. Effects of chronic stress on dendritic arborization in the central and extended amygdala. Brain Res. 2003 Mar 7;965(1-2):290-4. doi: 10.1016/s0006-8993(02)04162-8. PMID: 12591150.

Vyas A, Pillai AG, Chattarji S. Recovery after chronic stress fails to reverse amygdaloid neuronal hypertrophy and enhanced anxiety-like behavior. Neuroscience. 2004;128(4):667-73. doi: 10.1016/j.neuroscience.2004.07.013. PMID: 15464275.

Vyas A, Jadhav S, Chattarji S. Prolonged behavioral stress enhances synaptic connectivity in the basolateral amygdala. Neuroscience. 2006 Dec 1;143(2):387-93. doi: 10.1016/j.neuroscience.2006.08.003. Epub 2006 Sep 8. PMID: 16962717.

Wang HX, Gao WJ. Cell type-specific development of NMDA receptors in the interneurons of rat prefrontal cortex. Neuropsychopharmacology. 2009 Jul;34(8):2028-40. doi: 10.1038/npp.2009.20. Epub 2009 Feb 25. PMID: 19242405; PMCID: PMC2730038.

Wellman CL. Dendritic reorganization in pyramidal neurons in medial prefrontal cortex after chronic corticosterone administration. J Neurobiol. 2001 Nov 15;49(3):245-53. doi: 10.1002/neu.1079. PMID: 11745662.

Warren BL, Vialou VF, Iniguez SD, Alcantara LF, Wright KN, Feng J, Kennedy PJ, Laplant Q, Shen L, Nestler EJ, Bolanos-Guzman CA (2013) Neurobiological sequelae of witnessing stressful events in adult mice. Biol Psychiatry 73:7–14

Weikum, E. R., Knuesel, M. T., Ortlund, E. A., and Yamamoto, K. R. (2017). Glucocorticoid receptor control of transcription: precision and plasticity via allostery. Nat. Rev. Mol. Cell Biol. 18, 159–174. doi: 10.1038/nrm.20 16.152

Xu, L., Anwyl, R. and Rowan, M.J. (1997) Behavioral stress facilitates the induction of long-term depression in the hippocampus. Nature, 387: 497-500.

Xu, L., Anwyl, R. and Rowan, M.J. (1998) Spatial exploration induces a persistent reversal of long-term potentiation in rat hippocampus. Nature, 394: 891-894.

Yamamoto BK, Reagan LP. The glutamatergic system in neuronal plasticity and vulnerability in mood disorders. Neuropsychiatric Dis Treatment. 2006; 2:7–14.

Yang Y, Cui Y, Sang K, Dong Y, Ni Z, Ma S, Hu H. Ketamine blocks bursting in the lateral habenula to rapidly relieve depression. Nature. 2018 Feb 14;554(7692):317-322. doi: 10.1038/nature25509. PMID: 29446381.

Yehuda R, Hoge CW, McFarlane AC, Vermetten E, Lanius RA, Nievergelt CM, Hobfoll SE, Koenen KC, Neylan TC, Hyman SE. Post-traumatic stress disorder. Nat Rev Dis Primers. 2015 Oct 8;1:15057. doi: 10.1038/nrdp.2015.57. PMID: 27189040.

Yehuda R. Post-traumatic stress disorder. N Engl J Med. 2002 Jan 10;346(2):108-14. doi: 10.1056/NEJMra012941. PMID: 11784878.

Yuen EY, Liu W, Karatsoreos IN, Feng J, McEwen BS, Yan Z. Acute stress enhances glutamatergic transmission in prefrontal cortex and facilitates working memory. Proc Natl Acad Sci U S A. 2009 Aug 18;106(33):14075-9. doi: 10.1073/pnas.0906791106. Epub 2009 Jul 29. PMID: 19666502; PMCID: PMC2729022.

Yuen EY, Liu W, Karatsoreos IN, Ren Y, Feng J, McEwen BS, et al. Mechanisms for acute stress-induced enhancement of glutamatergic transmission and working memory. Mol Psychiatry. 2011; 16(2):156–170. [PubMed: 20458323]

Yuen EY, Wei J, Liu W, Zhong P, Li X, Yan Z. Repeated stress causes cognitive impairment by suppressing glutamate receptor expression and function in prefrontal cortex. Neuron. 2012; 73(5):962–977. [PubMed: 22405206]

Yuen EY, Zhong P, Li X, Wei J, Yan Z. Restoration of glutamatergic transmission by dopamine D4 receptors in stressed animals. J Biol Chem. 2013 Sep 6;288(36):26112-20. doi: 10.1074/jbc.M112.396648. Epub 2013 Jul 24. PMID: 23884421; PMCID: PMC3764814.

Zannas, A. S., Provencal, N. & Binder, E. B. Epigenetics of posttraumatic stress disorder: current evidence, challenges, and future directions. Biol. Psychiatry 78, 327–335 (2015).

Zarate CA Jr, Singh JB, Carlson PJ, et al. Arandomized trial of an N-methyl-D-aspartateantagonist in treatment-resistant major depression.Arch Gen Psychiatry. 2006;63(8):856-864.9.

Zeithamova D, Dominick AL, Preston AR. Hippocampal and ventral medial prefrontal activation during retrieval-mediated learning supports novel inference. Neuron. 2012 Jul 12;75(1):168-79. doi: 10.1016/j.neuron.2012.05.010. PMID: 22794270; PMCID: PMC3398403.

Zoladz, P. R. & Diamond, D. M. Current status on behavioral and biological markers of PTSD: a search for clarity in a conflicting literature. Neurosci. Biobehav. Rev. 37, 860–895 (2013)

References reported in Tab. I.1, from Flandreau and Toth (2018):

3. Andero R, Brothers SP, Jovanovic T, Chen YT, Salah-Uddin H, Cameron M, Bannister TD, Almli L, Stevens JS, Bradley B et al (2013) Amygdala-dependent fear is regulated by Oprl1 in mice and humans with PTSD. Sci Transl Med 5:188ra173

4. . Mitra R, Jadhav S, McEwen BS, Vyas A, Chattarji S (2005) Stress duration modulates the spatiotemporal patterns of spine formation in the basolateral amygdala. Proc Natl Acad Sci U S A 102:9371–9376

5. Kedia S, Chattarji S (2014) Marble burying as a test of the delayed anxiogenic effects of acute immobilisation stress in mice. J Neurosci Methods 233:150–154

6. Meerlo P, Easton A, Bergmann BM, Turek FW (2001) Restraint increases prolactin and REM sleep in C57BL/6J mice but not in BALB/cJ mice. Am J Physiol Regul Integr Comp Physiol 281:R846–R854

8. Harvey BH, Brand L, Jeeva Z, Stein DJ (2006) Cortical/hippocampal monoamines, HPA-axis changes and aversive behavior following stress and restress in an animal model of posttraumatic stress disorder. Physiol Behav 87:881–890

9. Richter-Levin G (1998) Acute and long-term behavioral correlates of underwater trauma – potential relevance to stress and post-stress syndromes. Psychiatry Res 79:73–83

10. Cohen H, Zohar J, Matar MA, Zeev K, Loewenthal U, Richter-Levin G (2004) Setting apart

the affected: the use of behavioral criteria in animal models of post traumatic stress disorder. Neuropsychopharmacology 29:1962–1970

11. Moore NL, Gauchan S, Genovese RF (2012) Differential severity of anxiogenic effects resulting from a brief swim or underwater trauma in adolescent male rats. Pharmacol Biochem Behav 102:264 268

13. Imanaka A, Morinobu S, Toki S, Yamawaki S (2006) Importance of early environment in the development of post-traumatic stress disorder-like behaviors. Behav Brain Res 173:129–137

14. Knox D, George SA, Fitzpatrick CJ, Rabinak CA, Maren S, Liberzon I (2012) Single prolonged stress disrupts retention of extinguished fear in rats. Learn Mem 19:43–49

15. Takahashi T, Morinobu S, Iwamoto Y, Yamawaki S (2006) Effect of paroxetine on enhanced contextual fear induced by single prolonged stress in rats. Psychopharmacology (Berl) 189:165–173

17. Yamamoto S, Morinobu S, Takei S, Fuchikami M, Matsuki A, Yamawaki S, Liberzon I (2009) Single prolonged stress: toward an animal model of posttraumatic stress disorder. Depress Anxiety 26:1110–1117

18. Wu Z, Tian Q, Li F, Gao J, Liu Y, Mao M, Liu J, Wang S, Li G, Ge D et al (2016) Behavioral changes over time in post-traumatic stress disorder: insights from a rat model of single prolonged stress. Behav Processes 124:123–129

20. Vanderheyden WM, George SA, Urpa L, Kehoe M, Liberzon I, Poe GR (2015) Sleep alterations following exposure to stress predict fear-associated memory impairments in a rodent model of PTSD. Exp Brain Res 233:2335–2346

29. Siegmund A, Wotjak CT (2007) A mouse model of posttraumatic stress disorder that distinguishes between conditioned and sensitised fear. J Psychiatr Res 41:848–860

30. Cullen PK, Gilman TL, Winiecki P, Riccio DC, Jasnow AM (2015) Activity of the anterior cingulate cortex and ventral hippocampus underlie increases in contextual fear generalization. Neurobiol Learn Mem 124:19–27

31. Louvart H, Maccari S, Ducrocq F, Thomas P, Darnaudery M (2005) Long-term behavioural alterations in female rats after a single intense footshock followed by situational reminders. Psychoneuroendocrinology 30:316–324

32. Mikics E, Baranyi J, Haller J (2008) Rats exposed to traumatic stress bury unfamiliar objects – a novel measure of hyper-vigilance in PTSD models? Physiol Behav 94:341–348

33. Mikics E, Toth M, Varju P, Gereben B, Liposits Z, Ashaber M, Halasz J, Barna I, Farkas I, Haller J (2008) Lasting changes in social behavior and amygdala function following traumatic experience induced by a single series of foot-shocks. Psychoneuroendocrinology 33:1198–1210

34. Philbert J, Pichat P, Beeske S, Decobert M, Belzung C, Griebel G (2011) Acute inescapable stress exposure induces long-term sleep disturbances and avoidance behavior: a mouse model of post-traumatic stress disorder (PTSD). Behav Brain Res 221:149–154

35. Pynoos RS, Ritzmann RF, Steinberg AM, Goenjian A, Prisecaru I (1996) A behavioral animal model of posttraumatic stress disorder featuring repeated exposure to situational reminders. Biol Psychiatry 39:129–134

75. Golden SA, Covington HE 3rd, Berton O, Russo SJ (2011) A standardized protocol for repeated social defeat stress in mice. Nat Protoc 6:1183–1191

78. Pulliam JV, Dawaghreh AM, Alema-Mensah E, Plotsky PM (2010) Social defeat stress produces prolonged alterations in acoustic startle and body weight gain in male Long Evans rats. J Psychiatr Res 44:106–111

80. Der-Avakian A, Mazei-Robison MS, Kesby JP, Nestler EJ, Markou A (2014) Enduring deficits in brain reward function after chronic social defeat in rats: susceptibility, resilience, and antidepressant response. Biol Psychiatry 76:542–549

90. Zoladz PR, Conrad CD, Fleshner M, Diamond DM (2008) Acute episodes of predator exposure in conjunction with chronic social instability as an animal model of post-traumatic stress disorder. Stress 11:259–281

93. Adamec R, Fougere D, Risbrough V (2010) CRF receptor blockade prevents initiation and consolidation of stress effects on affect in the predator stress model of PTSD. Int J Neuropsychopharmacol 13:747–757

97. Diamond DM, Park CR, Heman KL, Rose GM (1999) Exposing rats to a predator impairs spatial working memory in the radial arm water maze. Hippocampus 9:542–552

99. Woodson JC, Macintosh D, Fleshner M, Diamond DM (2003) Emotion-induced amnesia in rats: working memory-specific impairment, corticosterone-memory correlation, and fear versus arousal effects on memory. Learn Mem 10:326–336

100. Zoladz PR, Park CR, Fleshner M, Diamond DM (2015) Psychosocial predator-based animal model of PTSD produces physiological and behavioral sequelae and a traumatic memory four months following stress onset. Physiol Behav 147:183–192

119. Khan S, Liberzon I (2004) Topiramate attenuates exaggerated acoustic startle in an animal model of PTSD. Psychopharmacology (Berl) 172:225–229

120. Cassella JV, Davis M (1985) Fear-enhanced acoustic startle is not attenuated by acute or chronic imipramine treatment in rats. Psychopharmacology (Berl) 87:278–282

121. Davis M (1989) Sensitization of the acoustic startle reflex by footshock. Behav Neurosci 103:495–503

122. Rygula R, Abumaria N, Domenici E, Hiemke C, Fuchs E (2006) Effects of fluoxetine on behavioral deficits evoked by chronic social stress in rats. Behav Brain Res 174:188–192